

University of Montana

## ScholarWorks at University of Montana

---

Graduate Student Theses, Dissertations, &  
Professional Papers

Graduate School

---

2012

# THE ECOLOGY OF TICK-BORNE RELAPSING FEVER IN WESTERN NORTH AMERICA

Tammi Lynne Johnson  
*The University of Montana*

Follow this and additional works at: <https://scholarworks.umt.edu/etd>

**Let us know how access to this document benefits you.**

---

### Recommended Citation

Johnson, Tammi Lynne, "THE ECOLOGY OF TICK-BORNE RELAPSING FEVER IN WESTERN NORTH AMERICA" (2012). *Graduate Student Theses, Dissertations, & Professional Papers*. 985.  
<https://scholarworks.umt.edu/etd/985>

This Dissertation is brought to you for free and open access by the Graduate School at ScholarWorks at University of Montana. It has been accepted for inclusion in Graduate Student Theses, Dissertations, & Professional Papers by an authorized administrator of ScholarWorks at University of Montana. For more information, please contact [scholarworks@mso.umt.edu](mailto:scholarworks@mso.umt.edu).

THE ECOLOGY OF TICK-BORNE RELAPSING FEVER IN WESTERN NORTH AMERICA

by

TAMMI LYNNE JOHNSON

B.S. Biology, University of Mary, Bismarck, ND, 2000  
M.S. Biology, Kansas State University, Manhattan, KS, 2005

Dissertation  
presented in partial fulfillment of the requirements  
for the degree of

Doctor of Philosophy  
In  
Organismal Biology and Ecology

The University of Montana  
Missoula, MT

Spring 2012

Approved by:  
Sandy Ross, Associate Dean of The Graduate School

Dr. Kerry R. Foresman, Co-Chair  
Division of Biological Sciences, OBE

Dr. Tom G. Schwan, Co-Chair  
Laboratory of Zoonotic Pathogens, Rocky Mountain laboratories, National Institute of Allergy  
and Infectious Disease, National Institutes of Health

Dr. Fred W. Allendorf  
Division of Biological Sciences, OBE

Dr. Jonathan M. Graham  
Department of Mathematical Sciences

Dr. Vanessa O. Ezenwa  
Odum School of Ecology, University of Georgia

**The Ecology of Tick-borne Relapsing Fever in Western North America**

Co-chairperson: Kerry R. Foresman

Co-chairperson: Tom G. Schwan

In North America the primary cause of tick-borne relapsing fever (TBRF) is the spirochete *Borrelia hermsii* that is vectored by the tick *Ornithodoros hermsi*. Ecological investigations were combined with mathematical modeling and genetics to gain a clearer understanding of the interactions and mechanisms responsible for disease maintenance, distribution, and genetic diversity. The objectives of this research were to: 1) identify mammals associated with *B. hermsii* and *O. hermsi* by determining active infection and antibody presence, 2) develop a deterministic model to ascertain ecological and epidemiological parameters essential for disease persistence, 3) resolve the phylogeographic structure of *B. hermsii* and *O. hermsi* to identify dispersal events, and 4) determine the environmental requirements of *B. hermsii* and *O. hermsi*.

We identified 11 species of small mammals with antibodies to relapsing fever spirochetes, while pine squirrels (*Tamiasciurus hudsonicus*) and deer mice (*Peromyscus maniculatus*) had active infections. Interactions for the enzootic maintenance of *B. hermsii* include vectors and host(s). These interactions were incorporated into a SIR compartmental model to calculate  $R_0$ , the basic reproductive number of the disease system. The effect of antigenic variation of the spirochete was assessed by adding relapsing classes to the model, which resulted in an increase of  $R_0$ . We confirmed the suitability of coniferous forests at higher elevations for the presence *O. hermsi* and identified constraints on this distribution. *O. hermsi* and *B. hermsii* were sensitive to temperature extremes throughout the year. Models for global climate change predicted a shift in range of suitable conditions to higher elevations in the year 2050. Little is known about dispersal of these ticks and spirochetes. Phylogeographic analysis of single nucleotide polymorphisms in 49 *B. hermsii* isolates from western North America suggested that *B. hermsii* was introduced to Wild Horse Island, Montana, on at least three occasions. Further, sequence data from the mt16S rDNA of *O. hermsi* suggested that these ticks can move between the mainland and islands on Flathead Lake. Taken together these data define the complex dynamics of the underlying ecological interactions of an otherwise poorly understood system, and provide evidence for the potential emergence of this pathogen in naïve areas.

## Acknowledgements

I am grateful to my committee for allowing me to undertake an interdisciplinary-based dissertation project. Each of them provided invaluable knowledge that contributed to the development of each portion of my dissertation. I am thankful to Dr. Tom Schwan for his vast expertise of medical entomology, his interest in the ecology of infectious disease systems, and most importantly for the personal knowledge of the tick-borne relapsing fever system that he was able to impart to me as one of, if not the, leading authority on this disease system. Dr. Kerry Foresman has immeasurable experience and expertise in the field of mammalogy and field methods. His support and knowledge in these areas is greatly appreciated. Dr. Jon Graham has played a pivotal role in my knowledge and implementation of statistical and mathematical methods. Dr. Fred Allendorf is a renowned population and conservation geneticist and I am fortunate for his interest in my work and the helpful discussions we have had. Although Dr. Vanessa Ezenwa moved to the University of Georgia last year, I am grateful that she remained a member of my committee. Her vast knowledge of disease ecology and broad interests helped to motivate this research. I appreciate her involvement and the many discussions we have had about my research.

This research would not have been possible without support from many individuals and organizations. Special thanks go to Dr. Robert Fischer, a post-doc in Dr. Schwan's lab, and my partner in the field. Large field projects require the support and assistance from many people and entities. I thank the following individuals for their help in the field: Jake Bledsoe, Macaela Martinez, Eric Baggs, Brandi Williamson, Ben Krajacich, Lisa Wolff, Caroline Grunenwald, Beth Fischer, and Kristin McNally. I thank the staff at Flathead Lake Biological Station, especially Jack Stanford and Sue Gillespie. Working on islands on Flathead Lake certainly has its challenges; Zeff Kingsley, Jerry Sawyer, and Bryan Schwartz of Montana Fish Wildlife and Parks provided access to the islands. I am also thankful to the members of the Confederated Salish and Kootenai Tribes for allowing us to conduct field research on their land south of Flathead Lake. We would not have been able to conduct research on Wild Horse Island and Melita Island without the support and interest from property owners including the Harrington Family, the MacDonald Family, Mike Kadas and Martha Newell, and Barry Gordon, on Wild Horse Island, and on Melita Island, Howard Haslan and the Boy Scouts of America.

I received extensive support from the Genomics Unit at Rocky Mountain Laboratories (RML), and extend special thanks you to Steve Porcella, Craig Martens, Stacey Rickliffs, Dan Bruno, and Kent Barbian. Dr. Scott Miller, University of Montana, was always willing to talk with me about my research and provided many helpful discussions regarding prokaryotic phylogenetics. Logistic support for this research was very efficiently handled by Colleen Miller. Additionally, Anita Mora and Austin Athman from the RML Visual and Media Arts Department have been extremely helpful in the preparation of posters, maps, and figures.

I was fortunate to receive funding from the Montana Ecology of Infectious Diseases (MEID) program sponsored by the National Science Foundation Integrative Graduate Education and Research Traineeship (IGERT), and from the National Institutes of Health (NIH) Pre-doctoral Intramural Research Training Award (IRTA) program. I feel very fortunate to have received funding from these two establishments, not only because it allowed me to not be a poor starving graduate student, but because the MEID program was designed to be interdisciplinary program and I was extremely interested in this type of research, but knew little about the techniques I was most interested in. The MEID program provided me the opportunity to work closely with computer and mathematic modelers, and to form close collaborations and friendships. Chapter 3 is a direct result of my involvement with this program and is the product of a modeling collaboration between me and Dr. Erin Landguth, also a MEID fellow. Dr. Landguth is not only my colleague, she has become a close friend and confidant. I am very thankful to Dr. Landguth for her patience and willingness to take on such a complex modeling project. Also as a result of the MEID program, I have been fortunate to get to know and work with Ted Cosart. Ted has served as an invaluable resource in the fields of genetics and bioinformatics and has become a close friend. I would also like to thank all students and faculty involved with the MEID program. MEID provided an excellent forum of individuals with a broad range of interests and expertise to present research ideas and discuss potential research directions.

My involvement in the NIH IRTA program has undoubtedly provided me with experience in the laboratory that I likely otherwise would not have received. I especially extend thanks to all of the current and past members of Dr. Schwan's lab, the Laboratory of Zoonotic Diseases, National Institute of Allergy and Infectious Diseases, NIH. I began this project with zero experience in the laboratory. Everyone in Dr. Schwan's group was more than willing to

help me with even the most mundane laboratory tasks. Merry Schrumpf processed all of the Western Blots for the first two years of the project. Sandy Stewart is a wizard and has imparted vast knowledge on the molecular properties of *Borrelia hermsii*. Brandi Williamson and Paul Policastro do an amazing job of maintaining the tick colonies, and are always willing to answer questions and discuss ideas pertaining to my research. Job Lopez, a former post-doc in Dr. Schwan's lab was always interested and willing to talk about the ecology of infectious disease, and was a source of motivation for bringing lab-based concepts to the field and vice versa.

Finally, I could have never made it through my Ph.D. without the constant support and encouragement of my friends and family, especially my parents Jerry and Sharon Johnson. My parents have fully supported my every endeavor, taught me a strong work ethic, to always do the best job I can, and most importantly, to never give up. I dedicate this dissertation to them. Thanks Mom and Dad!

# Table of Contents

Abstract.....	ii
Acknowledgements.....	iii
Table of Contents.....	vi
List of Tables .....	x
List of Figures.....	xiv
Chapter 1 – Introduction to Tick-borne Relapsing Fever in North America	
1.1 Introduction.....	1
1.2 Methods.....	5
1.3 Results/Conclusions.....	8
Chapter 2 – Investigations of an Endemic Focus of Tick-borne Relapsing Fever in Lake County, Montana	
2.1 Abstract.....	13
2.2 Introduction.....	14
2.3 Methods.....	19
2.3.1 Small mammal trapping.....	19
2.3.2 Sample and laboratory analyses.....	20
2.3.3 Statistical analyses.....	23
2.3.4 Tick collection.....	24
2.4 Results.....	24
2.4.1 Small mammal and tick infection with <i>Borrelia hermsii</i> .....	24
2.4.2 Host species diversity and prevalence of relapsing fever antibodies.....	25
2.4.3 Spirochete isolation and genetic characterization.....	26

2.5 Discussion.....	27
Chapter 3 – Modeling relapsing disease dynamics in a host-vector community	
3.1 Abstract.....	47
3.2 Introduction.....	48
3.2.1 Study system.....	49
3.2.2 Dynamical systems model introduction.....	53
3.3 Methods.....	54
3.3.1 Parameter estimates.....	54
3.4 Single Host-vector System.....	57
3.4.1 Model description.....	57
3.4.2 Equilibrium analysis.....	59
3.4.3 $R_0$ analysis.....	62
3.5 Coupled Host-vector System.....	62
3.5.1 Model description.....	62
3.5.2 Equilibrium analysis.....	64
3.5.3 $R_0$ analysis.....	68
3.6 Discussion.....	69
Chapter 4 – Phylogeographic Structure of the Tick-borne Relapsing Fever Agent <i>Borrelia hermsii</i>	
4.1 Abstract.....	79
4.2 Introduction.....	80
4.3 Methods.....	84
4.3.1 <i>Borrelia hermsii</i> samples .....	84



4.3.2 Phylogenetic analysis.....	85
4.4 Results.....	86
4.4.1 GGI <i>B. hermsii</i> .....	87
4.4.2 GGII <i>B. hermsii</i> .....	87
4.5 Discussion.....	88
 Chapter 5 – The Potential Distribution of the Tick-borne Relapsing Fever Spirochete <i>Borrelia</i> <i>hermsii</i> and vector <i>Ornithodoros hermsi</i> in Western North America	
5.1 Abstract.....	101
5.2 Introduction.....	102
5.3 Methods.....	107
5.3.1 Presence data.....	107
5.3.2 Current and future climate data.....	108
5.3.3 Maxent modeling.....	109
5.4 Results.....	111
5.5 Discussion.....	113
 Appendix A – Virulence of Two Genomic Groups of <i>Borrelia hermsii</i> in deer mice ( <i>Peromyscus</i> <i>maniculatus</i> )	
A.1 Introduction.....	131
A.2 Methods.....	132
A.3 Results/Discussion.....	133
 Appendix B – Population Genetics of <i>Ornithodoros hermsi</i> , a Vector of Tick-borne Relapsing Fever in Western North America	
B.1 Introduction.....	139

B.2 Methods.....	139
B.3 Results.....	142
B.4 Discussion.....	143
References.....	152

## List of Tables

Table 2-1. Trap effort at all sites including dates trapped and number of total trap nights at each study site.....35

Table 2-2. Total animals captured and total animals with antibodies to tick-borne relapsing fever spirochetes at each study site during each year.....36

Table 2-3. Location of *O. hermsi* collected at Melita Island (MEL), Wild Horse Island (WHI), and Yellow Bay (YB). Stage = life stage of tick when collected, N = nymph, M = adult male, F = adult female, and stages separated by a comma represent ticks that molted after capture and being fed in the laboratory. Y = Yes, N = No.....37

Table 2-4. All isolates of *B. hermsii* obtained in Montana from this study as well as previous human outbreaks on Wild Horse Island, Lake Co., Montana. Isolate = name of isolate, source = source of infection from which the isolate was cultured, year = year of isolation, GG = genomic group, CoInf = coinfection with > 1 GG.....38

Table 3-1. Parameters and variable notation in the host-vector TBRF model for  $j - 1$  relapses between  $j$  infected compartments (rates are per month, competency values are probabilities (per bite)) and dimensionless forms (rescaled by  $\gamma$  or normalized by  $N(0)$ ). In the coupled system, additional subscripts with  $ps$  represent the pine squirrel host-vector system and  $dm$  represent the deer mouse host-vector system.....73

Table 3-2. Parameter values in the TBRF model for  $j-1$  relapses between  $j$  infected compartments (rates are per month, competency values are probabilities (per bite)). The subscripts  $ps$  and  $dm$  denote values used in the pine squirrel and deer mouse host-vector system, respectively. Note that if the subscripts do not appear, then the parameter is the same value in both systems.....74

Table 4-1a. GGI *B. hermsii* isolates included in SNP analysis. The name includes the state or province from where the isolate originated, the year of isolation, and the three letter isolate designation. The biological origin of each isolate is listed under source.....92

Table 4-1b. GGII *B. hermsii* isolates included in SNP analysis. The name includes the state or province from where the isolate originated, the year of isolation, and the three letter isolate designation. The biological origin of each isolate is listed under source.....93

Table 4-2a. Number of SNPs between all GGI *B. hermsii* isolates. LAK-4 and LAK-6 are grouped together because they were identical and thus all pair-wise differences between them and other isolates are also identical.....94

Table 4-2b. Number of SNPs between all GGII *B. hermsii* isolates.....95

Table 5-1. Description of 40 georeferenced presence locations of *O. hermsi*, *B. hermsii* infected hosts, hosts with antibodies specific to relapsing fever spirochetes, and isolates resulting from human cases with known site of exposure.....119

Table 5-2. Pearson correlation between 19 Bioclim variables and elevation. The 10 environmental variables included in the Maxent model are shown in bold. Bold numbers within the matrix indicate variables with a Pearson correlation  $\geq 0.75$ . A short description of each variable is given in the footnote of the table.....120

Table 5-3. Contribution of selected variables to the Maxent model. The five most influential variables contributed  $> 75\%$  to explain the distribution of *O. hermsi* and *B. hermsii*. Temperature-related variables contributed the most to explain the observed distribution produced by the model.....121

Table 5-4. Area (km<sup>2</sup>) of each probability class ( $< 0.05$ , 0.05-0.25, 0.25-0.50, 0.50-0.75, and  $> 0.75$ ) for the predicted distribution of *O. hermsi* by Maxent. Estimates are based on the

current distribution of 9 climate layers and elevation. Climatic requirements identified for current environmental conditions were projected onto future climate change models to predict the probability distribution of the tick in the year 2050. Three climate change models under two emissions scenarios were used; conservative (B2) and extreme (A2) emissions, created by the Canadian Centre for Climate Modelling and Analysis (CCCMA), the Commonwealth Scientific and Industrial Research Organisation (CSIRO), and the Hadley Centre for Climate Prediction and Research (HADCM), based on the Intergovernmental Panel on Climate Change 3<sup>rd</sup> Assessment (IPCC3).....122

Table A-1. Number and stage of *B. hermsii*-infected *O. hermsi* fed on each deer mouse (*P. maniculatus*). N = nymphal tick stage.....135

Table B-1. Location, origin, date of collection, and haplotype of 49 *O. hermsi* ticks from which mitochondrial 16S rDNA sequence was obtained. Tick samples consisted of *O. hermsi* maintained in laboratory colonies at Rocky Mountain Laboratories, Hamilton, MT and *O. hermsi* collected during field studies described in Chapter 2 (MIT, WHT, and YBT).  
 MTW = Mount Wilson colony, RML = Rocky Mountain Laboratory colony, SIS = Siskiyou County colony, WHI = Wild Horse Island colony, MIT = Melita Island ticks, WHT = Wild Horse Island tick, YBT = Yellow Bay tick.....145

Table B-2. Genetic characteristics of the seven haplotypes represented by the mt16S rDNA of 49 *Ornithodoros hermsi*.....146

Table B-3. Pair-wise  $F_{ST}$  values between collection sites (lower diagonal), and the  $p$ -values for pair wise  $F_{ST}$  comparisons (upper diagonal), (+) denotes a significant  $p$ -value ( $p < 0.05$ ), (-) denotes a non-significant  $p$ -value ( $p > 0.05$ ). MTW = Mount Wilson colony, RML =

Rocky Mountain Laboratory colony, SIS = Siskiyou County colony, WHI = Wild Horse  
Island, MIT = Melita Island ticks, YBT = Yellow Bay tick.....147

## List of Figures

- Figure 2-1. Map of study area of Flathead Lake, Lake Co., Montana (inset). Study sites included Cedar Island (CED), East Yellow Bay (EYB), Melita Island (MEL), Polson/Big Arm (PBA), Wild Horse Island (WHI), and Flathead Lake Biological Station at Yellow Bay (YB).....41
- Figure 2-2. Western blots targeting *Borrelia*-specific antibodies (whole-cell lysate in the left lane and recombinant GlpQ in the right lane) in the serum of field-caught rodents showing positive (+) and negative (-) examples for four species, *Tamiasciurus hudsonicus*, *Tamias ruficaudus*, *Peromyscus maniculatus*, and *Glaucomyssabrinus*. Molecular mass standards are shown on the left in kilodaltons.....42
- Figure 2-3. Analysis of Variance (ANOVA) of differences in species diversity among study sites. MEL was the least diverse site, while YB was the most diverse site ( $p = 0.01$ ). MEL was significantly less diverse than all sites except WHI, and WHI was significantly less diverse than YB.....43
- Figure 2-4. Analysis of Variance (ANOVA) of differences in seroprevalence among host species. *Tamiasciurus hudsonicus*, *Glaucomyssabrinus*, and *Tamias* spp. were significantly more seropositive for relapsing fever spirochetes than all other species ( $p < 0.0001$ ). *Tamiasciurus hudsonicus* and *Glaucomyssabrinus* were equally seropositive, while chipmunks were less seropositive than *Tamiasciurus hudsonicus* and *Glaucomyssabrinus* but more seropositive than the three other species. *Peromyscus maniculatus*, *Zapus princeps*, and *Microtus* spp. did not differ from each other and were significantly less seropositive than the other species.....44

Figure 2-5. Linear regression of seroprevalence and Shannon species diversity. There was a marginally significant trend between increasing species diversity and decreasing seroprevalence rates ( $p = 0.052$ ;  $R^2 = 0.69$ ). The dashed line represents the 95% confidence interval around the regression line.....45

Figure 2-6. Phylogenetic tree based on the concatenated DNA sequence of 4 genes (*glpQ*, *gyrB*, *flaB*, and *16S rRNA*; 5,197 bp) illustrating the genetic relationships among 27 *Borrelia hermsii* isolates obtained from humans, *Tamiasciurus hudsonicus*, and *Ornithodoros hermsi* ticks, and sequence from a single *Peromyscus maniculatus* near Flathead Lake, Lake Co., MT. Sequences were aligned using CLUSTAL W and the tree was constructed using the neighbor joining algorithm (Saitou and Nei 1987). Genomic group (GG) designations are shown on the right.....46

Figure 3-1. Conceptual models for the cross-infection dynamics between (a) a single host-vector system, which includes  $j - 1$  relapses between  $j$  infected compartments and (b) a coupled host-vector system with no relapses in either host. Dashed lines are vital rates for each population, where solid lines refer to interaction rates between compartments. See Table 1 for a summary of notation.....76

Figure 3-2. Increasing number of infected compartments are added to the single host-vector system and  $R_0$  is plotted (Equation 15).  $R_0$  becomes greater than 1 at 4 relapses.....77

Figure 3-3. An incompetent deer mouse (*Peromyscus maniculatus*) host system ( $c_{dm} = 0.2$ ) is coupled with a competent pine squirrel (*Tamiasciurus hudsonicus*) host system ( $c_{ps} = 0.9$ ).  $R_0$  is plotted (Equations 31-32) for the deer mouse host system that contained no relapses and the pine squirrel host system with increasing number of infected compartments.  $R_0$  becomes greater than 1 at 7 relapses.....78



Figure 4-1. Geographic locations by county of *B. hermsii* isolates included in SNP analysis (in black). Blue circles show locations of *B. hermsii* isolates and yellow triangles correspond to locations where *O. hermsii* and *B. hermsii* were found. Multiple isolates from a single county are denoted by a single symbol (See Table 4-1).....97

Figure 4-2. Alignment of concatenated chromosomal SNPs of 49 *B. hermsii*, a) genomic group 1 (GGI), b) genomic group 2 (GGII), created in BEAST. Black bars represent the presence of a SNP and grey areas represent sequence consensus. Isolates grouped by state of origin.....98

Figure 4-3. Coalescent-based phylogeny of concatenated chromosomal SNPs from 21 GGI *B. hermsii* isolates based on BEAST output created using TreeAnnotator and viewed using FigTree. Scale bar in bottom left corner is in years.....99

Figure 4-4. Coalescent-based phylogeny of concatenated chromosomal SNPs from 28 GGII *B. hermsii* isolates based on BEAST output created using TreeAnnotator and viewed using FigTree. Scale bar in bottom left corner is in years.....100

Figure 5-1. Map of 40 presence locations for infected hosts, hosts with *Borrelia* antibodies, *O. hermsii* collections and georeferenced points of bacterial isolates obtained from the blood of infected human patients.....125

Figure 5-2. Logistic predicted probability of occurrence/ecological suitability of *B. hermsii* and *O. hermsii*. Presence points (as defined in Figure 1) are shown in red, and probability of occurrence increases as the shading becomes darker.....126

Figure 5-3. Jackknife plots for: a) regularized training gain, b) regularized test gain, and c) AUC gain. Gain is how much better or worse the model performs based on the inclusion or exclusion of variables and is measured in three ways: the omission of a single variable,

the inclusion of only a single variable, and the inclusion of all variables. The red bar shows model performance with all variables included. Dark blue bars show model performance with only a single variable included, while the light blue bars display model performance when a single variable is omitted. Variables with the longest blue bars have the most individual influence on the model, while light blue bars that are the shortest contain the most information that is not present in other variables in the model. Training gain (a) shows variation in model performance of presence points included in the training dataset, test gain (b) is based on model performance based on 25% of presence points withheld to test model performance, and AUC gain (c) assesses model fit as a whole...127

Figure 5-4. Variable response curves produced by Maxent for the five most influential variables contributing to the model. Each curve shows the effect of an individual variable on the model and the dependence of the predicted suitability on each of the variables shown. Peaks for each curve correspond to the threshold at which the probability of presence is highest: 1) Min Temperature of Coldest Month = 18°F, 2) Mean Temperature of Wettest Quarter = 35°F, 3) Max Temperature of Warmest Month = 79°F, 4) Temperature Annual Range (BIO5-BIO6) = 61°F, and 5) Precipitation of Warmest Quarter = 3.13".....128

Figure 5-5. Predicted changes in distribution of *O. hermsi* and *B. hermsii* in western North America based on three climate change models under extreme emissions scenarios (A2) and more conservative emissions scenarios (B2) for the year 2050. Models were created by the Canadian Centre for Climate Modelling and Analysis (CCCMA), the Commonwealth Scientific and Industrial Research Organisation (CSIRO), and the Hadley Centre for Climate Prediction and Research (HADCM), based on the Intergovernmental Panel on Climate Change 3<sup>rd</sup> Assessment (IPCC3).....129

Figure 5-6. Overlay of Douglas squirrel (*Tamiasciurus douglasii*) and pine squirrel (*T.*

*hudsonicus*) distributions (hatched overlay with dark outline) and all chipmunks (*Tamias* spp.) (stippled overlay) in western North America on the: a) current and b) the year 2050 predicted distribution of *O. hermsi* and *B. hermsii* with a probability of presence > 0.50 (dark gray underlay), Center for International Earth Science Information Network (CIESIN), Columbia University. 2008. Species Distribution Grids [online data]. Palisades, NY: Socioeconomic Data and Applications Center (SEDAC), Columbia University. Available at <http://sedac.ciesin.columbia.edu/species> , retrieved [7/30/2011].....130

Figure A-1. Differences in susceptibility of deer mice to infection with GGI and GGII *B.*

*hermsii*. The number of spirochetes observed in 50 microscopic fields for 21 days after intraperitoneal needle inoculation of two deer mice (*P. maniculatus*). One mouse was inoculated with *B. hermsii* DAH (GGI) spirochetes (black box) and the other mouse was inoculated with *B. hermsii* MTW (GGII) spirochetes (red circle). P.I. = post-inoculation .....137

Figure A-2. Spirochete densities in the blood of four deer mice (*P. maniculatus*) infected with *B.*

*hermsii* MTW (GGII) via nymphal *O. hermsi* tick bite. Data for the fifth deer mouse are not shown because it died on day one post-exposure. Three out of four mice died on day 11 and therefore data are only presented for the first 11 days. P.I. = post-inoculation. No spirochetes were observed in the five mice fed upon by ticks infected with *B. hermsii* DAH (GGI) during the 21 days following exposure to infected ticks (*data not shown*).....138

Figure B-1. Geneious maximum likelihood alignment of the 421 bp sequences of the mitochondrial 16S rDNA of 49 *O. hermsi* and *O. coriaceus*. The green bar on top shows the base position and the consensus among ticks. Each row represents a different haplotype. Black bars show areas of disagreement among bases and gray regions depict identical bases.....149

Figure B-2. Alignment of seven haplotypes (shown in parentheses) identified for *O. hermsi* mitochondrial 16S rDNA sequences. The (•) represents agreement with the base call in Haplotype 1.....150

Figure B-3. A) Neighbor joining tree of *O. hermsi* (haplotypes shown in parentheses) and *O. coriaceus* as the outgroup. The evolutionary history was inferred using the Neighbor-Joining method. The bootstrap consensus tree inferred from 1000 replicates is shown. The tree is drawn to scale based on the number of base substitutions per site. All positions containing gaps and missing data were eliminated. Due to two deletions in *O. coriaceus*, there were 421 positions in the final dataset. Evolutionary analyses were conducted using MEGA5. B) Neighbor joining tree showing inset of *O. hermsi* and genetic relationships among seven haplotypes (shown in parentheses).....151

# Chapter 1 – Introduction to Tick-borne Relapsing Fever in North America

## 1.1 Introduction

The emergence or reemergence of infectious diseases poses a very real threat to human, domestic animal and wildlife populations throughout the world. Sixty percent of emerging infectious diseases are zoonotic (i.e. can be transmitted from animals to humans) and of these, >71% originate in wild animals (Jones *et al.* 2008). Understanding the biotic and abiotic interactions and identifying mechanisms that may contribute to disease emergence, establishment and persistence is necessary to assessing current and future disease risk. Ecological factors likely play a primary role in the emergence of infectious diseases (Morse 1995; Schrag and Wiener 1995; Gubler 1998; Daszak *et al.* 2000; Patz *et al.* 2000; Wilcox and Gubler 2005). Understanding the complete epidemiology of a disease is crucial to advancing the ability to predict and control outbreaks in human and wildlife populations. Sonenshine (2005) outlines the sequence of steps undertaken when attempting to understand the epidemiology of a given disease system. The pathway typically begins with the identification of a clinical syndrome, followed by discovery of the causative disease agent, and then the identification of the source of the agent in nature. The final step includes investigating the often complex biology and ecology of the hosts and/or vectors involved. Given the difficulty frequently encountered when attempting to study a disease in nature, the last step is often the most difficult. However, advances in computational modeling and molecular techniques, including advances in genetic sequencing capabilities, have contributed significantly to an increased understanding of natural disease systems.

Infectious diseases account for 30% of human morbidity and mortality and 25% of human deaths worldwide (Murray and Lopez 1996; WHO 2000). Several factors have been

attributed to the surge in pathogens, including increases in human population, global climate change, increases in global travel, and human encroachment into wildlife habitat (Morse 1995; Schrag and Wiener 1995; Daszak *et al.* 2000; Gubler *et al.* 2000; Patz *et al.* 2000; Wilcox and Gubler 2005). Understanding the underlying principles that influence the spatio-temporal patterns of diseases is vital to understanding the complete epidemiology of a disease, and is especially important when dealing with zoonotic diseases that are often characterized by complex interactions between wildlife reservoirs, arthropod vectors and humans. This research employs an integrated set of tools to examine poorly understood underlying ecological interactions of a vector-borne disease in western North America.

Tick-borne relapsing fever (TBRF) is a vector-borne zoonotic disease caused by infection with *Borrelia* spirochetes and is primarily transmitted by the bite of an infected *Ornithodoros* tick (Southern and Sanford 1969; Felsenfeld 1971). TBRF is endemic to the Americas, Africa, and Asia (Davis 1940). In North America, three species of *Ornithodoros* ticks, *O. hermsi*, *O. turicata*, and *O. parkeri*, vector *B. hermsii*, *B. turicatae*, and *B. parkeri*, respectively (Davis 1940; Felsenfeld 1971). The first report of tick-borne relapsing fever in western North America occurred in 1915 in Colorado (Meader 1915), although ticks were not implicated at that time. Endemicity to Colorado was established in 1939 with the discovery of the tick vector *O. hermsi* (Davis 1939). Additional disease foci of ticks, spirochetes and hosts exist in high coniferous forests throughout the western United States (Moursund 1942). Human cases of TBRF in North America are primarily associated with *B. hermsii* and have been reported from several regions of western North America including many popular tourist destinations near mountain lakes throughout the Cascade, Sierra Nevada, San Bernardino and Rocky Mountain ranges (Dworkin *et al.* 2002).

In the absence of human hosts (which likely serve as dead-end hosts), *B. hermsii* exists in an enzootic cycle involving *O. hermsi* and various vertebrate hosts. *O. hermsi* and *B. hermsii* have been found in association with a variety of rodent species, most notably, tree squirrels (*Tamiasciurus* spp.) and chipmunks (*Tamias* spp.), bats (*Myotis* spp.), and birds (Beck 1937; Porter *et al.* 1932; Davis 1940; Gregson 1949; Longanecker 1951; Dworkin *et al.* 1998; Thomas *et al.* 2002; Schwan *et al.* 2007; Fischer *et al.* 2009). Although several species of hosts have been identified as potentially being involved in the enzootic maintenance of *B. hermsii*, few studies have sought to further investigate the underlying ecology of this system, including the role of these vertebrate hosts in the maintenance, diversity, and distribution of the pathogen across the landscape.

Tick-borne relapsing fever represents an excellent opportunity to apply a multidisciplinary approach to investigate disease dynamics. There is currently very limited knowledge regarding the ecology of TBRF in North America; however, the molecular characteristics of *B. hermsii* have been and continue to be investigated extensively (Hinnenbusch *et al.* 1998; Barbour *et al.* 1991, 2000; Barbour and Restrepo 2000; Bunikis *et al.* 2004; Fritz *et al.* 2004; Barbour 2005; Porcella *et al.* 2005; Dai *et al.* 2006; Frank and Barbour 2006; Schwan *et al.* 2007). Tick-borne relapsing fever is characterized as a relapsing disease because the *Borrelia* spirochetes undergo antigenic variation via genetic recombination of surface protein genes to evade host immune defense. The pattern(s) of antigenic variation have been explored in the laboratory, but little is known pertaining to the behavior of the antigenic variation in natural host populations and the role this may play in pathogen genetic diversity and pathogen persistence in the environment (Burgdorfer and Mavros 1970; Hinnenbusch *et al.* 1998; Fritz *et al.* 2004). It is crucial to combine our molecular knowledge of *B. hermsii* with field studies to

assess potential mechanisms for the distribution and genetic diversity of *B. hermsii* in western North America. Elucidating the basic ecological factors of relapsing fever will provide valuable insights to our understanding of TBRF in North America and may provide clues to investigating TBRF systems in other regions of the world.

This research investigated the ecology of the TBRF system at Flathead Lake, Lake Co., Montana. The first documented human cases of relapsing fever caused by infection with *B. hermsii* in Montana occurred in 2002 on Wild Horse Island on Flathead Lake, Lake, Co., MT (Schwan *et al.* 2003); however, a retrospective study identified an individual from the Big Arm area near Flathead Lake, who was likely infected in 1984 (Dworkin *et al.* 2002). Human outbreaks occurred again in 2004 and 2009 on the island (Schwan *et al.* 2007, Schwan *unpublished data*). These outbreaks led to the isolation of *B. hermsii* and collection of *O. hermsi*, the first confirmation of the tick vector and pathogen in Montana. The objective of this research was to utilize an integrated set of tools including mathematical modeling and phylogenetics to elucidate the ecology of tick-borne relapsing fever in Montana and elsewhere in North America with hopes of gaining a better understanding of how *B. hermsii* is maintained on the landscape and to determine if the genetic structure of *B. hermsii* provides evidence of long distance geographic dispersal. The specific objectives of the study were:

- To identify mammals associated with *B. hermsii* and *O. hermsi* at Flathead Lake by determining active infection and antibody presence,
- To develop a deterministic model to ascertain ecological and epidemiological parameters essential for disease persistence,



- To resolve the phylogeographic structure of *B. hermsii* to investigate geographic structure and dispersal events, and
- To determine the environmental requirements of *B. hermsii* and *O. hermsi* in western North America.

Chapter 2 identified hosts involved in the enzootic maintenance of *B. hermsii* and *O. hermsi* at Flathead Lake and the effects of host diversity on the prevalence, genetic diversity and distribution of *B. hermsii*. Chapter 3 utilized a dynamical systems model to explore the temporal infection dynamics of *B. hermsii* and the conditions necessary for pathogen maintenance and introduction. Chapter 4 used large-scale genomic analyses to investigate the phylogeographic structure of *B. hermsii* for geographic structure and evidence of long-distance dispersal. Chapter 5 investigated the environmental conditions necessary for the presence of *B. hermsii* and *O. hermsi* throughout western North America.

## 1.2 Methods

Chapter 2 presents a serological survey of small mammals on islands and along the mainland of Flathead Lake for the presence of relapsing fever antibodies, identified animals actively infected with *B. hermsii*, and documented the presence of *O. hermsi* and the prevalence of infection of *B. hermsii* in this tick. These data were used to investigate the effects of host species diversity on pathogen prevalence, incidence, and genetic diversity. Whole-blood samples were collected from small mammals at three island sites and three mainland sites. Material collected from cavity and ground nests, as well as pine squirrel middens was collected

and *O. hermsii* were found in nest material collected from Wild Horse Island (WHI), Yellow Bay (YB) and Melita Island (MEL).

We documented the prevalence and diversity of small mammals infected with *B. hermsii* at each site, the number of small mammals possessing antibodies specific to relapsing fever spirochetes and isolated *B. hermsii* from infected individuals. Differences in host species diversity between island and mainland sites provided an opportunity to identify additional hosts not previously implicated in spirochete persistence. Data gathered regarding the distribution and prevalence of *B. hermsii* in vertebrate hosts and vectors contributed to our limited understanding of the ecological dynamics of tick-borne relapsing fever. Furthermore, these data were utilized in subsequent chapters to investigate the underlying ecological dynamics and the role of rodents in the persistence, genetic diversity, and distribution of relapsing fever spirochetes.

Chapter 3 was written in collaboration with Dr. E. Landguth (a programmatic requirement for MEID) and utilized a dynamical systems modeling approach to investigate the underlying dynamics of TBRF that contribute to pathogen maintenance and persistence. Compartmental models, such as the SIR models with susceptible, infectious, and removed compartments (Kermack and McKendrick 1927), have been applied to many disease systems in an effort to examine system dynamics. We utilized the essential summary parameter  $R_0$ , the basic reproductive rate or the expected number of secondary infections produced by a single infectious individual in a population of susceptible hosts (Dietz 1975), to assess driving forces in the model. A basic SIR model was developed to represent the TBRF system on Wild Horse Island. The basic model was extended to include host-vector interactions, a relapsing compartment was added to accurately represent the antigenic variation that *B. hermsii* undergoes to evade host immune defenses, and a coupled system was created with the addition of another

population of host species. We used field data and published data to parameterize the model and examine the underlying dynamics of this system. We calculated  $R_0$  and determined the parameters driving the estimate of  $R_0$ .

Chapter 4 employed coalescent-based genetic analyses to investigate the phylogeographic structure of *B. hermsii*. Genetics can provide valuable insights into key processes of parasite transmission (Paterson and Viney 2000; Goldberg *et al.* 2007; Archie *et al.* 2009). The phylogeographic structure of *B. hermsii* may provide clues to its potential for long-distance dispersal. Many isolates of *B. hermsii* have been established from human cases and are maintained at Rocky Mountain Laboratories (RML), National Institute of Allergy and Infectious Diseases, National Institutes of Health (Schwan *et al.* 2007, 2009). In addition to human isolates, we isolated *B. hermsii* from 12 pine squirrels and 9 *O. hermsi*. Forty-nine isolates of *B. hermsii* were provided to the Research Technologies Genomics Branch at RML for genome sequencing using a SOLiD 3 System (Applied Biosystems). Data generated by the SOLiD sequencer were analyzed using Bioscope (Applied Biosystems) and Zoom (Bioinformatics Solutions, Inc.) to identify single nucleotide polymorphisms (SNPs).

In Chapter 5, georeferenced presence points were incorporated into an ecological niche modeling program to predict the potential distribution of *O. hermsi* and *B. hermsii*. Forty presence points for *B. hermsii* and *O. hermsi* were combined with nine uncorrelated environmental variables and elevation to predict the potential distribution using the Maximum Entropy Species Distribution Model (Maxent) developed and described by Phillips *et al.* (2006). Additionally, the predicted distribution in the year 2050 was estimated under three climate change models and two climate change scenarios. Climate change models were based on the Intergovernmental Panel on Climate Change 3<sup>rd</sup> Assessment (IPCC3) and included models from

three modeling centers: the Canadian Centre for Climate Modelling and Analysis (CCCMA), the Commonwealth Scientific and Industrial Research Organization (CSIRO), and the Hadley Centre for Climate Prediction and Research (HADCM), and for extreme (A2) and conservative (B2) emissions scenarios.

### 1.3 Results/Conclusions

We caught 18 pine squirrels and 1 deer mouse (*Peromyscus maniculatus*) with active infections of *B. hermsii*, the first evidence that deer mice are susceptible to *B. hermsii* and the first documentations of natural infections in both species. A total of 11 small mammal species possessed antibodies to relapsing fever spirochetes (Chapter 2). Nest material collected from MEL, WHI, and YB yielded 31 *O. hermsi* and 13 ticks transmitted spirochetes to laboratory mice. *Borrelia hermsii* was isolated from 9 of 13 mice fed upon by infected *O. hermsi* collected from the field (Chapter 2). *Borrelia hermsii* was also isolated from 12 pine squirrels and infection was identified in 7 additional pine squirrels. Overall, most individuals were infected with GGII *B. hermsii*. Only one *O. hermsi* and one pine squirrel at WHI were infected with GGI<sub>A</sub>, two ticks were infected with GGI<sub>B</sub>, and the remaining individuals were infected with GGII *B. hermsii*. Three pine squirrels were dually infected with *B. hermsii*. A pine squirrel captured at MEL was dually infected with GGII and GGI<sub>A</sub> (Chapter 2, Table 2-4). Two squirrels at YB were dually infected with *B. hermsii* GGII and GGI<sub>B</sub> spirochetes (Chapter 2, Table 2-4). Species diversity was negatively correlated with seroprevalence; islands with less species diversity of hosts had higher rates of seroprevalence than mainland sites. Overall, pine squirrels, chipmunks and northern flying squirrels (*Glaucomys sabrinus*) were most seropositive for relapsing fever spirochetes than were the other species captured.

The basic interactions for the enzootic maintenance cycle of *B. hermsii* include interactions between infected and uninfected vectors and host(s). These interactions were incorporated into a SIR compartmental model and used to calculate  $R_0$ , the basic reproductive number of the disease system (Chapter 3). Breakdown of the model parameters composing the  $R_0$  equation showed that  $R_0$  was directly proportional to tick biting rate, the competency of ticks and hosts, and initial numbers of hosts and vectors. An inverse relationship existed between  $R_0$  and the death rate of ticks and the rate at which hosts were removed either by recovering or dying. The effect of antigenic variation was assessed with the addition of relapsing classes, and always resulted in an increase of  $R_0$ . Results from Chapter 2 suggest that several species may be involved in maintenance of *B. hermsii*, however, little is known about the susceptibility of these additional species to infection. The coupled SIR model showed that as long as the competence of the species added was  $< 1.0$ ,  $R_0$  was predicted to decrease over time.

The phylogeography of *B. hermsii* suggests a past history of dispersal of the pathogen and multiple introductions to diverse geographic areas (Chapter 4). Phylogenetic and coalescent-based trees that showed the relationship of GGI and GGII *B. hermsii* isolates indicated at least three introductions of *B. hermsii* to WHI; a single introduction of GGI and two introductions of GGII *B. hermsii*. The coalescent phylogeny showed that many isolates from close geographic areas grouped together; however, there was some mixing between geographic areas such as between Idaho and southern British Columbia, and between Washington and Idaho GGI isolates showed three divergent groups: 1) ALL and EST from Utah and Colorado, respectively, 2) WAD, MAN and ELD-2 from the Sierra Nevada Mountains in eastern California, and 3) all other isolates from northern California, eastern Washington, the Idaho panhandle and the three Wild Horse Island isolates grouped closely. Isolates belonging to GGII also showed three

distinct groups; 1) SIL, DOG, HAN, LAK-1 and LAK-2 were closely related and genetically distinct from all other isolates and represented collections from Idaho, Washington, and Montana; 2) the MTW isolate from near Los Angeles, California, was distinct from all other isolates; 3) the remaining isolates from Idaho, Washington, Montana, northern California and British Columbia grouped closely together (Figure 4-4a). With the exception of the five genetically divergent isolates from Montana, Idaho, and Washington, the coalescent-based phylogeny showed clear geographic clustering. All Montana isolates, with the exception of LAK-1 and LAK-2, were genetically similar and grouped by collection site.

The preferred habitat of *O. hermsi* and presence of *B. hermsii* associated with these habitats has been well noted in the past. These species occur in coniferous forests at varying but higher elevations in mountainous regions (Dworkin *et al.* 2002); however, the climatic factors driving the distribution are not well understood. The Maxent model described a restricted distribution of *B. hermsii* and *O. hermsi* that was highly dependent on minimum temperature during the coldest month, mean temperature of the wettest month, maximum temperature during the warmest month and annual temperature range (Chapter 4). Predicted shifts in distribution of the tick and spirochete based on all climate change models and both emissions scenarios for the year 2050 predicted an overall decline in the probability of their occurrence and a dramatic shift to higher elevations, which are presumably cooler and drier locations. Taken together with the genetic results presented in Chapter 4, and the known associations of *O. hermsi* and *B. hermsii* with several species of terrestrial and aerial vertebrates, there is a high probability that the tick and pathogen would be dispersed to new areas in the face of global climate change.

We found that several small mammal species were involved with the endemic focus of TBRF in Montana (Chapter 2). However, limited data exist on the susceptibility or competence

of many of these species to become infected with *B. hermsii* and subsequently transmit the infection to a naive tick. The prevalence of active infections and nearly 100% seroprevalence in pine squirrels demonstrate their importance in the maintenance of *B. hermsii*. The presence of relapsing fever antibodies in such a diverse sample of species indicates that these individuals are helping to sustain the tick population. Presumably, if all species are less competent than pine squirrels, which have been deemed here to be highly competent the SIR model showed that with time there should be a decrease in  $R_0$  (Chapter 3). However, unpublished data suggest that the virulence of spirochetes in different genomic groups exist and that GGII spirochetes may be more infectious in a wider range of species than just pine squirrels and chipmunks (Appendix A). Additionally, the longevity of the tick and the tick's ability to maintain infection with *B. hermsii* make it possible that despite an overall decrease in  $R_0$ , *B. hermsii* may persist in the environment. Results from the niche modeling (Chapter 5) combined with the phylogeography of *B. hermsii* (Chapter 4) suggest that these organisms can be dispersed across long geographic distances, which has important implications in the face of global climate change. In 2050, the predicted distribution of *B. hermsii* and *O. hermsi* indicate a substantial shift from the range due to climate change (Chapter 5). If these organisms are able to disperse across the landscape, new niches may likely be exploited in the future.

There is a clear need for ecological investigations of TBRF in North America and other regions of the world. This dissertation is the first comprehensive field study of TBRF in North America. Investigating this newly identified endemic focus using multiple techniques has allowed us to identify many new species that are involved with the enzootic maintenance of *B. hermsii*. Further, through the use of ecological niche modeling, we have a clearer understanding of the environmental niche occupied by these species, and thus the distribution on the landscape.

Genetic analyses revealed the potential for *B. hermsii* to be dispersed. The possibility of emerging or re-emerging relapsing fever around the world poses a very real threat to human populations (Parola and Raoult 2001; Cutler 2006, 2010). Therefore, understanding correlations between disease prevalence, the diversity of vertebrate hosts, and the distributions of hosts and vectors on the landscape is crucial to assessing the potential risk posed to human populations. It is my hope that this research will provide motivation for other researchers to study similar disease systems around the world that pose a significant threat to human wellbeing.



## Chapter 2 – Investigations of an Endemic Focus of Tick-borne Relapsing Fever in Lake County, Montana

### 2.1 Abstract

Tick-borne relapsing fever caused by the spirochete *Borrelia hermsii* is endemic to areas throughout the western United States. The causative agent and the vector responsible for transmission, *Ornithodoros hermsi*, were identified early in the 20<sup>th</sup> century. Mammalian hosts including Douglas squirrels (*Tamiasciurus douglasii*) and various chipmunk species (*Tamias* spp.) were identified early as potential hosts for the vector and spirochete. Here we examine the rodent hosts associated with a known focus of tick-borne relapsing fever in Lake County, Montana. We identified small mammals with antibodies to tick-borne relapsing fever spirochetes at species-rich mainland sites and species-poor island sites at Flathead Lake. We identified two species previously not documented to be infected with *B. hermsii* in the wild, pine squirrels (*Tamiasciurus hudsonicus*) and deer mice (*Peromyscus maniculatus*). We caught 19 individual mammals infected with *B. hermsii*, 18 pine squirrels, and one deer mouse, and 13 *O. hermsi* ticks; nine species of rodents were seropositive. Twenty one isolates of *B. hermsii* were cultured from infected individuals. Pine squirrels, chipmunks (*Tamias* spp.), and northern flying squirrels (*Glaucomys sabrinus*) were significantly more likely to be seropositive than other species trapped. Host species diversity was negatively correlated with seroprevalence. The presence of antibodies to *B. hermsii* in such a diversity of small mammal species suggests that several of these species likely play a role in the maintenance of *B. hermsii* on the landscape, however, the extent of this role has yet to be determined.

## 2.2 Introduction

Tick-borne relapsing fever is a vector-borne zoonotic disease that is endemic throughout Africa, central Asia and the Americas (Davis 1940). The causative agents of relapsing fever, spirochetes of the genus *Borrelia*, were identified by Obermeier in 1867 in association with louse-borne relapsing fever, a non-zoonotic disease in which infection is spread by contact with infected human body lice (*Pediculus humanus*) (Mackie 1907). Spirochetes causing tick-borne relapsing fever are transmitted by the bite of infected *Ornithodoros* ticks or occasionally through coxal fluid emitted from the tick during or immediately after feeding (Southern and Sanford 1969; Felsenfeld 1971). In North America, relapsing fever spirochetes are vectored by a variety of soft-bodied (Argasid) ticks of the genus *Ornithodoros*. Each tick species serves as a vector for a specific species of relapsing fever spirochete. The three primary species of relapsing fever spirochetes in North America are *B. hermsii*, *B. turicatae*, and *B. parkeri*, vectored by *O. hermsi*, *O. turicata*, and *O. parkeri* respectively (Davis 1940; Felsenfeld 1971).

The first recognized report of tick-borne relapsing fever in western North America occurred in 1915 in Colorado (Meader 1915); endemicity to Colorado was established in 1939 with the discovery of the tick vector *O. hermsi* (Davis 1939). In California, human cases of tick-borne relapsing fever were reported as early as 1921 in the Sierra Nevada mountain range and again in the early 1930s (Porter *et al.* 1932). The cases in the 1930s occurred at three locations, Lake Tahoe, Packer Lake, and Big Bear Lake. Additional disease foci of ticks, spirochetes and hosts exist in high coniferous forests throughout the western United States (Moursund 1942). Our research focused exclusively on *B. hermsii* relapsing fever spirochetes vectored by *O. hermsi*.

*B. hermsii* is maintained in an enzootic cycle involving the vector, *O. hermsi*, and vertebrate hosts and has a wide geographic distribution in western North America. *O. hermsi* is found at elevations ranging to >8,000 ft., and is often found in association with rodents such as tree squirrels (*Tamiasciurus* spp.) and chipmunks (*Tamias* spp.) (Porter *et al.* 1932; Beck 1937; Davis 1940; Dworkin *et al.* 1998). Humans become infected as a result of unintentional contact with infected ticks and most likely do not serve as a source of infection for uninfected ticks. Human contact with the ticks usually occurs while sleeping in rustic cabins located within coniferous forests. Currently, tick-borne relapsing fever is a reportable disease in 12 states: Arizona, California, Colorado, Idaho, Montana, Nevada, New Mexico, Oregon, Texas, Utah, Washington, and Wyoming (Tick Borne Relapsing Fever Disease Trends, Centers for Disease Control and Prevention, [http://www.cdc.gov/ncidod/dvbid/RelapsingFever/TBRF\\_DiseaseTrends.html](http://www.cdc.gov/ncidod/dvbid/RelapsingFever/TBRF_DiseaseTrends.html)). Despite the potential distribution of suitable hosts and habitat for *O. hermsi* in Western North America, human cases are relatively rare, possibly due to under reporting because of a lack of diagnosis (Dworkin *et al.* 1998).

Previous field-based investigations of tick-borne relapsing fever occurred primarily during the early part of last century. During the 1930s a series of field investigations in response to human relapsing fever outbreaks led to the collection of several infected *T. douglasii* and chipmunks (*Tamias* spp.) in California (Beck 1937). Early field investigations identified infected individuals from these two genera, yet noted the presence of several other species present at study sites. A laboratory-based susceptibility study on field-caught rodent hosts was carried out in 1970, and discovered that different host species had different competencies for infection with *B. hermsii* (Burgdorfer and Mavros 1970). These investigators infected pine

squirrels (*T. hudsonicus*), yellow pine chipmunks (*Tamias amoenus*) and meadow voles (*Microtus pennsylvanicus*) but were unable to infect additional species noted during other outbreaks.

We now have the capability to test for the presence of antibodies to relapsing fever spirochetes in the serum of a blood sample. A surveillance program of forest service facilities and public campgrounds was implemented in California through a joint effort between the U. S. Forest Service, the California Department of Public Health, Vector-borne Disease Section, and the Rocky Mountain Laboratories, National Institutes of Health initiated in 2005 and continued in 2008 (California Department of Public Health 2005, 2008). Species positive for relapsing fever antibodies included golden-mantled ground squirrels (*Spermophilus lateralis*) and California ground squirrels (*S. beecheyi*). One other study examined rodents for the presence of *Borrelia* antibodies and identified two seropositive brush mice (*Peromyscus boylii*) (Schwan *et al.* 2009).

Species observed in association with human relapsing fever cases but never identified as infected or seropositive in the wild included pine squirrels (*T. hudsonicus*), other chipmunks (*Tamias* spp.), wood rats (*Neotoma* spp.), and deer mice (*P. maniculatus*) (Wynns and Beck 1935; Beck 1937; Porter *et al.* 1932; Davis 1940; Thompson *et al.* 1969; Boyer *et al.* 1977; Centers for Disease Control, Morbidity and Mortality Weekly Report 2003; Schwan *et al.* 2003). Because few studies have identified *B. hermsii* infections in wild mammals and only two studies have examined wildlife species for retrospective infection, i.e. presence of antibodies against relapsing fever spirochetes, we sought to identify potential rodent hosts of *B. hermsii* in Montana where human infections have occurred.

The first documented human cases of relapsing fever caused by *B. hermsii* in Montana occurred in 2002 on Wild Horse Island (WHI) on Flathead Lake, Lake Co., MT (Schwan *et al.* 2003). However, a retrospective study of hospital case histories identified an individual from the Big Arm area near Flathead Lake, who was likely infected in 1984 (Dworkin *et al.* 2002). Human outbreaks occurred again in 2004 and 2009 on WHI (Schwan *et al.* 2007, Schwan *unpublished data*). These outbreaks led to the isolation of *B. hermsii* and the collection of *O. hermsi*, the first confirmation of the tick vector and pathogen in Montana.

The genetic diversity of *B. hermsii* has been well characterized at several genetic loci, which shows a dramatic divergence among isolates examined that represent two distinct genomic groups, GGI and GGII (Porcella *et al.* 2005; Schwan *et al.* 2007). The human isolates obtained from WHI belonged to both genomic groups, which demonstrated the presence of both genomic groups of *B. hermsii* on the island. A diverse array of rodent species has been reported in relation to *B. hermsii*; however, early visits to Wild Horse Island indicated that the island was only inhabited by two species of rodents, pine squirrels and deer mice. This led us to question the role of host species diversity in this system.

Species diversity can affect the maintenance and prevalence of zoonotic pathogens by either increasing pathogen abundance and/or persistence (amplification) or by decreasing them (dilution) (Begon 2008). Each of these scenarios is equally difficult to show empirically and few examples of each can be found in the literature, especially for vector-borne zoonotic diseases. When differences in host competency are known, and interspecific transmission occurs, it would be expected that an increase in the number of incompetent host species, i.e. hosts that are unlikely to result in passage of a pathogen to a naïve vector, should decrease pathogen prevalence by essentially serving as a dead-end host for the pathogen. The effects of host

diversity and the resulting dilution effect have been well studied in the Lyme disease system (*B. burgdorferi*) (Ostfeld and Keesing 2000a, b; Schmidt and Ostfeld 2001). Ostfeld and Keesing (2000b) outline four attributes of a disease system considered necessary to test for the dilution effect: 1) The vector must be a generalist, 2) most vectors must acquire the infection from biting an infectious host, rather than becoming transovarially infected, 3) there must be differences in host competency, and 4) the most competent species must be present in both species-rich and species-poor communities.

The islands of Flathead Lake have a low diversity of small mammals (H. Haslan *personal communication*; Carson 2008), which provided a good opportunity to ask diversity-based questions about the TBRF system in the Flathead Lake region of Montana. The first goal of this research was to assess the prevalence of *B. hermsii* and provide a serological survey for antibodies in small mammals on islands and along the mainland of Flathead Lake. Attempts were made to isolate *B. hermsii* from actively infected animals and to document the presence of *O. hermsii* and the prevalence of infection with *B. hermsii* in them. Additionally, we sought to answer the following questions regarding the prevalence and diversity of TBRF at Flathead Lake: 1) Which species are actively infected with *B. hermsii* and which species possess antibodies to the spirochete? 2) Which species of rodents are more likely to be infected with the spirochete? 3) Are there differences between the species diversity and seroprevalence (number of individuals with TBRF antibodies) among island and mainland study sites? 4) Is there gender-biased transmission in this system?

## 2.3 Methods

### 2.3.1 Small mammal trapping

Small mammals were trapped on three islands on Flathead Lake and three mainland sites around Flathead Lake, Lake Co., Montana (47°54'24"N, 114°06'57"W), between May and August 2008-2010 (Figure 2-1). WHI is the largest island (~2100 acres), and like other islands on Flathead Lake, is only inhabited by a limited number of rodent species. We included 2 other islands in this study that are devoid of chipmunks and primarily inhabited by pine squirrels. Sites included Cedar Island (CED), East Yellow Bay (EYB), Melita Island (MEL), Polson/Big Arm (PBA), Wild Horse Island (WHI), and Flathead Lake Biological Station at Yellow Bay (YB). Sites were trapped a variable number of times depending on circumstances including inclement weather and accessibility throughout the study (Table 2-1). Animals were trapped with 3" x 3.5" x 9" Sherman live traps (HB Sherman Traps, Tallahassee, FL) and 6" x 6" x 24" Tomahawk wire mesh live traps (Tomahawk Live Trap Company, Tomahawk, WI). Because the primary goal of the study was to find infected or seropositive animals, pine squirrels were initially targeted because of their assumed (but not proven) role as a primary host for *B. hermsii*. Traps were set in transects with stations of one Tomahawk and two Sherman traps selectively placed to target pine squirrels. Once the presence of *B. hermsii* was confirmed, a 12 x 12 grid with 15m spacing was established at each site and one Sherman trap was placed at each grid stake. Standardized grid trapping should maximize the diversity of habitat types sampled and thus increase the likelihood of capturing a diversity of species. Tomahawk traps were set along transects targeting squirrels. Each site was trapped for four consecutive days/nights and traps were checked every four hours during daylight.

Animals were captured alive and anesthetized with Isoflurane in a vaporizer. Individuals were weighed, standard body measurements taken, identified to species (except *Microtus* and *Sorex* spp.) and gender, implanted subcutaneously with a 9mm passive integrated transponder (PIT) tag (Biomark, Inc., Boise, ID) for identification upon recapture, inspected for ectoparasites, and a blood sample was obtained. Up to 200 uL of blood was collected from pine squirrels and ground squirrels from the tail or saphenous vein; blood was collected from all other species from the retro-orbital sinus. Animals were allowed to recover in the trap before being released at the point of capture. Animals recaptured during the same week were scanned for identification but not reprocessed. Because we were not setting traps specifically to catch shrews, and shrews are difficult to keep alive for extended periods in a trap, we released live shrews without processing them and attempted to collect a blood sample only from dead shrews. Additionally, we did not attempt to identify shrews and voles to species, and they will herein be referred to as *Sorex* and *Microtus* spp. All field and laboratory procedures were approved by Rocky Mountain Laboratories Animal Care and Use Committee and the University of Montana Animal Care and Use Committee (2007-39; 2010-53; 027-08KFDBS-060608).

### **2.3.2 Sample and laboratory analyses**

Blood samples were acquired to: 1) prepare thin and thick smears for direct microscopic detection of spirochetes, allowing for the identification of currently spirochetemic animals from which to culture spirochetes, 2) perform serology targeting *B. hermsii* antibodies, and 3) to extract DNA for performing a polymerase chain reaction (PCR) to identify the presence and genetic identity of *B. hermsii*.



Thin smears were prepared in the field by placing 2.5 uL of blood on a slide, then, using another clean slide, the drop of blood was drawn back and then pushed out onto the slide to create a feathered edge. Slides were air-dried, fixed with methanol, stained using a modified Wright-Giemsa stain following manufacturer's directions (Quick III Statpak differential stain kit, Astral Diagnostics, Inc.), rinsed in de-ionized water, and allowed to air dry. Slides were examined with a light microscope (Nikon Eclipse E800) at 600x magnification and oil immersion. Fifty fields were examined on each slide for the presence of spirochetes. Thick smears were prepared by placing 3 uL of blood on the slide, covering with a 22mm x 22 mm cover slip and examining fifty fields with a dark field microscope at 400x magnification. This method allowed us to identify the presence of motile viable spirochetes. Upon detection of live spirochetes, up to 200 uL of rodent blood (non-*Peromyscus*) was inoculated into a laboratory mouse via intraperitoneal injection. Laboratory mice (RML Colony Strain, *Mus musculus*) were monitored daily for the presence of spirochete infection by examining a blood smear (<3 uL) obtained from the tail vein by nicking the tip of the tail. When an adequate level of spirochetemia was reached (10 or more spirochetes per field), we euthanized the mouse, collected blood by intracardiac puncture, and placed 500 uL of infected blood into 5 mL of BSK-H (Sigma-Aldrich<sup>®</sup>) culture medium with 12% rabbit serum.

DNA was extracted from field-collected whole-blood samples using the QIAGEN DNeasy Blood and Tissue Kit according to the manufacturer's instructions. PCR was performed using both the DNA from whole-blood samples of infected individuals as well as for cultured spirochetes from infected laboratory mice. PCR was performed using the Promega GoTaq Flexi DNA polymerase (Promega Corp, USA) and primers for *B. hermsii* genes *glpQ*, *flaB*, *gyrB* and *16S rRNA* (Porcella *et al.* 2005). The PCR conditions were as follows: initial denaturation 96°C

for 3 min, followed by 35 cycles of 94°C, 30 s, 55°C, 30 s and 72°C, 2 min 30 s followed by a final extension of 7 min at 72°C. Samples were analyzed by agarose (2%) gel electrophoresis and positive samples were submitted for Sanger sequencing for comparison to other laboratory isolates of *B. hermsii*. Base calls were visualized and ambiguous base calls were manually edited with the sequence chromatogram using Sequencher v. 5.0 (Gene Codes Corporation, Ann Arbor, MI). Sequences were aligned using the CLUSTAL W function, trimmed and concatenated using the MegAlign program (Lasergene, DNASTAR, Inc., Madison, WI). A phylogenetic tree of the four concatenated genes (*glpQ*, *flaB*, *gyrB* and *16S rRNA*; 5,197 bp) was created using MegAlign. MegAlign utilizes the Kimura distance method which results in a pair-wise genetic distance matrix used to create a neighbor-joining tree (Saitou and Nei 1987).

Western blot analysis was used to detect antibodies common to *Borrelia* spirochetes, as well as antibodies specific to relapsing fever *Borrelia* species. Western blot analysis was performed using whole-cell lysates of *B. hermsii* and a recombinant purified GlpQ protein from *B. hermsii* (Schwan *et al.* 1996). The protein preparations were electrophoresed onto Novex® 4-20% Tris-Glycine ZOOM® Gels 1.0 mm, IPG well (Invitrogen, Life Technologies, USA), and transferred to a nitrocellulose membrane using the iBlot® Gel Transfer Device according to manufacturer's directions (Invitrogen, Life Technologies, USA). Membranes were blocked in Tropix® I-BLOCK (Applied Biosystems, Life Technologies, USA) at room temperature for one hour. Serum samples (1:100) were prepared by placing 50 uL of serum collected from the whole-blood sample into 5 mL of I-BLOCK and incubated with the membrane at room temperature for one hour. Membranes were removed from the serum samples, washed with I-BLOCK, and incubated with HRP conjugated recombinant Protein A (1:4000)(Invitrogen, Life Technologies, USA). The membranes were washed in I-BLOCK for two hours, changing the

wash solution at least four times, and then developed for 30 seconds using ECL® Western Blotting Detection Reagents (GE Healthcare, UK). Positive and negative control samples were obtained from infected and uninfected laboratory mice. Positive individuals were required to show a strong and diverse antibody response to both the lysates and reactivity to the purified GlpQ.

### 2.3.3 Statistical analyses

We calculated the Shannon-Weiner diversity index ( $H'$ ) (Equation 1) and variance of  $H'$  (Equation 2) for all sites and years,

$$H' = \sum p_i (\ln p_i) \quad (1)$$

$$\text{var}(H') \approx \frac{\sum_{i=1}^S p_i (\ln p_i)^2 - \sum_{i=1}^S (p_i \ln p_i)^2}{N} - \frac{S-1}{2N^2} \quad (2)$$

where,  $p_i$  is the proportion of individuals of species  $i$ ,  $S$  is the total number of species, and  $N$  is the total number of individuals. The Shannon-Weiner diversity index accounts for both species richness and evenness of captures. Over the course of this study, field methods were continually updated and trap efforts were not consistent among sites or among years so we were unable to test for year effects and weighted all statistical analyses accordingly. To determine if some species of rodents were more likely to possess antibodies to relapsing fever spirochetes than others, we used a weighted analysis of variance (ANOVA), weighted by the number of captures for each species and included site as a fixed effects variable, the assumption of normality was confirmed using the Shapiro-Wilk test. We also used weighted ANOVA (weighted by  $\text{var}(H')$ ) to test for significant differences in species diversity among study sites. We used weighted ( $\text{var}(H')$ ) linear regression to test for a significant relationship between species diversity and

seroprevalence over sites and years. Finally, we tested for significant differences in seroprevalence between males and females of each species using z-tests to compare proportions. Because of the low number of captures at CED, we excluded it from the analysis. Also, we excluded species with < 10 captures from the gender-based analysis. The Tukey method was used for all multiple comparison testing. All statistical analyses were conducted with the statistical package R v 2.11 and GraphPad Prism v 5 and an alpha level of 0.05 was used to test for statistical significance.

#### **2.3.4 Tick collection**

In an effort to find the specific tick vector *O. hermsi*, we collected nest material and loose dirt and wood from cavity nests in trees, snags, squirrel middens and ground burrows at all study sites except PBA. Material from nests was placed in Ziploc bags and brought back to Rocky Mountain Laboratories for processing in Berlese extraction funnels. Ticks collected from nest material were allowed to feed on laboratory mice to determine if they were infected with *B. hermsii*. Laboratory mice were monitored for infection as described above for two weeks and spirochetes were cultured and isolates were obtained and analyzed as described above.

## **2.4 Results**

### **2.4.1 Small mammal and tick infection with *Borrelia hermsii***

We trapped 666 small mammals during 14,336 trap nights at 6 study sites on and around Flathead Lake, between 2008 and 2010 (Table 2-1, 2-2). Individuals infected with *B. hermsii* were found at WHI, MEL and YB. Only pine squirrels and a single deer mouse were infected with *B. hermsii* upon capture. Active *B. hermsii* infections were found in 18 pine squirrels, 9

male and 9 female, (WHI=4, MEL=7, YB=7) and 1 female deer mouse (WHI). We isolated *B. hermsii* from 12 of the 18 infected pine squirrels and identified *B. hermsii* in the six other squirrels. We collected 31 *O. hermsi* from six nests taken from YB, MEL, and WHI. We identified 13 ticks infected with *B. hermsii*, as determined by infection of laboratory mice fed on by individual ticks. Infected ticks were found at all three sites (Table 2-3) and we isolated and genetically characterized the spirochetes in nine ticks (Table 2-4).

#### **2.4.2 Host species diversity and prevalence of relapsing fever antibodies**

Overall, we trapped small mammals representing nine species of rodents, one mustelid, and at least two species of shrews (*Sorex spp.*) (Table 2-2). All study sites except CED had at least one individual that was positive via Western Blot analyses for antibodies to relapsing fever spirochetes. Seroprevalence varied with site and species present (Table 2-2). At least one or more individuals of each species trapped, except *Mustela erminea* and *Neotoma cinerea*, were seropositive for *B. hermsii* (Table 2-2, Figure 2-2). Species diversity differed significantly among study sites ( $p = 0.01$ ); MEL was significantly less diverse than all other sites except WHI and WHI was significantly less diverse than YB (Figure 2-3). Pine squirrels, one of the most frequently captured species, had the highest seroprevalence (EYB 100% (N=5), MEL 85% (N=40), YB 68% (N=74), WHI 95% (N=41)). Red-tailed chipmunks (*T. ruficaudus*) though captured less frequently, also had a high prevalence of seropositive individuals (EYB 62% (N=21), PBA 32% (19), YB 50% (N=4)). Overall, pine squirrels, chipmunks and flying squirrels (*Glaucomys sabrinus*) were more seropositive than all other species ( $p < 0.0001$ ; Figure 2-4). Deer mice, despite being the most frequently captured species at the sites where they occurred, had low numbers of seropositive individuals (EYB 11% (N=44), PBA 5% (N=43), YB 5%

(N=164), WHI 4% (N=117)). There were no differences in infection rate or seroprevalence between males and females of any host species ( $p > 0.05$ ). Finally, there was a marginally significant relationship between species diversity and the seroprevalence at a site ( $p = 0.052$ ,  $R^2 = 0.69$ ,  $n = 5$ ), where overall seroprevalence rates decreased with increased host species diversity (Figure 2-5).

### 2.4.3 Spirochete isolation and genetic characterization

We cultured and isolated *B. hermsii* from 12 of 18 infected pine squirrels and nine of 13 infected *O. hermsi* ticks. We obtained genetic sequence data for the spirochetes infecting the deer mouse. Sequence analyses of concatenated *glpQ*, *flaB*, *gyrB* and *16S rRNA* genes identified the genomic groups of infected individuals (Figure 2-6). A single squirrel (WHS90) was infected with *B. hermsii* GGI spirochetes while all other squirrels were infected with GGII *B. hermsii* spirochetes (Figure 2-6). All but three ticks transmitted spirochetes belonging to GGII, a single tick from WHI was infected with GGI (WHT8), while the remaining two ticks collected from MEL transmitted *B. hermsii* spirochetes genetically similar to those described from Thomas *et al.* (2002) and Fischer *et al.* (2009). These *B. hermsii* are distinct from both GGI and GGII types, but more genetically close to GGI leading to a new designation of genomic groups of GGI<sub>A</sub>, GGI<sub>B</sub>, and GGII (Figure 2-6). There were 116 base differences among the 27 *B. hermsii* isolates. GGI spirochetes differed from GGII spirochetes at 113 bases and GGI<sub>A</sub> spirochetes differed from GGI<sub>B</sub> spirochetes at 42 sites and there was a nine base pair deletion in GGI<sub>B</sub> spirochetes as compared with all other samples. All GGI<sub>A</sub> spirochetes were identical to each other, as were all GGI<sub>B</sub> spirochetes. GGII spirochetes form two groups, one including LAK-1 and LAK-2 and the other contained the remaining GGII spirochetes. LAK-1 and LAK-2 differed

from the other GGII spirochetes by only two base differences. There are now 27 isolates of *B. hermsii* originating from the Flathead Lake region of Montana, three GGI<sub>A</sub>, 22 GGII and two belonging to a newly identified genomic group GGI<sub>B</sub>. Overall, GGI isolates represented the minority of isolates from the Flathead Lake area. Human isolates obtained from WHI between 2002 and 2009 included two GGI isolates and four GGII isolates.

We observed pine squirrels with dual spirochete infections, i.e. infections of both genomic groups in a single individual. Dually infected individuals were identified by comparing genetic sequences of DNA obtained directly from pine squirrel blood and DNA resulting from infected laboratory mice. A pine squirrel from MEL was dually infected with GGI<sub>A</sub> spirochetes and GGII spirochetes. Two squirrels from YB (YBS60 and YBS1171) were dually infected with a GGII spirochete and a spirochete in the newly identified genomic group (GGI<sub>B</sub>) of *B. hermsii* (Fischer *et al.* 2009). The newly identified genomic group of *B. hermsii* had identical sequences to those obtained for the spirochetes from a Northern Spotted Owl (*Strix occidentalis*) (Thomas *et al.* 2002; Fischer *et al.* 2009).

## 2.5 Discussion

This research confirmed that *B. hermsii* is endemic to this region of western Montana. We documented the presence of infected pine squirrels, deer mice and infected and uninfected *O. hermsi* vectors. The presence of *B. hermsii* and *O. hermsi* on WHI prompted our research there and with the inclusion of other islands on Flathead Lake, provided an ideal opportunity to ask questions related to species diversity involved with this disease system. The islands in our study system had less diverse rodent communities compared to the mainland surrounding Flathead Lake, and WHI and MEL were devoid of chipmunks. Although voles were not known to occur

on WHI and MEL, we trapped one vole on both islands (Carson 2008). Pine squirrels inhabited CED, however we captured only one individual that was uninfected and seronegative.

This study is the first comprehensive field effort to document prevalence of *B. hermsii* and prevalence of antibodies to *B. hermsii* in small mammals in Montana. We sought to identify potential reservoir species of spirochetes by identifying actively infected individuals and quantifying the prevalence of exposed individuals, i.e. those possessing antibodies to relapsing fever spirochetes. We found evidence of exposure to *B. hermsii* in five species not previously known to be susceptible to infection with the spirochete: northern flying squirrels, deer mice, Columbian ground squirrels (*S. columbianus*), shrews (*Sorex* spp.), and jumping mice (*Zapus princeps*). Two species, pine squirrels and deer mice, had individuals with active infections of *B. hermsii* when captured. We recaptured a single squirrel at YB that was seropositive both times. Little is known about the persistence of antibodies to *B. hermsii* in any of these species, therefore it is impossible to determine when exposure occurred or if there have been repeated infections. A juvenile squirrel was seronegative when captured at MEL in June 2010 however, upon recapture in August 2010, the individual had seroconverted. The presence of antibodies to *B. hermsii* in such a diversity of small mammal species suggests that several of these species likely play a role in the maintenance of *B. hermsii* and its tick vector on the landscape.

When interspecies transmission occurs and generalist vectors are involved, species diversity of the hosts can affect the risk of infection by either amplifying or diluting it. An amplification effect may occur when interspecific transmission exceeds intraspecific transmission, or when there is a spillover event from one host to another (Begon 2008). Although theory predicts that the amplification effect should be observable in many zoonotic disease systems, little empirical evidence exists. Species richness of bird host communities



increases the human risk of Lyme disease (Ostfeld and Keesing 2000a). Another study observed an increase in abundance of a plant virus in more diverse plant host communities, but the authors suggest this was due to the overwhelming effects of a single, highly competent host species that was present in all communities (Power and Mitchell 2004). Dilution of disease risk with an increase in host species diversity has been shown for several systems including Lyme disease, West Nile virus, *Bartonella* and hantavirus (Ostfeld and Keesing 2000a,b; Keesing *et al.* 2006; Swaddle and Calos 2008; Allen *et al.* 2009; Suzán *et al.* 2009).

In the case of vector-borne diseases, the dilution effect results from an increase in dead-end transmission events to incompetent hosts. The introduction of additional host species that provide blood meals to generalist vectors but yet are unable to transmit pathogens to uninfected vector creates a new “link” in this system. This new link between infectious individuals and incompetent hosts will generate fewer new infections than if all hosts were equally competent. The Lyme disease system represents one of the better studied systems for determining the effects of increased species diversity on disease risk (Ostfeld and Keesing 2000 a, b; Schmidt and Ostfeld 2001; Keesing *et al.* 2006). Lyme disease spirochete *B. burgdorferi*, is vectored by *Ixodes scapularis* in the eastern United States, and white-footed mice (*P. leucopus*) are the primary source of infection for larval and nymphal ticks. White-footed mice are highly competent hosts for the transmission of *B. burgdorferi* to these ticks, while other small mammal species are poor or less competent hosts. Increased host species diversity results in fewer interactions between infectious mice and uninfected ticks. We wondered if host diversity would have a similar effect on the prevalence of tick-borne relapsing fever.

We observed a negative relationship between seroprevalence and species diversity, suggesting that a dilution of transmission may exist in highly diverse host communities. The

presence of antibodies in multiple species suggested that *O. hermsi* were feeding on these species, although very little is known about the competence of these species for transmission of *B. hermsii*. Differences in host species competences for their susceptibility to *B. hermsii* infection have been demonstrated (Burgdorfer and Mavros 1970). Based on their results, we expected to observe marked differences in seroprevalence among study sites however, the prevalence of antibodies may not provide the level of specificity required to test the dilution effect. The presence of antibodies in an animal does not prove that the animal was a competent host for ticks to acquire the spirochete. A dynamical system model including relapsing compartments and interactions of two host species with one vector population showed that the addition of a second, incompetent host species decreased pathogen prevalence (Chapter 3). We caught so few infected individuals compared with the number of seropositive individuals that it was not possible to use infected hosts to ask diversity-based questions. However, seroprevalence is not an adequate surrogate for infection/transmission data in the relapsing fever system.

The effects of increasing host diversity in this system may be dampened by several properties of the tick and spirochete. Argasid ticks of the genus *Ornithodoros* that transmit relapsing fever spirochetes are long-lived and acquire many blood meals throughout their lifespan, which can be > 15 years (Francis 1938). A single *O. hermsi* tick has the potential to outlive several generations of host species and cause infection in all of them. Once these ticks become infected with relapsing fever spirochetes, they can maintain the infection and transmit spirochetes for the remainder of their life (Barbour 2005). Transovarial transmission in this system, when an infected female tick passes the infection to her offspring, also decreases the potential to observe a strong dilution effect with greater host diversity.

*O. hermsi* is the reservoir for *B. hermsii*, not only because of the tick's longevity and the acquisition of multiple blood meals, but also because once infected, *O. hermsi* maintains infection (Barbour 2005). For *O. hermsi* to serve as the reservoir for *B. hermsii*, the tick must also function as a maintenance vector capable of maintaining the pathogen through transovarial and transstadial transmission in the absence of a competent host. Transstadial transmission of *B. hermsii* in *O. hermsi* is well known, however there remains uncertainty concerning the frequency of transovarial transmission in *O. hermsi* (Longanecker 1951, Burgdorfer and Varma 1967, Barbour 2005, T. Schwan *unpublished data*). If transovarial transmission does not occur or occurs infrequently in *O. hermsi*, rodents may be essential to the persistence of *B. hermsii*. Alternatively, if transovarial transmission occurs with a higher frequency, *O. hermsi* may be capable of maintaining *B. hermsii* on the landscape for extended periods of time without competent vertebrate hosts. Although rodents are not the reservoir of *B. hermsii* in North America, their role as hosts for tick survival is essential.

Numerous details of the ecology of tick-borne relapsing fever, including the role played by sylvatic rodents in the persistence and diversity of tick-borne relapsing fever spirochetes, remain unknown. Prior to the implementation of a surveillance program by the California Department of Health and the United States Forest Service beginning in 2005, efforts to document the presence of relapsing fever spirochetes in wild rodents occurred primarily in the first half of the twentieth century (Beck 1937). Beck (1937) sampled rodents at several popular recreation sites in California, including Big Bear Lake, Lake Tahoe, and Packer Lake. Her studies documented the presence of spirochetes in Douglas squirrels (*T. douglasii*) and at least two species of chipmunks (*Tamias* spp.). However, Beck also noted the presence and abundance of other species including unidentified "field mice", flying squirrels and especially golden-

mantled and California ground squirrels. Beck (1937) only identified active infections and was unable to document previous exposure (detection of antibodies) to relapsing fever spirochetes. Other animals encountered by Beck may have been uninfected because they were refractory to infection with *B. hermsii* or were spirochetemic for only short periods of time. Species other than squirrels and chipmunks caught in early studies may not have showed any positive infections because they may be refractory to infection or only remain spirochetemic for short periods of time and were not spirochetemic when examined.

Beck (1942) recognized early on the potential role of rodent hosts to the ecology of the *B. hermsii* system, stating, "...the rodent host is the determining factor in the ecology of *O. hermsii*. Biologically, these animal reservoirs are an absolute necessity to this species of tick for the existence of relapsing fever...". To further investigate the potential role of different rodent hosts, Burgdorfer and Mavros (1970) attempted to infect wild-caught rodents with *B. hermsii* by needle inoculation of infectious tick material or by allowing infected ticks to feed on the animals. Burgdorfer and Mavros (1970) were able to infect pine squirrels, yellow pine chipmunks, and meadow voles; however, deer mice, northern flying squirrels, golden mantled ground squirrels, and bushy-tailed wood rats were not susceptible to infection. Our results show a rather high rate of seroprevalence in flying squirrels and a lower but considerable prevalence of seropositive deer mice, indicating that both of these species are susceptible to infection with *B. hermsii*. The competency of these hosts and their role in the maintenance of *B. hermsii* remain unclear. Small mammals are important to maintain *B. hermsii* in the wild although the role all of these animals play in vector and pathogen persistence is unclear. Incompetent hosts may only serve as a source of blood for the tick, making them important for vector persistence but dead-end hosts for the pathogen.

Rodents may be important for the movement of spirochetes to new areas via dispersal of infected animals. In addition to rodent hosts, the potential role of airborne vertebrates in spirochete dispersal should be considered in the future. Birds and bats may be involved in the tick-borne relapsing fever system at Flathead Lake. During a previous outbreak of tick-borne relapsing fever on WHI, nest material was collected from an affected cabin and included carcasses of deer mice and robin chicks (*Turdus migratorius*), possibly implicating these species (Schwan *et al.* 2003). A pine squirrel caught at YB exhibited a dual infection with *Borrelia* spirochetes belonging to GGII and a newly identified genomic group GGI<sub>B</sub>. Genomic DNA from this squirrel revealed a 100% genetic match with spirochete genomic DNA obtained from a Spotted Owl (*Strix occidentalis*) found dead in Washington (Thomas *et al.* 2002; Fischer *et al.* 2009), providing further support for pathogen and/or vector dispersal via airborne vertebrates.

Spirochetes could also be dispersed by infected ticks being moved about by aerial hosts. *O. hermsi* has been found in the nests of a variety of wild birds and will feed on laboratory chickens and quail (*Colinus virginianus*) (Schwan *et al.* 2007). *O. hermsi* have been found in the nests of wild blue birds (*Sialia* sp.) (Gregson 1949; Longanecker 1951), house sparrows (*Passer domesticus*), California gulls (*Larus californicus*) (Furman and Loomis 1984) and American robins (*Turdus migratorius*) (Schwan *et al.* 2003). Bats (*Myotis* sp.) may also disperse *O. hermsi*. Longanecker (1951) found several *O. hermsi* occupying dead tree snags and in attics containing bats; one bat had an *O. hermsi* attached. Additional fieldwork should include non-terrestrial vertebrates as potential hosts of *B. hermsii*.

Tick-borne relapsing fever caused by infection with *B. hermsii* spirochetes has been known in North America since the early 20<sup>th</sup> century, yet there are still large gaps in the knowledge of the ecology of this system. *B. hermsii* is quite prevalent in the Flathead Lake

region of western Montana. Pine squirrels were the most frequently captured infected host, however, we documented a large range of host species with antibodies to relapsing fever. Equally striking was the diversity of spirochetes infecting these animals. Both previously known genomic groups of *B. hermsii* were found, but an additional genomic group was also documented. GGI<sub>A</sub> spirochetes were only found at WHI and MEL, the sites with the lowest host species diversity. We documented only GGII and GGI<sub>B</sub> at all other sites. However, we did not detect significant differences in seroprevalence at sites with high host species diversity, perhaps because of the presence of multiple genomic groups of *B. hermsii*. Currently, there is no way to identify *B. hermsii* genomic group based on serology, however, this may provide insight into the relationship between spirochete genetic diversity and host species diversity. Preliminary evidence suggests that GGII spirochetes are able to infect deer mice, whereas GGI *B. hermsii* are unable to reach high levels of spirochetemia, and are thus unlikely to be transmitted back to a tick (Appendix A). If the three genomic groups of *B. hermsii* are capable of causing infection in different host species, host diversity may have differing effects on the system depending on the proportions of genomic groups present. Information pertaining to the prevalence of *B. hermsii* genomic groups may provide better information concerning the effects of host diversity on spirochete persistence. Future field investigations could benefit from trapping sites for extended periods of time to elucidate the susceptibility of individual hosts to repeated infections with spirochetes in the same or different genomic groups.

Table 2-1. Trap effort at all sites including dates trapped and number of total trap nights at each study site.

<b>Study Site</b>	<b>Years Trapped</b>	<b>Number of Trap nights</b>
Wild Horse Island (WHI)	2008 – 2010	4476
Yellow Bay (YB)	2008-2010	2632
East Yellow Bay (EYB)	2009, 2010	2032
Melita Island (MEL)	2009, 2010	2032
Polson/Big Arm (PBA)	2008, 2010	1732
Cedar Island (CED)	2010	1432
<b>Total</b>		<b>14,336</b>

Table 2-2. Total animals captured and total animals with antibodies to tick-borne relapsing fever spirochetes at each study site during each year.

		Yellow Bay			Wild Horse Island			Polson/Big Arm		East Yellow Bay		Melita Island		Cedar Island	Total
		2008	2009	2010	2008	2009	2010	2008	2010	2009	2010	2009	2010	2010	
<i>Peromyscus</i>	Total	67	33	64	53	10	52	7	36	17	27	0	0	0	366
<i>maniculatus</i>	Seropositive	4	2	2	3	2	0	0	2	3	2	0	0	0	20
<i>Tamiasciurus</i>	Total	16	30	28	26	12	3	0	0	5	0	7	33	1	161
<i>hudsonicus</i>	Seropositive	12	20	18	24	12	3	0	0	5	0	7	27	0	128
<i>Microtus sp.</i>	Total	3	4	24	0	1	0	0	12	1	5	1	0	0	51
	Seropositive	2	0	1	0	0	0	0	0	0	0	0	0	0	3
<i>Tamias</i>	Total	3	1	0	0	0	0	1	18	15	6	0	0	0	44
<i>ruficaudus</i>	Seropositive	2	0	0	0	0	0	1	5	10	3	0	0	0	21
<i>Zapus</i>	Total	5	3	3	0	0	0	0	0	0	1	0	0	0	12
<i>princeps</i>	Seropositive	1	0	0	0	0	0	0	0	0	0	0	0	0	1
<i>Glaucomys</i>	Total	2	6	1	0	0	0	0	0	2	0	0	0	0	11
<i>sabrinus</i>	Seropositive	1	6	1	0	0	0	0	0	2	0	0	0	0	10
<i>Sorex sp.*</i>	Total	1	4	1	0	0	0	0	1	0	0	0	0	0	7
	Seropositive	1	0	1	0	0	0	0	0	0	0	0	0	0	2
<i>Tamias</i>	Total	2	0	0	0	0	0	2	1	0	0	0	0	0	5
<i>amoenus</i>	Seropositive	2	0	0	0	0	0	0	0	0	0	0	0	0	2
<i>Spermophilus</i>	Total	0	0	0	0	0	0	0	4	0	0	0	0	0	4
<i>columbianus</i>	Seropositive	0	0	0	0	0	0	0	2	0	0	0	0	0	2
<i>Mustela</i>	Total	0	1	2	0	0	0	0	0	0	0	0	0	0	3
<i>erminea</i>	Seropositive	0	0	0	0	0	0	0	0	0	0	0	0	0	0
<i>Neotoma</i>	Total	0	1	0	0	0	0	0	0	0	1	0	0	0	2
<i>cinerea</i>	Seropositive	0	0	0	0	0	0	0	0	0	0	0	0	0	0
Total	Total	99	83	123	79	23	55	10	72	40	40	8	33	1	666
	Seropositive	25	28	23	27	14	3	1	9	20	5	7	27	0	189

\* *Sorex sp.* found dead in trap.



Table 2-3. Location of *O. hermsi* collected at Melita Island (MEL), Wild Horse Island (WHI), and Yellow Bay (YB). Stage = life stage of tick when collected, N = nymph, M = adult male, F = adult female, and stages separated by a comma represent ticks that molted after capture and being fed in the laboratory. Y = Yes, N = No.

Location	Nest	Date Collected	Tick #	Stage	Transmitted	Isolate
YB	16A	02/09	1	M	N	
			2	N,F	N	
			3	N,M	N	
	16B	07/09	4	N,M	N	
			5	N	N	
			6	N	N	
			7	N	Y	YBT7
WHI	3	06/09	8	M	Y	WHT8
			9	N	N	
			10	N	Y	YBT10
YB	3B	11/09	11	N	N	
			12	N	Y	YBT12
			13	N	Y	YBT13
			14	N	N	
			15	N,M	N	
			16	N	N	
			17	N,F	Y	YBT17
			18	N	Y	YBT18
			19	N	N	
			20	N	Y	YBT20
			21	N,M	Y	*
MEL	LOG	5/09	22	N	N	
			23	N	N	
			24	M	Y	*
			25	F	N	
			26	F	Y	MIT26
			27	N	Y	*
			28	F	N	
			29	F	Y	*
			30	N	N	
			31	N	N	

\* Tick transmitted to laboratory mouse but spirochetes did not grow up in culture and were not isolated.

Table 2-4. All isolates of *B. hermsii* obtained in Montana from this study as well as previous human outbreaks on Wild Horse Island, Lake Co., Montana. Isolate = name of isolate, source = source of infection from which the isolate was cultured, year = year of isolation, GG - genomic group, CoInf = coinfection with > 1 GG.

Location	Isolate	GG	Source	Year	CoInf
WHI	LAK1*	II	Human	2002	
WHI	LAK2*	II	Human	2002	
WHI	LAK3*	II	Human	2004	
WHI	LAK4*	I <sub>A</sub>	Human	2004	
WHI	LAK5*	II	Human	2004	
WHI	LAK6	I <sub>A</sub>	Human	2009	
WHI	WHS40	II	<i>T. hudsonicus</i>	2008	
WHI	WHS81	II	<i>T. hudsonicus</i>	2008	
WHI	WHS88	II	<i>T. hudsonicus</i>	2008	
WHI	WHS90	I <sub>A</sub>	<i>T. hudsonicus</i>	2008	
YB	YBS60	II	<i>T. hudsonicus</i>	2008	I <sub>B</sub>
YB	YBS70	II	<i>T. hudsonicus</i>	2008	
YB	YBS266	II	<i>T. hudsonicus</i>	2009	
WHI	DM31**	II	<i>P. maniculatus</i>	2008	
YB	YBT7	I <sub>B</sub>	<i>O. hermsi</i>	2010	
YB	YBT10	II	<i>O. hermsi</i>	2010	
YB	YBT12	I <sub>B</sub>	<i>O. hermsi</i>	2010	
YB	YBT13	II	<i>O. hermsi</i>	2010	
YB	YBT17	II	<i>O. hermsi</i>	2010	
YB	YBT18	II	<i>O. hermsi</i>	2010	
YB	YBT20	II	<i>O. hermsi</i>	2010	
MEL	MIS1014	II	<i>T. hudsonicus</i>	2010	
MEL	MIS491	II	<i>T. hudsonicus</i>	2010	I <sub>A</sub>
MEL	YBS479	II	<i>T. hudsonicus</i>	2010	
YB	YBS1143	II	<i>T. hudsonicus</i>	2010	
YB	YBS1171	II	<i>T. hudsonicus</i>	2010	I <sub>B</sub>
MEL	MIT26	II	<i>O. hermsi</i>	2010	
WHI	WHT8	I <sub>A</sub>	<i>O. hermsi</i>	2010	

\* Described in, Porcella *et al.* 2005; Schwan *et al.* 2007.

\*\* No isolate of DM-31 was made but several genes were sequenced.

Figure 2-1. Map of study area of Flathead Lake, Lake Co., Montana (inset). Study sites include Cedar Island (CED), East Yellow Bay (EYB), Melita Island (MEL), Polson/Big Arm (PBA), Wild Horse Island (WHI), and Flathead Lake Biological Station at Yellow Bay (YB).

Figure 2-2. Western blots targeting *Borrelia*-specific antibodies (whole-cell lysate in the left lane and recombinant GlpQ in the right lane) in the serum of field-caught rodents showing positive (+) and negative (-) examples for four species, *Tamiasciurus hudsonicus*, *Tamias ruficaudus*, *Peromyscus maniculatus*, and *Glaucomys sabrinus*. Molecular mass standards are shown on the left in kilodaltons

Figure 2-3. Analysis of Variance (ANOVA) of differences in species diversity among study sites. MEL is the least diverse site, while YB is the most diverse site ( $p = 0.01$ ). MEL was significantly less diverse than all sites except WHI, and WHI was significantly less diverse than YB. Bars indicate means of observations.

Figure 2-4. Analysis of Variance (ANOVA) of differences in seroprevalence among host species. *Tamiasciurus hudsonicus*, *Glaucomys sabrinus*, and *Tamias* spp. were significantly more seropositive for relapsing fever spirochetes than all other species ( $p < 0.0001$ ). *Tamiasciurus hudsonicus* and *Glaucomys sabrinus* were equally seropositive, while chipmunks were less seropositive than *Tamiasciurus hudsonicus* and *Glaucomys sabrinus* but more seropositive than the three other species. *Peromyscus maniculatus*, *Zapus princeps*, and *Microtus* spp. did not differ from each other and were significantly less seropositive than the other species.

Figure 2-5. Linear regression of seroprevalence and Shannon species diversity. There was a marginally significant trend between increasing species diversity and decreasing

seroprevalence rates ( $p = 0.052$ ;  $R^2 = 0.69$ ). The dashed line represents the 95% confidence interval around the regression line.

Figure 2-6. Phylogenetic tree based on the concatenated DNA sequence of 4 genes (*glpQ*, *gyrB*, *flaB*, and *16S rRNA*; 5,197 bp) illustrating the genetic relationships among 27 *Borrelia hermsii* isolates obtained from humans, *Tamiasciurus hudsonicus*, and *Ornithodoros hermsi* ticks, and a sequences from single *Peromyscus maniculatus* near Flathead Lake, Lake Co., MT. Sequences were aligned using CLUSTAL W and the tree was constructed using the neighbor joining algorithm (Saitou and Nei 1987). Genomic group (GG) designations are shown on the right.

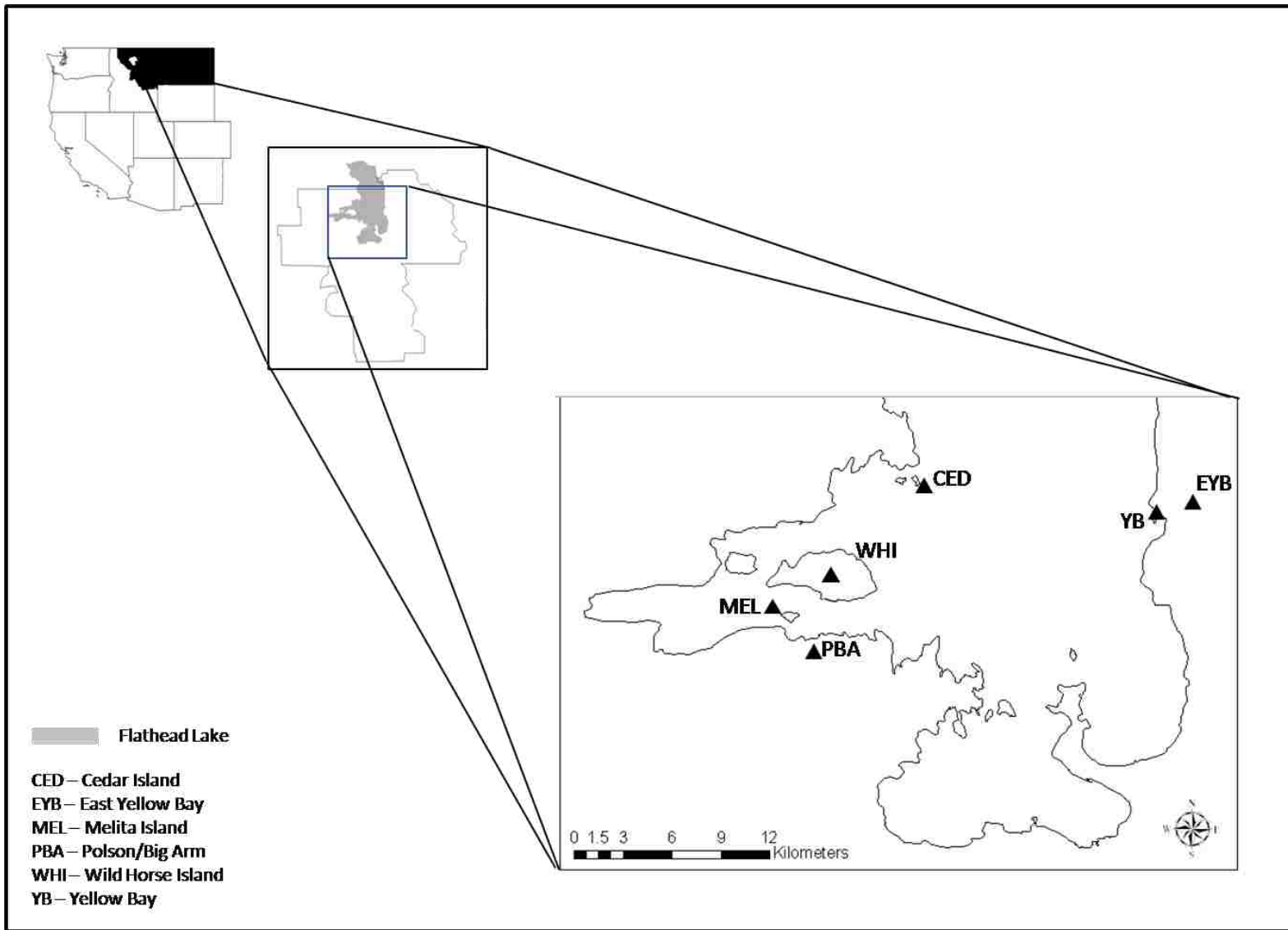


Figure 2-1.

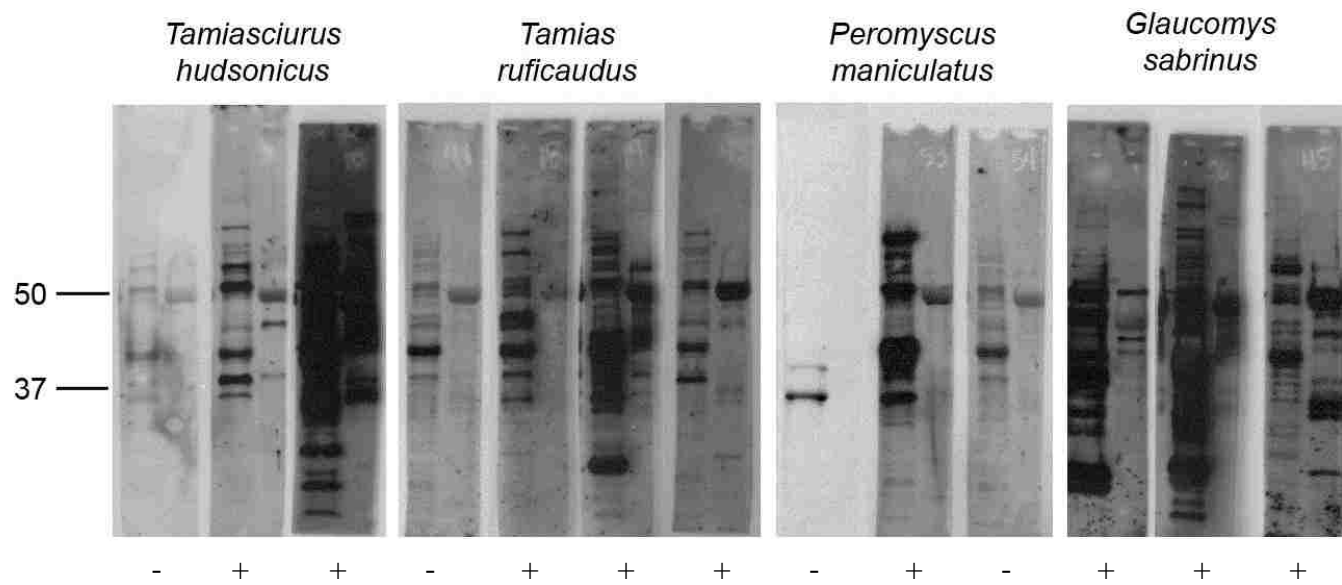


Figure 2-2.

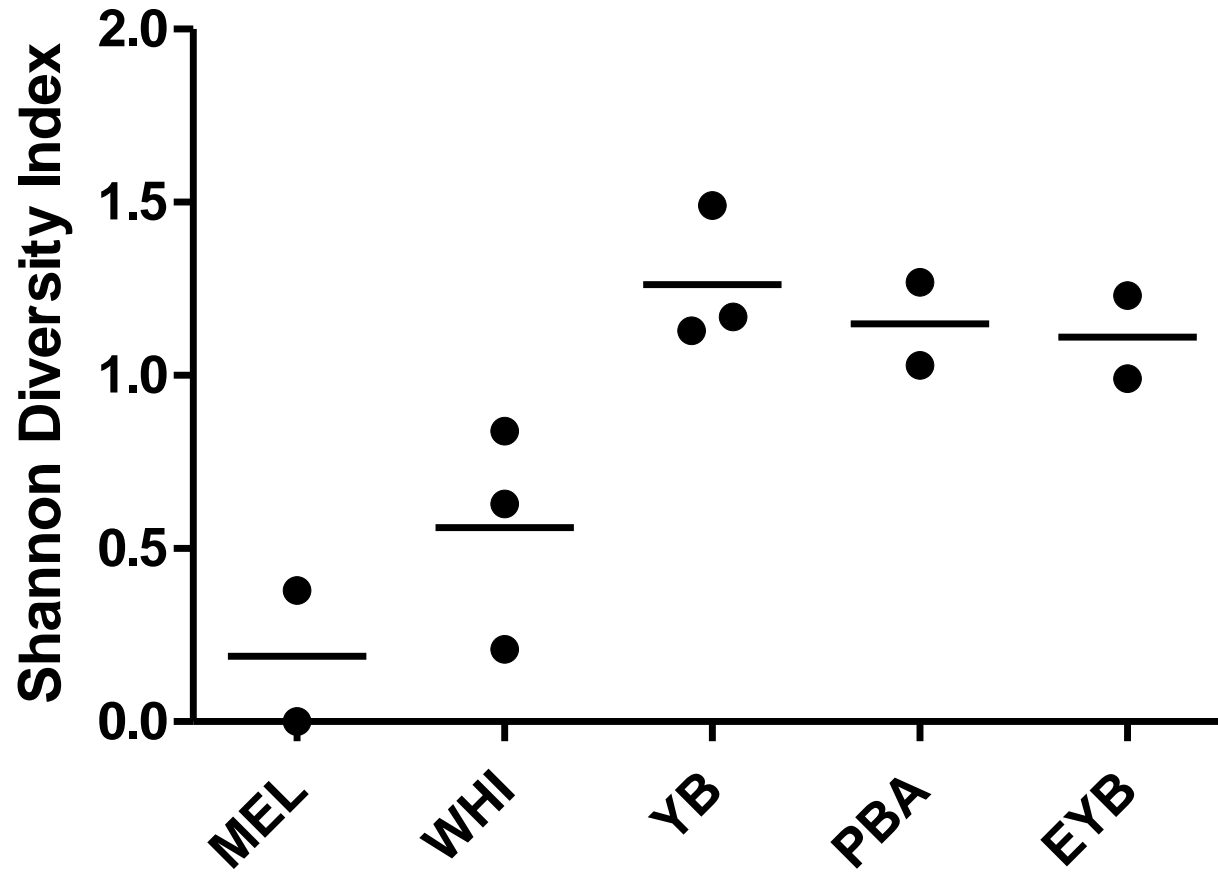


Figure 2-3.

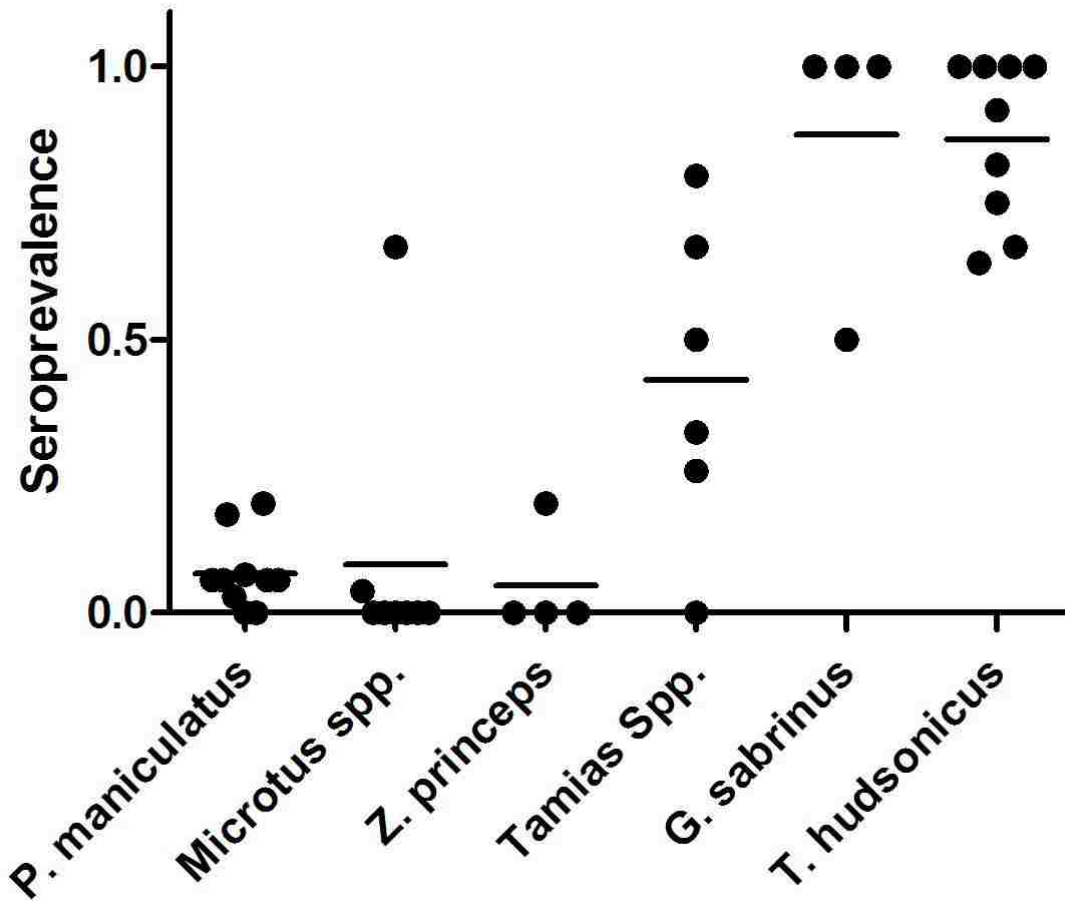


Figure 2-4.



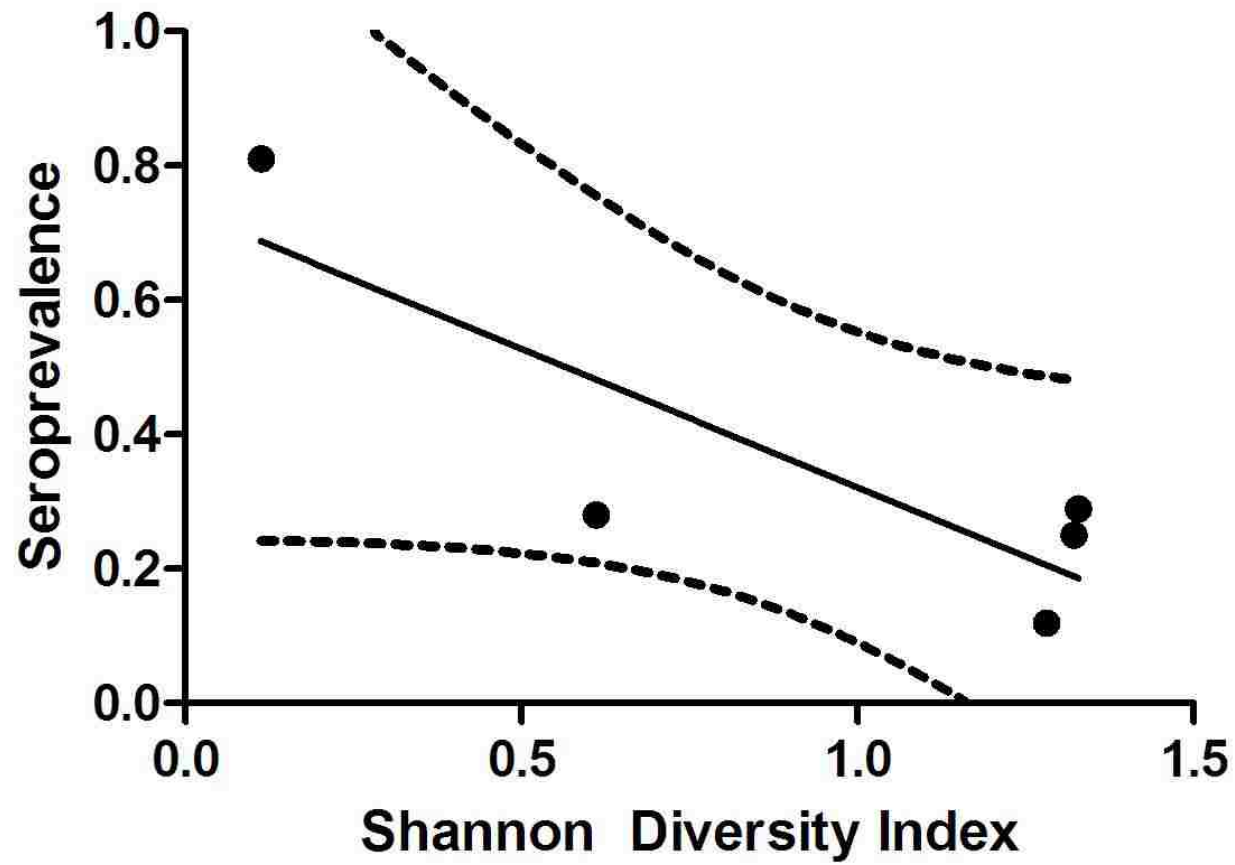


Figure 2-5.

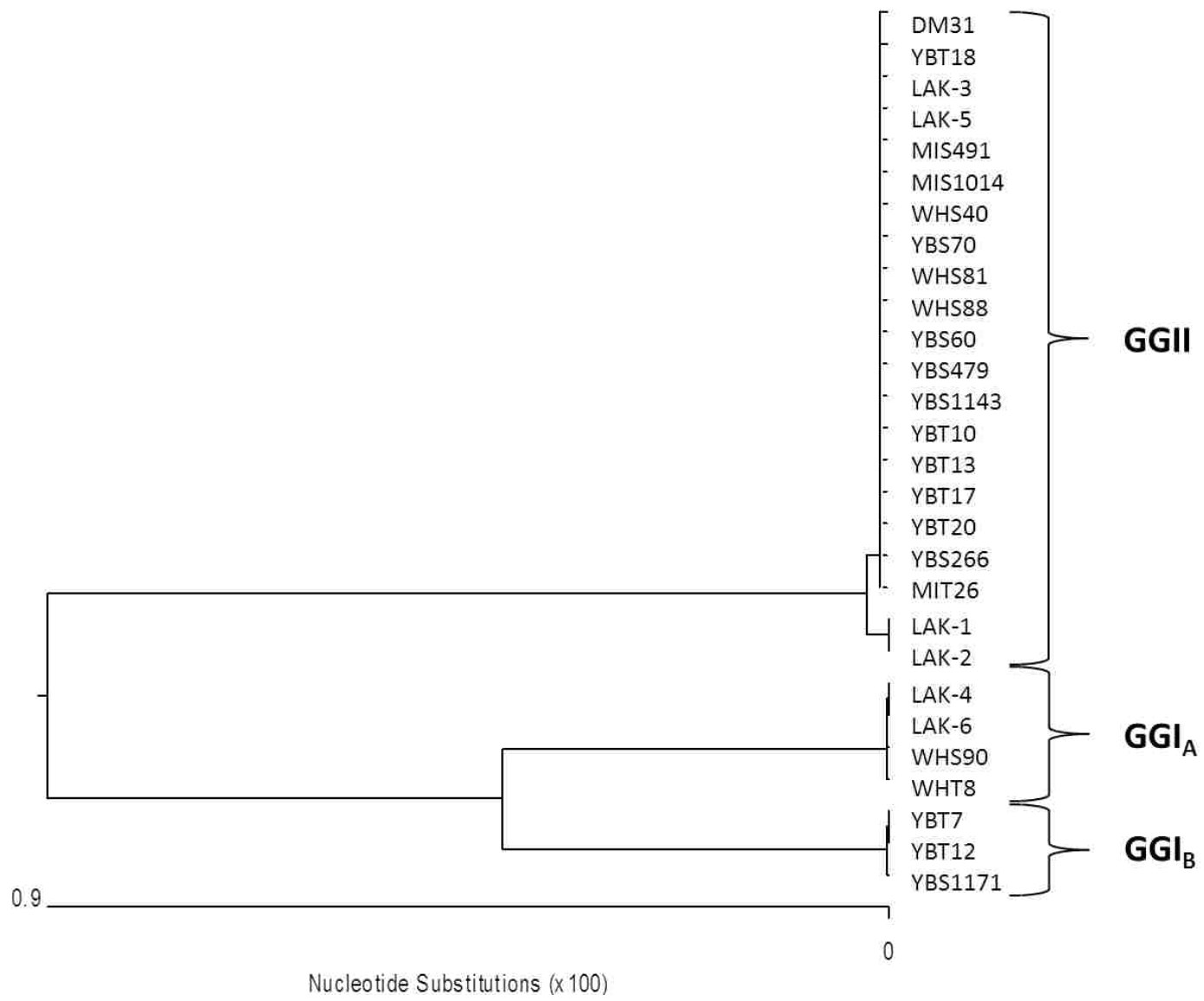


Figure 2-6.

## Chapter 3 – Modeling Relapsing Disease Dynamics in a Host-vector

### Community

\*This is a collaborative chapter with MEID Fellow Erin Landguth who did the mathematical modeling involved in this chapter.

#### 3.1 Abstract

Vector-borne diseases represent a threat to human and wildlife populations and mathematical models provide a means to understand and control epidemics involved in complex host-vector systems. The disease model studied here is a host-vector system with a relapsing class of host individuals, used to investigate tick-borne relapsing fever (TBRF). Equilibrium analysis is performed for models with increasing numbers of relapses and multiple hosts and the disease reproduction number,  $R_0$ , is generalized to establish parameter thresholds that would result in the elimination of the disease. Specific literature and field research investigating TBRF on Wild Horse Island, Lake Co., MT, is presented, showing that four relapses in a single host-vector system is needed to maintain endemic states on the island. In addition, we show that the addition of an incompetent second host system with no relapses increases the number of relapses to seven in the first host system needed for maintaining the pathogen. The coupled two host-vector system produces some interesting dynamics, which may be very important to understanding pathogen persistence in diverse host communities. Coupling of the system with hosts of differing competencies will always reduce  $R_0$ , making it more difficult for the system to reach an endemic state. This study advances the understanding of a complex disease system and provides specific predictions about TBRF.

## 3.2 Introduction

Globally, the emergence or reemergence of infectious diseases poses a very real threat to human, domestic animal and wildlife populations (Daszak *et al.* 2000). Sixty percent of emerging infectious diseases are zoonotic (i.e., can be transmitted from animals to humans) and of these, >71% originate in wild animals (Jones *et al.* 2008). Understanding the biotic and abiotic interactions and identifying mechanisms that may contribute to disease emergence, establishment and persistence is necessary to assessing current and future disease risk, as well as developing effective control strategies (Anderson and May 1991). An important development in the study of infectious diseases is the application of mathematical models to understand the interplay between various factors that determine epidemiological processes. Many systems show a rich variety of dynamics that arise from nonlinear interactions (due to the mixing of different infectious populations) or temporal forcing (caused by changes in the average contact rate) (Keeling *et al.* 2001). Vector-borne diseases are additionally complex with interactions between multiple host and vector species (Ostfeld and Keesing 2000 a, b; Dobson *et al.* 2006).

Compartmental models, such as the SIR models with susceptible, infectious, and removed compartments (Kermack and McKendrick 1927), have been applied to many disease systems in an effort to examine system dynamics. In these epidemic models, susceptible individuals pass into the infective class, from which they transition to the removed class. For some diseases, recovered individuals may relapse with a reactivation of infection and revert back to an infective class. An example of such a system is found in van den Driessche *et al.* (2007), which includes a relapsing rate between the susceptible and the same infected compartment. An advantage of these types of models is the ability to vary parameters while monitoring the overall effect on the disease system. These types of models allow researchers to explore aspects of the

system that may not be well understood. Adding additional infected compartments simulates disease systems in which there is a relapsing component, leading to a prolonged infectious period, presumed to be important to disease persistence. To our knowledge, the addition of a relapsing component has not been applied to a host-vector system. Noteworthy vector-borne relapsing diseases include tick-borne relapsing fever and malaria. Here, we model a vector-borne disease system, tick-borne relapsing fever (TBRF) caused by infection with *Borrelia hermsii* and vectored by *Ornithodoros hermsi*, which occurs throughout higher elevations of the western United States.

### 3.2.1 Study System

Tick-borne relapsing fever is a vector-borne zoonotic disease endemic to central Asia, Africa, and the Americas (Davis 1940). TBRF is caused by infection with *Borrelia* spirochetes and all but one species of relapsing fever spirochetes are vectored by soft ticks (*Ornithodoros* spp.) (Felsenfeld 1971). Louse-borne relapsing fever is transmitted by the human body louse *Pediculus humanus*. Relapsing fever is characterized by recurring febrile episodes and generalized symptoms including headache, chills, myalgia, nausea, and vomiting (Dworkin *et al.* 2002). There is a rapid onset of disease symptoms, with a febrile episode lasting 3-6 days, after which symptoms subside, only to return in 7-10 days. Symptoms are associated with large numbers of spirochetes present in the bloodstream (spirochetemia). Symptoms subside when the host mounts an immune response, producing antibodies to outer surface proteins of the *Borrelia*, thus eliminating bacteria with specific surface proteins. However, through a process known as antigenic variation, the spirochetes are able to switch a series of antigenic outer surface proteins, resulting in relapse of the spirochetes in the blood stream, and another febrile episode (Barbour

1990; Dai *et al.* 2006). *Borreliae* producing new outer membrane proteins can avoid destruction by antibodies directed against the original outer surface protein. Eventually, the host immune system targets the new surface protein being produced and eliminates this “version” from the bloodstream. There are > 60 outer surface proteins that can be varied in *B. hermsii* (Barbour *et al.* 2000; Dai *et al.* 2006). Laboratory experiments on RML colony strain Swiss Webster mice (*Mus musculus*) always show at least three relapses (*unpublished data*). In humans, there is an average relapse rate of three febrile episodes without treatment, but up to 13 relapses have been observed (Trevejo *et al.* 1998).

There is a species-specific relationship between relapsing fever spirochetes and their tick vector; each species of *Ornithodoros* tick is capable of transmitting only a single species of relapsing fever spirochete. In North America, three species of *Ornithodoros* ticks *O. hermsi*, *O. turicata*, and *O. parkeri* serve as vectors to three distinct species of *Borrelia* spirochetes that take the name of the tick vector, i.e. *B. hermsii*, *B. turicatae*, and *B. parkeri*. This research focuses on TBRF caused by *B. hermsii* and vectored by *O. hermsi*. *O. hermsi* is a long-lived, fast feeding vector. *Ornithodoros* ticks are known to live > 10 years, and have been shown to survive for up to five years without feeding (Francis 1938). *O. hermsi* are nest dwelling ticks that rarely leave the confines of the host nest or burrow and are able to obtain a blood meal and detach from the host in < 90 min. Additionally, soft ticks only obtain a blood meal about once every 3 months; even when presented with the opportunity to feed daily. *O. hermsi* ticks require several months between feedings and can survive years between feeding. The longevity of these ticks means that they outlive their rodent hosts, affording the potential to infect several cohorts of rodents over the course of the tick lifespan. Once infected with *B. hermsii*, *O. hermsi* remain infected and infectious for the duration of their lifespan.

Tick-borne relapsing fever has been considered endemic in western North America since the 1930s. The first recognized report of tick-borne relapsing fever in western North America occurred in 1915 in Colorado (Meader 1915); endemicity to Colorado was established in 1939 with the discovery of the tick vector *O. hermsi* (Davis 1939). In California, human cases of tick-borne relapsing fever were reported as early as 1921 in the Sierra Nevada range and again in the early 1930s (Porter *et al.* 1932). The cases in the 1930s occurred at three locations, Lake Tahoe, Packer Lake, and Big Bear Lake. Additional disease foci of ticks, spirochetes and hosts exist in high coniferous forests throughout the western United States (Moursund 1942). Despite a long history of causing human infection, the underlying ecological interactions maintaining the TBRF pathogen are understudied.

Early site investigations of human exposures in California identified spirochete infections in squirrels (*Tamiasciurus douglasii*) and chipmunks (*Tamias* spp.) (Porter *et al.* 1932; Beck 1937). Burgdorfer and Mavros (1970) infected wild-caught rodents from Montana with *B. hermsii* and showed that different host species had different competencies for infection with *B. hermsii*. Three species showed observable spirochetemia; pine squirrels (*Tamiasciurus hudsonicus*) reached the highest spirochete levels, underwent the most relapses, and remained infected for the longest amount of time. Chipmunks (*Tamias amoenus*) and meadow voles (*Microtus pennsylvanicus*) were less susceptible yet still became spirochetemic and maintained infection through > 1 relapse. Several rodent species did not become infected with detectible levels of spirochetes, including deer mice (*Peromyscus maniculatus*), northern flying squirrels (*Glaucomys sabrinus*), Columbian ground squirrels (*Spermophilus columbianus*), and wood rats (*Neotoma cinerea*).

Aside from identifying infected wild animals, the technology now exists to allow for the identification of individuals that have been exposed to *B. hermsii*, by identifying the presence of antibodies to relapsing fever spirochetes in the blood of rodents. Field investigations of rodents on and around Flathead Lake, Lake Co., MT, revealed that at least 8 species of rodents and 2 species of shrew (*Sorex* sp.) had antibodies to relapsing fever spirochetes, indicating tick bite and exposure to TBRF spirochetes (Chapter 2). Many of these species were those that were challenged by Burgdorfer and Mavros (1970) and unsuccessfully infected with *B. hermsii*. The presence of antibodies in these species indicates that despite being incompetent hosts for *B. hermsii* they may be important to tick survival. Field studies at Flathead Lake showed a vast difference in host species diversity between mainland and island study sites, yet two islands and one mainland site had spirochetemic individuals and all sites harbored seropositive individuals. We sought to develop a model based on disease dynamics on Wild Horse Island (WHI), the largest island on Flathead Lake.

The first documented human cases of TBRF in Montana occurred in 2002 on WHI, however, a retrospective study likely identified an individual from the Big Arm area near Flathead Lake, who was infected in 1984 (Dworkin *et al.* 2002). Human outbreaks occurred again in 2004 and 2009 on WHI (Schwan *et al.* 2003, 2007; Schwan *unpublished data*). These outbreaks lead to the isolation of *B. hermsii* and collection of *O. hermsi*, the first documentation of the tick vector and pathogen in Montana. WHI is the largest island (~2100 acres) on Flathead Lake and like other islands on the lake has a limited diversity of rodent host species. WHI is almost exclusively inhabited by deer mice (*Peromyscus maniculatus*) and pine squirrels (*Tamiasciurus hudsonicus*) as the terrestrial rodents and provided an important opportunity to



develop and parameterize a model including only two hosts and to compare results with field observations.

### 3.2.2 Dynamical systems model introduction

Careful consideration of the formulation of every biological model must be made, as these assumptions drive the mathematical structure and thus the outcome predictions. A key assumption for host-vector disease modeling is the definition of the transmission term, which represents the contact between hosts and vectors. The formulation of the transmission term affects the reproduction number,  $R_0$ , which is a central prediction of disease systems (Wonham *et al.* 2006). For host-vector disease models, the transmission term includes the vector biting rate. This rate controls the pathogen transmission both from the vector-to-host and from the host-to-vector. The TBRF model follows frequency-dependent transmission assumptions through the biting rate, since a blood meal is only required approximately once every three months regardless of the host population density. Following this framework, hosts would likely experience an increasing number of bites as the vector population increased.

Given a mathematical model for disease spread,  $R_0$  is an essential summary parameter. It is defined as the average number of secondary infections produced when one infected individual is introduced into a completely susceptible host population (Dietz 1975). When  $R_0 < 1$ , the disease free equilibrium (DFE) at which the population remains in the absence of disease is locally asymptotically stable. However, if  $R_0 > 1$ , then the DFE is unstable and invasion is always possible (see Hethcote 2000) and a new endemic equilibrium (EE) exists. For this study,  $R_0$  was extracted following the methodology developed in van den Driessche *et al.* 2002 (see also Diekmann *et al.* 1990; Roberts *et al.* 2003) for general compartmental disease models, which can

be extended to more complicated host-vector disease systems (Wonham *et al.* 2004; Lewis *et al.* 2006).

The overall goal of this study was to develop a mathematical model using TBRF dynamics to describe a host-vector system with a relapsing class of host individuals. First, using specific information about WHI, a model for the dynamics of a single host-vector interaction was developed. For models with increasing numbers of relapses and multiple hosts, equilibrium analysis was performed and  $R_0$  was generalized. Parameter values were considered in the model to provide theoretical criteria for population stability and to determine the parameter thresholds that would result in elimination of the disease. Finally, single and coupled host-vector systems were explored, focusing on the addition of less competent hosts and the number of relapses needed in order to maintain an endemic equilibrium. We use the model to ask several important biological questions pertaining to the TBRF system including: 1) what effect does adding relapsing classes have on pathogen persistence, 2) what is the effect of multiple host species with varying competency for acquiring and transmitting *B. hermsii*, and 3) how do tick life-history characteristics affect *B. hermsii* persistence?

### **3.3 Methods**

#### **3.3.1 Parameter estimates**

Specific parameter values for this system have not yet been determined, but can be estimated from similar studies and from data collected on *O. hermsi* from laboratory experiments. The units of the rates are individuals per month. Table 3-1 summarizes the notation for all system parameters and variables. See Table 3-2 for specific model values used in all of

the host-vector models. Note that parameters denoted with additional subscripts of  $ps$  and  $dm$  refers to values specific to the pine squirrel and deer mouse host-vector systems, respectively.

The birth rates for host and vector are each set to a constant value ( $\beta$  and  $\beta_v$ , respectively) and the compartmental death rates (for host and vector) are identical and set equal to birth rate.

Then the death rates must be

$$\mu_s = \mu_{i1} = \dots = \mu_{ij} = \mu_r = \frac{\beta}{j+2} \quad (1)$$

and

$$\mu_{sv} = \mu_{iv} = \frac{\beta_v}{2}. \quad (2)$$

The growth rate of pine squirrels ( $\beta_{rs} = 0.33$  individuals per month) is an average of the rates found in the literature, i.e., four individuals per litter at 1 litter per year (Steel 1998). The growth rate of deer mice is also taken from average estimates from the literature; we estimate growth rate based on an average of three litters per year and four young per litter, ( $\beta_{dm} = 1$  individual per month) (Sullivan 1995). The death rates are determined from equation (1), which depends on the number of relapses in the system. For example, for a pine squirrel host-vector system with one relapse, all death rates would be 0.0825. Life history dynamics of *O. hermsi* are not well documented and virtually nothing is known about the reproductive behavior and survival of these ticks in nature. Conservative estimates from the laboratory show that soft-bodied ticks lay an average five clutches over their approximately 10 year lifespan with roughly 50 eggs per clutch (Herms 1956; T. Schwan *unpublished data*). Thus, the vector birth rate is  $\beta_v = 2.08$  individuals per month. Following equation (2), we get death rates of  $\mu_{sv} = \mu_{iv} = 1.04$  for the vector compartments.

The rate at which an individual transitions among infected compartments and to the removed compartment is fixed and is assumed to be the same for all compartments. As more

infected compartments are added to the system, the corresponding constant rates are  $\gamma = \alpha = \alpha_1 = \dots = \alpha_{j-1}$ , for  $j$  infected compartments. Field parameter estimates have not yet been made for these transition rates (i.e., relapse and recovery rates). Laboratory results from three pine squirrels indicate a transition rate of approximately 4.35 individuals per month for a single compartment (Burgdorfer and Mavros 1970). Then  $\gamma = \alpha = \alpha_1 = \dots = \alpha_{j-1} = 4.35$ .

Ticks are assumed to bite a host once every three months (i.e.,  $f = 0.33$ ). Competency values are between 0 and 1 and thus modify the transmission rate of the infection by multiplying the biting rate. Burgdorfer and Mavros (1970) observed a high competency in pine squirrels, successfully transmitting *B. hermsii* to pine squirrels by either allowing infected ticks to feed on individual squirrels or by crushing up and injecting infected ticks directly into the squirrel. They successfully infected 3/3 squirrels. Using the same methods, they challenged deer mice with *B. hermsii* and were unsuccessful in establishing infection. Thus, we used competency values  $c_v = 0.95$  for the probability of transmission for vectors,  $c_{ps} = 0.90$  for pine squirrels, and  $c_{dm} = 0.10$  for deer mice.

The carrying capacity for the pine squirrel and deer mouse system is determined specifically for WHI. On WHI there are approximately 425 ha of suitable habitat for pine squirrels with up to a maximum of 2 individuals per suitable habitat patch and approximately 850 ha of suitable deer mouse habitat with a conservative estimate of just less than 12 mice per ha (Sullivan 1995). Thus, the total number of pine squirrels ( $N_{ps}$ ) is estimated at 850 and total number of deer mice ( $N_{dm}$ ) is estimated at 10,000. The soft bodied tick population ( $N_v$ ) is virtually unknown, however, we assume that they are limited to the nests of their hosts. Initial field collections have found as many as 14 ticks in one nest on the island; other collection efforts show > 300 ticks can be collected from a single nest or snag (Davis 1941). Because the

estimates of ticks per nest vary largely between our limited collection on WHI and the literature we chose a conservative number of ticks. We estimate that each squirrel has less than 1 nest (because of juveniles in the system), and each nest is inhabited by 14 ticks. We found no ticks in nest material collected from deer mice, however, nest material collected during the human outbreak in 2002 yielded 14 *O. hermsi*; the carcasses of two deer mice were found nearby and American Robins (*Turdus migratorius*) had been nesting there (Schwan *et al.* 2003). Thus it is nearly impossible to estimate the average number of ticks in a deer mouse nest, or if in fact they are coming in contact with ticks while visiting other nests. We used an estimate of 20,000 total ticks on the island split equally among host systems. We chose a conservative estimate of 1% of all ticks are infected. Thus, we used  $S_v(0) = 9,900$  ticks for the single host-vector system and  $S_v(0) = 19,800$  ticks for the coupled host-vector system.

### **3.4 Single Host-vector System**

#### **3.4.1 Model description**

A model for the dynamics of TBRF in a single host-vector system is considered (see Figure 3-1a). The following assumptions are used to establish a model that is appropriate for the WHI TBRF system for the host pine squirrel and soft tick vector, *O. hermsi*. 1) The only sources of infection occur between the bite of an infective vector and susceptible host and between a bite of a susceptible vector and infective host (i.e. there are no horizontal or vertical transmissions). 2) The vector becomes infected and infectious for life immediately upon biting an infectious host. 3) The transmission terms are frequency-dependent through the biting rate,  $f$ . 4) The hosts relapse to different infected compartments (i.e. different serotypes within the hosts caused by antigenic variation) at rate  $\alpha$  and recover from the disease at rate  $\gamma$ . 5) Though mortality rates are

noted to differ for each compartment, we assume a constant total population for both hosts and vectors ( $N$  and  $N_v$ , respectively). Thus, recruitment (or birth) and the sum of the removal (or death) rates from each compartment must be equal (Equations 1-2).

The generalized system for the infection dynamics in a single host-vector system with  $j - 1$  relapsing rates for  $j = 1$  infected compartments describes the number of susceptible hosts  $S(t)$ , infectious hosts  $I_k(t)$ , removed hosts  $R(t)$ , susceptible vectors  $S_v(t)$ , and infected vectors  $I_v(t)$ , where the total host population is  $N = S + \sum_{k=1}^j I_k + R$  and the total vector population is  $N_v = S_v + I_v$  (see Figure 1a for a compartmental diagram and Table 1 for parameter definitions). The equations are

Host equations (3):

$$\begin{aligned}\dot{S} &= \beta S - fc_v I_v \frac{S}{N} - \mu_s S \\ \dot{I}_1 &= fc_v I_v \frac{S}{N} - \alpha_1 I_1 - \mu_{i1} I_1 \\ \dot{I}_2 &= \alpha_1 I_1 - \alpha_2 I_2 - \mu_{i2} I_2 \\ &\vdots \\ \dot{I}_{j-1} &= \alpha_{j-2} I_{j-2} - \alpha_{j-1} I_{j-1} - \mu_{i(j-1)} I_{j-1} \\ \dot{I}_j &= \alpha_{j-1} I_{j-1} - \gamma_j I_j - \mu_{ij} I_j \\ \dot{R}_j &= \gamma_j I_j - \mu_r R.\end{aligned}$$

Vector equations (4):

$$\begin{aligned}\dot{S}_v &= \beta_v S_v - \frac{fc S_v}{N} \sum_{i=1}^j I_i - \mu_{sv} S_v \\ \dot{I}_v &= \frac{fc S_v}{N} \sum_{i=1}^j I_i - \mu_{iv} I_v.\end{aligned}$$

### 3.4.2 Equilibrium analysis

In the absence of disease, the system steady state is  $(S^*, I_1^*, \dots, I_j^*, R^*, S_v^*, I_v^*) = (S(0), 0, \dots, 0, S_v(0), 0)$  for  $j$  infected compartments, where now the total populations become  $N = S(0)$  and  $N_v = S_v(0)$ . This steady state is defined to be the disease free equilibrium (DFE). An equilibrium stability analysis is performed on the DFE by the extraction of  $R_0$ . A single host-vector model with no relapses ( $j = 1$ ) is first analyzed. The variables in this model are the number of susceptible hosts  $S(t)$ , infectious hosts  $I_1(t)$ , removed hosts  $R(t)$ , susceptible vectors  $S_v(t)$ , and infected vectors  $I_v(t)$ . The total host population is  $N = S + I_1 + R$ , and the total vector population is  $N_v = S_v + I_v$ . The mathematics is simplified by considering an equivalent non-dimensional system. First a new time scale is defined,  $\tau = \gamma t$ , and the equations are scaled by the initial host population,  $N(0)$ . The resulting rescaled host variables,  $s$ ,  $i_1$ , and  $r$ , indicate the fraction of the initial population in the susceptible, infectious, and recovered classes, and the total non-dimensional host population becomes  $n = s + i_1 + r$ . The vector compartments,  $s_v$  and  $i_v$ , represent susceptible and infectious vectors, respectively, normalized by  $N(0)$ . The total vector population thus becomes  $n_v = s_v + i_v$ . The resulting dimensionless system is

Host equations (5):

$$\begin{aligned}\frac{ds}{d\tau} &= an - ki_v \frac{s}{n} - b_s s \\ \frac{di_1}{d\tau} &= ki_v \frac{s}{n} i_1 - i_1 - b_{i1} i_1 \\ \frac{dr}{d\tau} &= i_1 - b_r r.\end{aligned}$$

Vector equations (6):

$$\frac{ds_v}{d\tau} = a_v s_v - l s_v \frac{i_1}{n} - b_{sv} s_v$$

$$\frac{di_v}{d\tau} = l s_v \frac{i_1}{n} - b_{iv} i_v.$$

where parameters are as shown in Table 1.

To evaluate the invasiveness of the disease in this system, we extract  $R_0$  following the techniques developed by van den Driessche and Watmough (2002). The size of the system is first reduced by considering only  $i_1$  and  $i_v$ , and the rate of appearance of new infections and the rate of transfer between compartments for all other processes respectively,

$$\frac{d}{d\tau} \begin{bmatrix} i_1 \\ i_v \end{bmatrix} = w - v = \begin{bmatrix} k i_v \frac{s}{n} \\ l s_v \frac{i_1}{n} \end{bmatrix} - \begin{bmatrix} i_1 + b_{i1} i_1 \\ b_{iv} i_v \end{bmatrix}. \quad (7)$$

The Jacobians of the vector fields  $w$  and  $v$  evaluated at the DFE describe the linearization about the DFE in terms of new infection occurrences and are

$$W \left( 1, 0, 0, \frac{S_v(0)}{N(0)}, 0 \right) = \begin{bmatrix} 0 & k \\ l \frac{S_v(0)}{N(0)} & 0 \end{bmatrix} \text{ and } V \left( 1, 0, 0, \frac{S_v(0)}{N(0)}, 0 \right) = \begin{bmatrix} 1 + b_{i1} & 0 \\ 0 & b_{iv} \end{bmatrix}. \quad (8)$$

The basic reproductive number,  $R_0$ , is given by the dominant eigenvalue of  $WV^{-1}$  (see Theorem 2 from van den Driessche and Watmough 2002), which is written in terms of the original variables and parameters as

$$R_0 = f \sqrt{\frac{cc_v S_v(0)}{\mu_{iv} N(0)} \left[ \frac{1}{\gamma + \mu_{i1}} \right]}. \quad (9)$$

For the system with one relapse ( $j = 2$  infected compartments), the host compartments,  $s$ ,  $i_1$ ,  $i_2$ , and  $r$ , indicate the fractions of the initial population in the susceptible, infectious, and recovered classes, so that the total rescaled host population is  $n = s + i_1 + i_2 + r$ . The vector compartments,  $s_v$  and  $i_v$ , represent susceptible and infectious vectors, respectively, scaled to the initial number of hosts. The total vector population thus becomes  $n_v = s_v + i_v$ . The resulting dimensionless system is



Host equations (10):

$$\begin{aligned}\frac{ds}{d\tau} &= an - ki_v \frac{s}{n} - b_s s \\ \frac{di_1}{d\tau} &= ki_v \frac{s}{n} i_1 - q_1 i_1 - b_{i1} i_1 \\ \frac{di_2}{d\tau} &= q_1 i_1 - i_2 - b_{i2} i_2 \\ \frac{dr}{d\tau} &= i_2 - b_r r.\end{aligned}$$

Vector equations (11):

$$\begin{aligned}\frac{ds_v}{d\tau} &= a_v s_v - l s_v \frac{i_1}{n} - l s_v \frac{i_2}{n} - b_{s_v} s_v \\ \frac{di_v}{d\tau} &= l s_v \frac{i_1}{n} + l s_v \frac{i_2}{n} - b_{i_v} i_v.\end{aligned}$$

Computing  $R_0$  the reduced set of equations become

$$\frac{d}{d\tau} \begin{bmatrix} i_1 \\ i_2 \\ i_v \end{bmatrix} = w - v = \begin{bmatrix} ki_v \frac{s}{n} \\ 0 \\ l s_v \frac{i_1}{n} + l s_v \frac{i_2}{n} \end{bmatrix} - \begin{bmatrix} q_1 i_1 + b_{i1} i_1 \\ -q_1 i_1 + i_2 + b_{i2} i_2 \\ b_{i_v} i_v \end{bmatrix}. \quad (12)$$

Note that only progression from  $s$  to  $i_1$  and  $s_v$  to  $i_v$  are considered to be new infections. The corresponding Jacobian matrices of  $w$  and  $v$  evaluated at the DFE are

$$W = \begin{bmatrix} 0 & 0 & k \\ 0 & 0 & 0 \\ l \frac{S_v(0)}{N(0)} & l \frac{S_v(0)}{N(0)} & 0 \end{bmatrix} \text{ and } V = \begin{bmatrix} q_1 + b_{i1} & 0 & 0 \\ -q_1 & 1 + b_{i2} & 0 \\ 0 & 0 & b_{i_v} \end{bmatrix} \quad (13)$$

and the dominant eigenvalue of  $WV^{-1}$ , which, in terms of the original variables and parameters is

$$R_0 = f \sqrt{\frac{cc_v S_v(0)}{\mu_{i_v} N(0)} \left[ \frac{1}{\alpha_1 + \mu_{i1}} \left[ 1 + \frac{\alpha_1}{\gamma + \mu_{i2}} \right] \right]}. \quad (14)$$

The form of  $R_0$  can now be inferred for  $j - 1$  relapsing rates between  $j$  infected compartments as

$$R_0 = f \sqrt{\frac{cc_v \frac{S_v(0)}{N(0)}}{\mu_{iv}} \left[ \frac{1}{\alpha_1 + \mu_{i1}} \left[ 1 + \frac{\alpha_1}{\alpha_2 + \mu_{i2}} \left[ \dots \left[ 1 + \frac{\alpha_{j-1}}{\gamma + \mu_{ij-1}} \right] \right] \right] \right] \right]}. \quad (15)$$

### 3.4.3 $R_0$ analysis

$R_0$  is directly proportional to the biting rate ( $f$ ), competency values ( $c$  and  $c_v$ ), and the ratio of initial vectors to initial hosts ( $\frac{S_v(0)}{N(0)}$ ) and inversely proportional to the vector death rate ( $\mu_{iv}$ ) and the rate that moves individuals out of the infected compartments ( $\alpha_1, \dots, \alpha_{j-1}, \mu_{i1}, \dots, \mu_{ij}$ , and  $\gamma$ ). In addition, a pattern emerges as more infected compartments are added: a nesting sequence of terms that increase the value of  $R_0$  and potentially contribute to a change in stability of the DFE. To illustrate this concept, we used the pine squirrel host parameters (Table 3-2) for increasing number of infected compartments and plotted  $R_0$ . Figure 2 shows that  $R_0$  crosses 1 at between  $j = 4$  and  $j = 5$  infected compartments (i.e., 4 relapses).

## 3.5 Coupled Host-vector System

### 3.5.1 Model description

Here the single host-vector model is expanded to include two hosts, namely pine squirrels and deer mice. Figure 1b is a compartmental diagram for the two systems with no relapses. The first host-vector system ( $S_{ps}, I_{I,ps}, R_{rs}, S_{v,ps}, I_{v,ps}$ ) is coupled with the second system ( $S_{dm}, I_{I,dm}, R_{dm}, S_{v,dm}, I_{v,dm}$ ) through ticks biting either host species, with parameter  $f$ , and is further controlled by competency values of either the ticks ( $c_v$ ) or hosts ( $c_{ps}$  or  $c_{dm}$  for pine squirrel and deer mice, respectively). Transmission occurs through three mechanisms: 1)  $fc_v$ , which is the biting rate modified by the tick competency through which an infected tick bites a host from each system,

2)  $fc_{ps}$ , which is the biting rate modified by the pine squirrel competency in that a susceptible tick bites an infected pine squirrel, and 3)  $fc_{dm}$ , which is the biting rate modified by the deer mouse competency, such that a susceptible tick bites an infected deer mouse. The parameters remain as in the single host vector system, denoted with additional subscripts to represent the respective host-vector system (either  $ps$  or  $dm$ ), and are explained in Tables 1-2.

The generalized system for the infection dynamics in a coupled host-vector system with  $j$  - 1 relapsing rates for  $j = 1$  infected compartments describes the pine squirrel system with the number of susceptible hosts  $S_{ps}(t)$ , infectious hosts  $I_{k,ps}(t)$ , and removed hosts  $R_{ps}(t)$ . The total pine squirrel host population is  $N_{ps} = S_{ps} + \sum_{k=1}^j I_{k,ps} + R_{ps}$ . Likewise, the deer mouse host system consists of susceptible hosts  $S_{dm}(t)$ , infectious hosts  $I_{k,dm}(t)$ , and removed hosts  $R_{dm}(t)$  with a total deer mouse host population of  $N_{dm} = S_{dm} + \sum_{k=1}^j I_{k,dm} + R_{dm}$ . The vector compartments are susceptible vectors  $S_v(t)$ , infected vectors  $I_v(t)$  and a total vector population of  $N_v = S_v + I_v$ .

The equations are

Pine squirrel host system (16):

$$\begin{aligned}
 \dot{S}_{ps} &= \beta S_{ps} - fc_v I_v \frac{S_{ps}}{N_{ps}} - \mu_{s,sp} S_{ps} \\
 \dot{I}_{1,ps} &= fc_v I_v \frac{S_{ps}}{N_{ps}} - \alpha_{1,ps} I_{1,ps} - \mu_{i1,ps} I_{1,ps} \\
 \dot{I}_{2,ps} &= \alpha_{1,ps} I_{1,ps} - \alpha_{2,ps} I_{2,ps} - \mu_{i2,ps} I_{2,ps} \\
 &\quad \vdots \\
 \dot{I}_{j-1,ps} &= \alpha_{j-2,ps} I_{j-2,ps} - \alpha_{j-1,ps} I_{j-1,ps} - \mu_{i(j-1),ps} I_{j-1,ps} \\
 \dot{I}_{j,ps} &= \alpha_{j-1,ps} I_{j-1,ps} - \gamma_{j,ps} I_{j,ps} - \mu_{ij,ps} I_{j,ps} \\
 \dot{R}_{j,ps} &= \gamma_{j,ps} I_{j,ps} - \mu_{r,ps} R_{ps}.
 \end{aligned}$$

Deer mouse host system (17):

$$\begin{aligned}
\dot{S}_{dm} &= \beta S_{dm} - f c_v I_v \frac{S_{dm}}{N_{dm}} - \mu_{s,dm} S_{dm} \\
\dot{I}_{1,dm} &= f c_v I_v \frac{S_{dm}}{N_{dm}} - \alpha_{1,dm} I_{1,dm} - \mu_{i1,dm} I_{1,dm} \\
\dot{I}_{2,dm} &= \alpha_{1,dm} I_{1,dm} - \alpha_{2,dm} I_{2,dm} - \mu_{i2,dm} I_{2,dm} \\
&\vdots \\
\dot{I}_{j-1,dm} &= \alpha_{j-2,dm} I_{j-2,dm} - \alpha_{j-1,dm} I_{j-1,dm} - \mu_{i(j-1),dm} I_{j-1,dm} \\
\dot{I}_{j,dm} &= \alpha_{j-1,dm} I_{j-1,dm} - \gamma_{j,dm} I_{j,dm} - \mu_{ij,dm} I_{j,dm} \\
\dot{R}_{j,dm} &= \gamma_{j,dm} I_{j,dm} - \mu_{r,dm} R_{dm}.
\end{aligned}$$

Coupled vector system (18):

$$\begin{aligned}
\dot{S}_v &= \beta_v S_v - \frac{f c_{ps} S_v}{N_{ps}} \sum_{i=1}^j I_{i,ps} - \frac{f c_{dm} S_v}{N_{dm}} \sum_{i=1}^j I_{i,dm} - \mu_{sv} S_v \\
\dot{I}_v &= \frac{f c_{ps} S_v}{N_{ps}} \sum_{i=1}^j I_{i,ps} + \frac{f c_{dm} S_v}{N_{dm}} \sum_{i=1}^j I_{i,dm} - \mu_{iv} I_v.
\end{aligned}$$

### 3.5.2 Equilibrium analysis

To understand the effect of an additional host system, a coupled host-vector model with no relapses is first analyzed following the techniques from the single host-vector system. The resulting dimensionless system is

Pine squirrel host system (19):

$$\frac{ds_{ps}}{d\tau} = a_{ps} s_{ps} - k i_v \frac{s_{ps}}{n_{ps}} - b_{s,ps} s_{ps}$$

$$\begin{aligned}\frac{di_{1,ps}}{d\tau} &= ki_v \frac{S_{ps}}{n_{ps}} - i_{1,ps} - b_{i_{1,ps}} i_{1,ps} \\ \frac{dr_{ps}}{d\tau} &= i_{1,ps} - b_{r,ps} r_{ps}.\end{aligned}$$

Deer mouse host system (20):

$$\begin{aligned}\frac{ds_{dm}}{d\tau} &= a_{dm} s_{dm} - ki_v \frac{S_{dm}}{n_{dm}} - b_{s,dm} s_{dm} \\ \frac{di_{1,dm}}{d\tau} &= ki_v \frac{S_{dm}}{n_{dm}} - i_{1,dm} - b_{i_{1,dm}} i_{1,dm} \\ \frac{dr_{dm}}{d\tau} &= i_{1,dm} - b_{r,dm} r_{dm}.\end{aligned}$$

Coupled vector system (21):

$$\begin{aligned}\frac{ds_v}{d\tau} &= a_v s_v - l_{rs} s_v \frac{i_{1,ps}}{n_{ps}} - l_{dm} s_v \frac{i_{1,dm}}{n_{dm}} - b_{s_v} s_v \\ \frac{di_v}{d\tau} &= l_{ps} s_v \frac{i_{1,ps}}{n_{ps}} + l_{dm} s_v \frac{i_{1,dm}}{n_{dm}} - b_{i_v} i_v.\end{aligned}$$

where parameters are as shown in Table 1.

In the absence of disease, the system steady state is  $(S_{ps}^*, I_{1,ps}^*,$

$R_{ps}^*, S_{v,ps}^*, I_{v,ps}^*, S_{dm}^*, I_{1,dm}^*, R_{dm}^*) = (S_{ps}(0), 0, 0, S_v(0), S_{dm}(0), 0, 0)$ . The total population becomes,  $N_{ps} = S_{ps}(0), N_{dm} = S_{dm}(0), N_v = S_v(0)$ . This steady state is the DFE for the coupled host-vector system with no relapses.

The size of the system is reduced by considering only  $i_{1,ps}$ ,  $i_v$ , and  $i_{1,dm}$  and the rate of appearance of new infections and the rate of transfer between compartments for all other processes respectively,

$$\frac{d}{d\tau} \begin{bmatrix} i_{1,ps} \\ i_v \\ i_{1,dm} \end{bmatrix} = w - v = \begin{bmatrix} ki_v \frac{S_{ps}}{n_{ps}} \\ l_{ps} s_v \frac{i_{1,ps}}{n_{ps}} + l_{dm} s_v \frac{i_{1,dm}}{n_{dm}} \\ ki_v \frac{S_{dm}}{n_{dm}} \end{bmatrix} - \begin{bmatrix} i_{1,ps} + b_{i_{1,ps}} i_{1,ps} \\ b_{i_v} i_v \\ i_{1,dm} + b_{i_{1,dm}} i_{1,dm} \end{bmatrix}.$$

(22)

The Jacobians of the vector fields  $w$  and  $v$  evaluated at the DFE are

$$W = \begin{bmatrix} 0 & k & 0 \\ l_{ps} \frac{S_v(0)}{N(0)} & 0 & l_{dm} \frac{S_v(0)}{N(0)} \\ 0 & k & 0 \end{bmatrix}, \text{ and } V = \begin{bmatrix} 1 + b_{i1,ps} & 0 & 0 \\ 0 & b_{iv} & 0 \\ 0 & 0 & 1 + b_{i1,dm} \end{bmatrix} \quad (23)$$

and the dominant eigenvalue of  $WV^{-1}$  written in terms of the original variables and parameters is

$$R_0 = f \sqrt{\frac{f c_v S_v(0)}{\mu_{iv}} \left[ \frac{c_{ps}}{N_{ps}(0)} \left[ \frac{1}{(\gamma + \mu_{i1,ps})} \right] + \frac{c_{dm}}{N_{dm}(0)} \left[ \frac{1}{(\gamma + \mu_{i1,dm})} \right] \right]}. \quad (24)$$

For the system with one relapse ( $j = 2$  infected compartments), the host compartments,  $s$ ,  $i_1$ ,  $i_2$ , and  $r$ , indicate the fractions of the initial population in the susceptible, infectious, and recovered classes, so that the total rescaled host population is  $n = s + i_1 + i_2 + r$ . The vector compartments,  $s_v$  and  $i_v$ , represent susceptible and infectious vectors, respectively, scaled to the initial number of hosts. The total vector population thus becomes  $n_v = s_v + i_v$ . The resulting dimensionless system is

Pine squirrel host system (25):

$$\begin{aligned} \frac{ds_{ps}}{d\tau} &= a_{ps} s_{ps} - k i_v \frac{s_{ps}}{n_{ps}} - b_{s,ps} s_{ps} \\ \frac{di_{1,ps}}{d\tau} &= k i_v \frac{s_{ps}}{n_{ps}} - q_{1,ps} i_{1,ps} - b_{i1,ps} i_{1,ps} \\ \frac{di_{2,ps}}{d\tau} &= q_{1,ps} i_{1,ps} - i_{2,ps} - b_{i2,ps} i_{2,ps} \\ \frac{dr_{ps}}{d\tau} &= i_{1,ps} - b_{r,ps} r_{ps}. \end{aligned}$$

Deer mouse host system (26):

$$\begin{aligned} \frac{ds_{dm}}{d\tau} &= a_{dm} s_{dm} - k i_v \frac{s_{dm}}{n_{dm}} - b_{s,dm} s_{dm} \\ \frac{di_{1,dm}}{d\tau} &= k i_v \frac{s_{dm}}{n_{dm}} - i_{1,dm} - b_{i1,dm} i_{1,dm} \end{aligned}$$

$$\begin{aligned}\frac{di_{2,dm}}{d\tau} &= q_{1,dm}i_{1,dm} - i_{2,dm} - b_{i2,dm}i_{2,dm} \\ \frac{dr_{dm}}{d\tau} &= i_{1,dm} - b_{r,dm}r_{dm}.\end{aligned}$$

Coupled vector system (27):

$$\begin{aligned}\frac{ds_v}{d\tau} &= a_v s_v - l_{rs} s_v \frac{i_{1,ps}}{n_{ps}} - l_{ps} s_v \frac{i_{2,ps}}{n_{ps}} - l_{dm} s_v \frac{i_{1,dm}}{n_{dm}} - l_{dm} s_v \frac{i_{2,dm}}{n_{dm}} - b_{sv} s_v \\ \frac{di_v}{d\tau} &= l_{ps} s_v \frac{i_{1,ps}}{n_{ps}} + l_{ps} s_v \frac{i_{2,ps}}{n_{ps}} + l_{dm} s_v \frac{i_{1,dm}}{n_{dm}} + l_{dm} s_v \frac{i_{2,dm}}{n_{dm}} - b_{iv} i_v.\end{aligned}$$

For computing  $R_0$  the reduced set of equations are

$$\frac{d}{d\tau} \begin{bmatrix} i_{1,ps} \\ i_{2,ps} \\ i_v \\ i_{1,dm} \\ i_{2,dm} \end{bmatrix} = w - v = \begin{bmatrix} ki_v \frac{s_{ps}}{n_{ps}} \\ 0 \\ l_{ps} s_v \frac{i_{1,ps}}{n_{ps}} + l_{dm} s_v \frac{i_{1,dm}}{n_{dm}} \\ 0 \\ ki_v \frac{s_{dm}}{n_{dm}} \end{bmatrix} - \begin{bmatrix} q_{1,ps} i_{1,ps} + b_{i1,ps} i_{1,ps} \\ -q_{1,ps} i_{1,ps} + i_{2,ps} + b_{i2,ps} i_{2,ps} \\ b_{iv} i_v \\ q_{1,dm} i_{1,dm} + b_{i1,dm} i_{1,dm} \\ -q_{1,dm} i_{1,dm} + i_{2,dm} + b_{i2,dm} i_{2,dm} \end{bmatrix}.$$

(28)

The Jacobians of the vector fields  $w$  and  $v$  evaluated at the DFE are

$$W = \begin{bmatrix} 0 & 0 & k & 0 & 0 \\ 0 & 0 & 0 & 0 & 0 \\ l_{ps} \frac{s_v(0)}{N(0)} & l_{ps} \frac{s_v(0)}{N(0)} & 0 & l_{dm} \frac{s_v(0)}{N(0)} & l_{dm} \frac{s_v(0)}{N(0)} \\ 0 & 0 & 0 & 0 & 0 \\ 0 & 0 & k & 0 & 0 \end{bmatrix},$$

and

$$V = \begin{bmatrix} q_{1,ps} + b_{i1,ps} & 0 & 0 & 0 & 0 \\ -q_{1,ps} & 1 + b_{i2,ps} & 0 & 0 & 0 \\ 0 & 0 & b_{iv} & 0 & 0 \\ 0 & 0 & 0 & q_{1,dm} + b_{i1,dm} & 0 \\ 0 & 0 & 0 & -q_{1,dm} & 1 + b_{i2,dm} \end{bmatrix}$$

(29)

and the dominant eigenvalue of  $WV^{-1}$  written in terms of the original variables and parameters is

$$R_0 =$$

$$f \sqrt{\frac{f c_v S_v(0)}{\mu_{iv}} \left[ \frac{c_{ps}}{N_{ps}(0)} \left[ \frac{1}{(\alpha_{1,ps} + \mu_{i1,ps})} \left[ 1 + \frac{\alpha_{1,ps}}{\gamma + \mu_{i2,ps}} \right] \right] + \frac{c_{dm}}{N_{dm}(0)} \left[ \frac{1}{(\alpha_{1,dm} + \mu_{i1,dm})} \left[ 1 + \frac{\alpha_{1,dm}}{\gamma + \mu_{i2,dm}} \right] \right] \right]}. \quad (30)$$

The form of  $R_0$  can now be inferred for  $j - 1$  relapsing rates between  $j$  infected compartments.

$$R_0 = f \sqrt{\frac{f c_v S_v(0)}{\mu_{iv}} [PS + DM]}. \quad (31)$$

where

$$PS = \frac{c_{ps}}{N_{ps}(0)} \left[ \frac{1}{(\alpha_{1,ps} + \mu_{i1,ps})} \left[ 1 + \frac{\alpha_{1,ps}}{\alpha_{2,ps} + \mu_{i2,ps}} \left[ \dots \left[ 1 + \frac{\alpha_{j-1,ps}}{\gamma + \mu_{ij,ps}} \right] \dots \right] \right] \right]$$

and

$$DM = \frac{c_{dm}}{N_{dm}(0)} \left[ \frac{1}{(\alpha_{1,dm} + \mu_{i1,dm})} \left[ 1 + \frac{\alpha_{1,dm}}{\alpha_{2,dm} + \mu_{i2,dm}} \left[ \dots \left[ 1 + \frac{\alpha_{j-1,dm}}{\gamma + \mu_{ij,dm}} \right] \dots \right] \right] \right]. \quad (32)$$

### 3.5.3 $R_0$ analysis

From the coupled host-vector system it is apparent that  $R_0$  has the additional dependency for both the host competency values ( $c_{ps}$  and  $c_{dm}$ ). Since competency values are probabilities between 0 and 1, then they will always decrease the value of  $R_0$  as they decrease. Like the single host-vector system, a pattern emerges as more infected compartments are added to each host system (Equations 31-32): a nested sequence of terms that increase the value of  $R_0$  and potentially contribute to a change in stability of the DFE. To compare the results of the number of relapses needed for  $R_0 > 1$  in the coupled host-vector system with the single host-vector, we



added an incompetent deer mouse host system ( $c_{dm} = 0.2$ ) and increased the number of relapses in a pine squirrel host system until  $R_0$  reached 1. Figure 3-3 shows that  $R_0$  crosses 1 at between  $j = 7$  and  $j = 8$  infected compartments (7 relapses).

### 3.6 Discussion

Incorporating a relapsing component into a host-vector SIR modeling framework represents a step towards a better understanding and representation of complex disease systems. We investigated the disease dynamics of TBRF and used the model to better understand the underlying dynamics and interactions among spirochetes, rodent hosts, and tick vectors that contribute to pathogen persistence. A disease model was presented that describes 1) a single host-vector system with a single relapsing class of host individuals, and generalized to  $j-1$  relapsing host classes and 2) a coupled host-vector model generalized as above to  $j-1$  relapsing host classes. Analytical techniques allowed for the generalization of  $R_0$  with increasing numbers of relapses, and parameters were identified that affect the elimination or persistence of the pathogen (e.g., biting rates, competency values, and population numbers).

In the single host-vector system,  $R_0$  is directly proportional to the biting rate ( $f$ ), competency values ( $c$  and  $c_v$ ), and the ratio of initial vectors to initial hosts ( $\frac{S_v(0)}{N(0)}$ ). An inverse relationship exists between  $R_0$  and the vector death rate ( $\mu_{iv}$ ) and the rate that moves individuals out of the infected compartments ( $\alpha_1, \dots, \alpha_{j-1}, \mu_{i1}, \dots, \mu_{ij}$ , and  $\gamma$ ). When additional relapsing classes are added to the system,  $R_0$  always increases because of the addition of a nested sequence of terms that is always  $> 1$  (Equation 15). The coupled host-vector system has similar dependencies with additional interesting dynamics that may be very important to understanding pathogen persistence and host diversity. Coupling of the system with hosts of lower

competencies will always reduce  $R_0$  (Equations 31-32). As the number of incompetent hosts available as blood meals for infected ticks increases, an effect comparable to the dilution effect occurs and  $R_0$  always decreases, leading to DFE. The dilution effect states that in the presence of a second, less competent species, competent host-vector encounters leading to transmission events may be replaced by incompetent host-vector encounters that do not end in a pathogen transmission event, thus decreasing  $R_0$  (Ostfeld and Keesing 2000 a, b).

The model presented here addresses the presence of multiple hosts with varying competencies and a single pathogen, however, the model can be extended to address not only differences in host species diversity but also the presence of >1 pathogen strain. The genetics of *B. hermsii* have been well characterized and isolates have been shown to fall into two distinct genomic groups, referred to as genomic group I and II (GGI, GGII) (Porcella *et al.* 2005; Schwan *et al.* 2007). The presence of both genomic groups of *B. hermsii* has been documented on WHI, while only GGII *B. hermsii* has been found to date on the mainland around Flathead Lake where host species diversity is greater than that of the WHI.

Field investigations of rodents on WHI confirmed infection in a single deer mouse (*Peromyscus maniculatus*) infected with GGII *B. hermsii* (Chapter 2). This prompted a laboratory experiment in which we infected deer mice with both GGI and GGII *B. hermsii* and monitored them for infection. We challenged deer mice with infection via needle inoculation and infectious tick bite and observed that deer mice show no susceptibility to GGI but are highly susceptible to GGII spirochetes (Appendix A). These findings were in contrast with Burgdorfer and Mavros (1970) who were unable to establish infection in deer mice, however, they were likely using infected ticks from a TBRF outbreak near Spokane, WA, U.S.A., which resulted in isolation of GGI *B. hermsii*.

The coupled system presented here could be used to examine the effects of not only host species with varying competencies, but also diverse host communities in the presence of *B. hermsii* in both genomic groups. The presence of both genomic groups simultaneously may result in a dampening of the dilution effect if GGII is able to infect a diverse array of host species even though GGI is more species limited. Rodent trapping and tick collection on WHI showed one squirrel and one tick infected with GGI and three squirrels infected with GGII. On WHI, 95% of all pine squirrels captured were seropositive for relapsing fever spirochetes while only 4% of deer mice possessed antibodies (Chapter 2). All infected individuals at mainland sites with diverse host species were infected with GGII spirochetes.

This model is an important first step in understanding a relapsing host-vector disease system; however, all known complexities of the system could not be addressed at this time. There is conflicting evidence at the rate which transovarial transmission of *B. hermsii* occurs in *O. hermsi*, however if it occurs with any frequency, it will most likely have large impacts on the system dynamics. The existence of transovarial transmission would provide insight into the implication of *O. hermsi* serving as the reservoir for *B. hermsii*, i.e., the ability to maintain infectious ticks in a prolonged absence of competent hosts and/or hosts in general. Further, the model could be used to explore the presence of both genomic groups of *B. hermsii* as well as drivers in the host and vector communities. Prevention strategies may be explored to identify the effectiveness of host control versus vector control, which may provide insight into human protective measures and the effectiveness of control strategies such as host vaccination. Simulations could be run to assess the efficacy of control programs such as vaccination regimes and vector control.

Ecological factors including biotic and abiotic interactions may play a primary role in the emergence and persistence of infectious diseases (Morse 1995, Schrag and Wiener 1995, Gubler 1998, Daszak 2000, Patz *et al.* 2000, Wilcox and Gubler 2005). Understanding the complete epidemiology of a disease is crucial to advancing the ability to predict and control outbreaks in human and wildlife populations, however, this is rarely an attainable goal. Sonenshine (2005) outlines the sequence of steps typically undertaken when attempting to understand the epidemiology of a given system. The pathway typically begins with the identification of a clinical syndrome, followed by discovery of the causative disease agent, and then the identification of the source of the agent in nature. The final step includes investigating the often complex biology and ecology of the hosts and/or vectors involved. Given the difficulty frequently encountered when attempting to study a disease in nature, the last step is often the most difficult. The application of advanced modeling techniques to poorly understood systems is often the only way to begin to understand the drivers of these systems.

The ecological dynamics of relapsing fever systems around the world are poorly understood. Here we use a North American system of relapsing fever caused by *B. hermsii*; however, information gathered from this modeling exercise can be applied to TBRF systems around the world. TBRF remains a major public health threat in Africa (Cutler 2010). In addition to other TBRF systems, the ideas presented here may provide the groundwork for relapsing components to be included in other disease systems with greater public health implications such as malaria.

Table 3-1. Parameters and variable notation in the host-vector TBRF model for  $j - 1$  relapses between  $j$  infected compartments (rates are per month, competency values are probabilities (per bite)) and dimensionless forms (rescaled by  $\gamma$  or normalized by  $N(0)$ ). In the coupled system, additional subscripts with  $ps$  represent the pine squirrel host-vector system and  $dm$  represents the deer mouse host-vector system.

<b>Notation</b>	<b>Description</b>	<b>Dimensionless</b>
$S$	Host susceptible	$s = S / N(0)$
$I_j$	Host infected from infected population $j$	$i_j = I_j / N(0)$
$R$	Host removed	$r = R / N(0)$
$N$	Host total	$n = N / N(0)$
$c$	Host competency	$l = fc / \gamma$
$\gamma$	Host recovery rate	$1$
$\alpha_{j-1}$	Host relapse rate for $j$ infected compartments	$q_{j-1} = \alpha_{j-1} / \gamma$
$\beta$	Host growth rate	$a = \beta / \gamma$
$\mu$	Host death rates	$b = \mu / \gamma$
$S_v$	Vector susceptible	$s_v = S_v / N(0)$
$I_v$	Vector infected	$i_v = S_v / N(0)$
$N_v$	Vector total	$n_v = N_v / N(0)$
$c_v$	Vector competency	$k = fc_v / \gamma$
$\beta_v$	Vector growth rate	$a_v = \beta_v / \gamma$
$\mu_v$	Vector death rates	$b_v = \mu_v / \gamma$
$f$	Biting rate between vector-host system	$l = fc / \gamma; k = fc_v / \gamma$

Table 3-2. Parameter values in the TBRF model for  $j$ -1 relapses between  $j$  infected compartments (rates are per month, competency values are probabilities (per bite)). The subscripts  $ps$  and  $dm$  denote values used in the pine squirrel and deer mouse host-vector system, respectively. Note that if the subscripts do not appear, then the parameter is the same value in both systems.

Notation	Description	Value
$S_{ps}(0), S_{dm}(0)$	Initial host susceptible	850, 10,000
$I_{j,ps}(0), I_{j,dm}(0)$	Initial host infected from infected population $j$	0
$R_{ps}(0), R_{dm}(0)$	Initial host removed	0
$N_{ps}(0), N_{dm}(0)$	Initial host total	850
$C_{ps}$	Pine squirrel host competency	0.9
$c_{dm}$	Deer mouse host competency (coupled system)	0.2
$\gamma, \alpha_1, \dots, \alpha_{j-1}$	Host transition rates	4.35
$\beta_{ps}, \beta_{dm}$	Host growth rate	0.33, 1.0
$\mu_{s,ps}, \mu_{s,dm}$	Host susceptible death rate	0.33/( $j+2$ ), 1.0/( $j+2$ )
$\mu_{ij,ps}, \mu_{ij,dm}$	Host infected death rate from infected population $j$	0.33/( $j+2$ ), 1.0/( $j+2$ )
$\mu_{r,ps}, \mu_{r,dm}$	Host removed death rate	0.33/( $j+2$ ), 1.0/( $j+2$ )
$S_{v,ps}(0), S_{v,dm}(0)$	Initial vector susceptible	9,900
$I_{v,ps}(0), I_{v,dm}(0)$	Initial vector infected	100
$N_{v,ps}(0), N_{v,dm}(0)$	Initial vector total	10,000
$c_v$	Vector competency	0.95
$\beta_v$	Vector growth rate	2.08
$\mu_{sv} = \mu_{iv}$	Vector death rates	1.04
$f$	Vector biting rate	0.33

Figure 3-1. Conceptual models for the cross-infection dynamics between (a) a single host-vector system, which includes  $j - 1$  relapses between  $j$  infected compartments and (b) a coupled host-vector system with no relapses in either host. Dashed lines are vital rates for each population, where solid lines refer to interaction rates between compartments. See Table 1 for a summary of notation.

Figure 3-2. Increasing number of infected compartments are added to the single host-vector system and  $R_0$  is plotted (Equation 15).  $R_0$  becomes greater than 1 at 4 relapses.

Figure 3-3. An incompetent deer mouse (*Peromyscus maniculatus*) host system ( $c_{dm} = 0.2$ ) is coupled with a competent pine squirrel (*Tamiasciurus hudsonicus*) host system ( $c_{ps} = 0.9$ ).  $R_0$  is plotted (Equations 31-32) for the deer mouse host system that contained no relapses and the pine squirrel host system with increasing number of infected compartments.  $R_0$  becomes greater than 1 at 7 relapses.

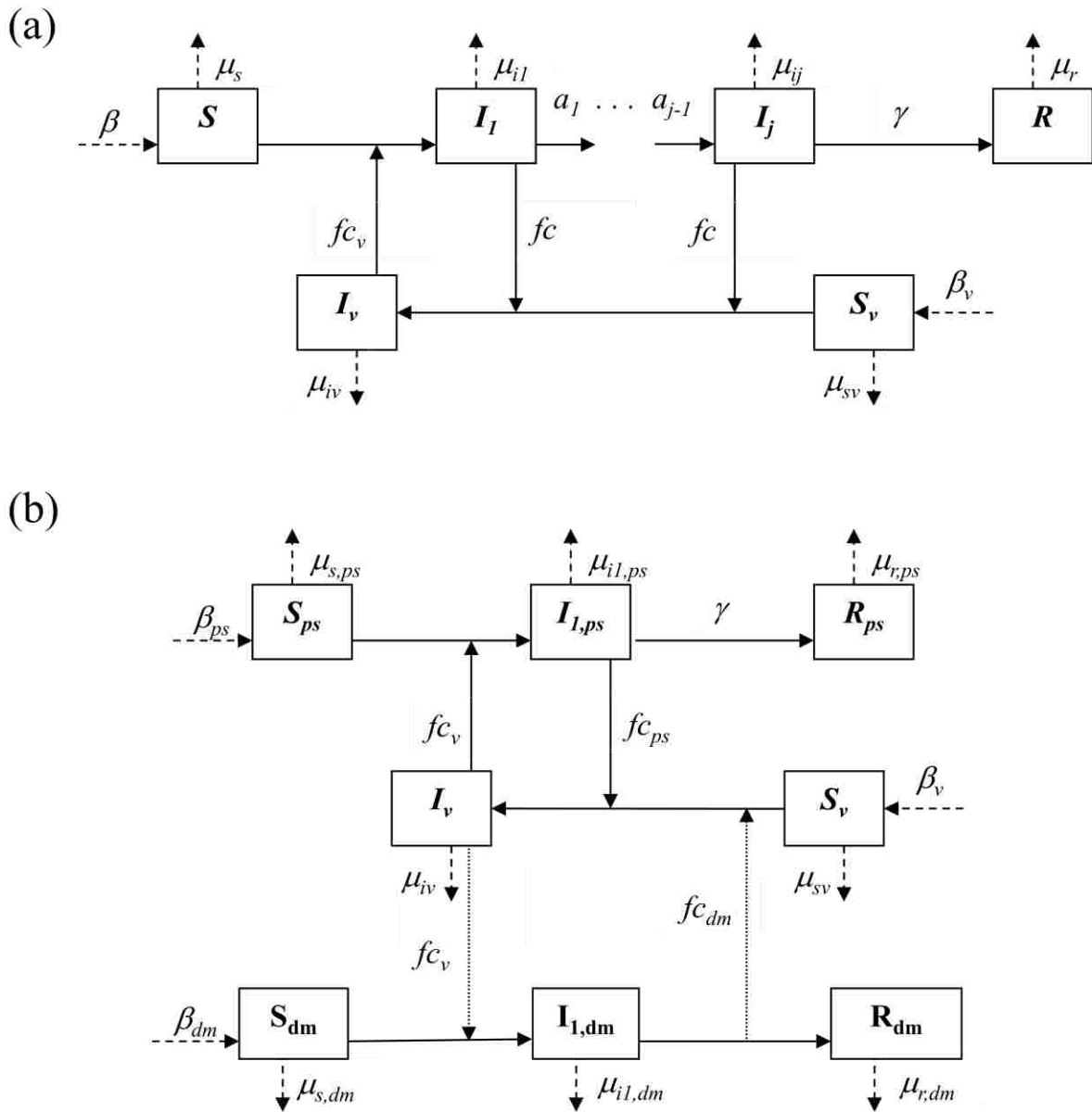


Figure 3-1.



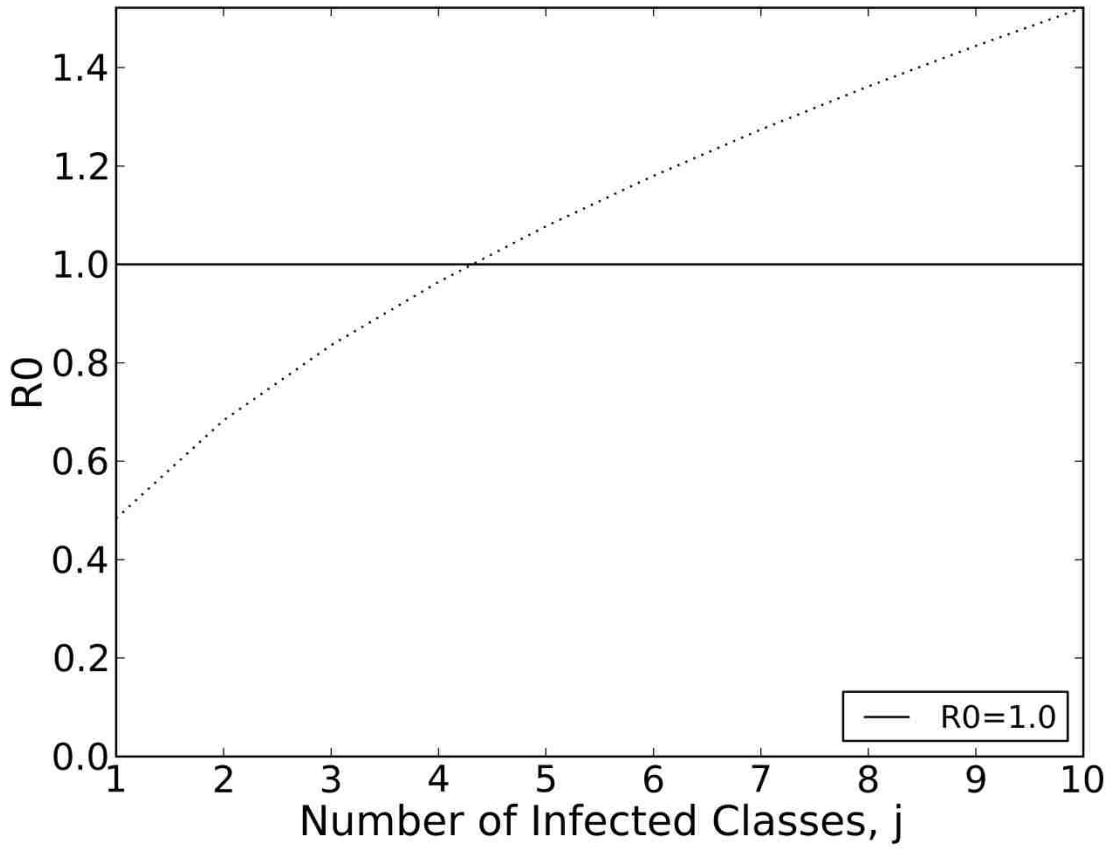


Figure 3-2.

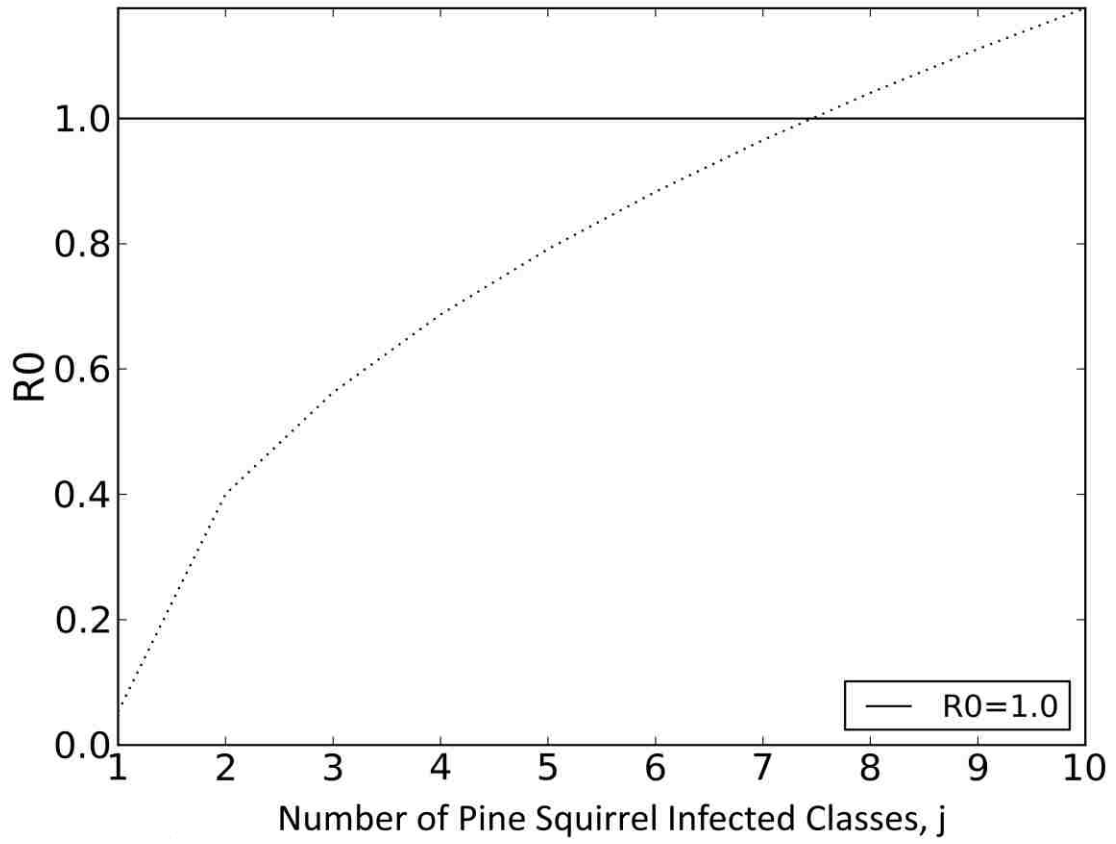


Figure 3-3.

## Chapter 4 – Phylogeographic Structure of Tick-borne Relapsing Fever

### *Agent Borrelia hermsii*

#### 4.1 Abstract

Tick-borne relapsing fever (TBRF) caused by *Borrelia hermsii* spirochetes and vectored by *Ornithodoros hermsi*, a soft-bodied, nest-dwelling tick, occurs throughout western North America, causing human illness on an annual basis. The genetic diversity of *B. hermsii* isolates has been previously documented; however, the molecular epidemiology of TBRF is less well understood. *Borrelia hermsii* spirochetes fall into two genomic groups (GGI and GGII) based on previous genetic analyses. GGI and GGII spirochetes co-exist both geographically and may co-infect the same host or tick. Here, we utilized whole-chromosome sequences to investigate the phylogeographic structure of *B. hermsii*. We identified single nucleotide polymorphisms (SNPs) along the chromosome of 49 isolates of *B. hermsii* and used Bayesian coalescent-based methods to compare the genetic structure among the isolates. Although both genomic groups are found in Montana, only three of 21 isolates were GGI, and all of these were found on Wild Horse Island. GGII spirochetes were documented at two island study sites and one mainland study site at Flathead Lake, Montana. The data suggest one GGI introduction and at least two separate introductions of GGII *B. hermsii* to Wild Horse Island. Resulting phylogenies showed that GGII isolates from Montana separated into the two distinct clades. GGII isolates from squirrels and ticks from the mainland and two islands showed very little genetic diversity. Two human isolates from Wild Horse Island were genetically distinct from other GGII isolates from Montana but were highly similar to isolates from Idaho and Washington.

## 4.2 Introduction

The dynamics of parasite transmission are important to understanding host-parasite interactions (McCallum *et al.* 2001); the rates and routes of parasite transmission are fundamental to the epidemiology of disease systems. Population genetics can provide valuable insight into key processes of parasite transmission (Paterson and Viney 2000; Goldberg *et al.* 2007; Archie *et al.* 2009). Parasite genetic markers can be used to assess parasite spread both temporally and spatially and can be used to infer pathogen population history, goals that can be difficult to address with traditional epidemiological approaches (Archie *et al.* 2009). Techniques to classify bacterial strains including multi-locus sequence typing (MLST) and variable number tandem repeat (VNTR) analyses are being replaced with genome-wide analyses made possible by new sequencing technologies. Advances in next generation technologies allow sequencing large numbers of genes from many individuals, large portions of genomes to identify single nucleotide polymorphisms (SNPs), and sequencing entire genomes is becoming widespread. Whole genome studies have been utilized primarily to study rapidly evolving RNA viruses with small genomes. More recently, whole-genome and whole-chromosome SNP mapping was used to determine the population genetic structure and phylogeography of bacterial organisms including *Yersinia pestis*, *Staphylococcus aureus*, *Mycobacterium tuberculosis*, and *Bacillus anthracis* (Gutacker *et al.* 2002, 2006; Van Ert *et al.* 2007; Nübel *et al.* 2008; Cummings *et al.* 2010; Harris *et al.* 2010; Morelli *et al.* 2010).

Here we used whole-chromosome sequences from 49 isolates of *Borrelia hermsii*, a causative agent of tick-borne relapsing fever. These isolates were collected between 1960 and 2010 across the western United States and southern British Columbia and were used to construct phylogenies to investigate the phylogeographic structure of this system. Tick-borne relapsing

fever (TBRF) is endemic to central Asia, Africa, and the Americas (Davis 1940); worldwide, all but one species of relapsing fever spirochete, *B. recurrentis*, are vectored by soft ticks (*Ornithodoros* spp.) (Felsenfeld 1971). The louse-borne relapsing fever spirochete *B. recurrentis* is transmitted by the human body louse (*Pediculus humanus*). TBRF occurs throughout western North America and most human cases are caused by infection with *B. hermsii* spirochetes. *Borrelia hermsii* is maintained in enzootic cycles involving spirochete transmission between the tick vector *O. hermsi* and a variety of vertebrate hosts, most often rodents. Human cases of TBRF occur each year in North America (Dworkin *et al.* 2008), and patient samples are frequently sent to the National Institutes of Health, Rocky Mountain Laboratories, Hamilton, MT, for diagnosis. These samples of *B. hermsii* have been catalogued along with other samples obtained from infected ticks (*O. hermsi*) and a chipmunk (*Tamias* sp.).

The genome of *B. hermsii* is unique, segmented and complex. These spirochetes contain a single linear chromosome (920 – 922 kb) and numerous linear and circular plasmids, which compose approximately one third of the genome (> 500 kb). There are seven to eight linear plasmids ranging in size from 18 kb to 200 kb and at least five 32 kb circular plasmids (Stevenson *et al.* 2000; Dai *et al.* 2006; Lopez *et al.* 2008).

Many molecular characteristics of *B. hermsii* including antigenic variation have been examined extensively (Hinnenbusch *et al.* 1998, Barbour *et al.* 1991, 2000; Barbour and Restrepo 2000, Bunikis *et al.* 2004; Barbour 2005; Fritz *et al.* 2004; Porcella *et al.* 2005; Dai *et al.* 2006; Frank and Barbour 2006; Schwan *et al.* 2007). Antigenic variation is a mechanism by which *B. hermsii* evades the host immune system by switching the abundant outer surface protein, called a variable major protein (Vmp), whose gene is a single locus expressed on a linear plasmid (Dai *et al.* 2006). This switch causes the host immune system to produce a new antibody in response to

the new major antigen. The variable tick protein (Vtp) is produced by *B. hermsii* upon uptake by the tick vector. Upon re-entry into a vertebrate host, *vtp* is no longer expressed and one of the variable major proteins involved in antigenic variation is again produced. Horizontal gene transfer and recombination have been demonstrated to occur at the *vtp* locus, located on a 53 kb linear plasmid (Porcella *et al.* 2005; Barbour 2005). Evidence of recombination among *B. hermsii* isolates has not been reported for chromosomal loci (Porcella *et al.* 2005; Schwan *et al.* 2007).

All isolates of *B. hermsii* that have been characterized previously segregate into two distinct genomic groups, designated Genomic Group I (GGI) and Genomic Group II (GGII) (Porcella *et al.* 2005; Schwan *et al.* 2007). The separation of these spirochetes into these groups is based on multi-locus sequence typing (MLST) of several highly conserved genes including *16S rRNA*, *flaB*, *gyrB*, *glpQ*, *fhbA* and the noncoding intergenic spacer region (IGS). All members within each group have an identical *16S rRNA* sequence, but between the two groups there are 5 bp differences (99.6% identity). The other loci are less similar, such as *glpQ*, which varies by only 2 or 3 bp within each group but between the two groups there are 36 or 37 bp differences (96.4% identity). The other loci show similar levels of sequence divergence with fewer differences within each group compared to more differences between the two groups. *Borrelia hermsii* is transmitted only by *O. hermsi*, and historically the relapsing fever spirochetes were identified and named based on the species of tick that transmitted them in nature. Given that the spirochetes in both genomic groups of *B. hermsii* are transmitted by *O. hermsi*, the investigators who described the two genomic groups chose to maintain the current nomenclature and designate the spirochetes as belonging to two genomic groups rather than establish a newly named species.

There is geographic overlap between the distribution of GGI and GGII spirochetes (Schwan *et al.* 2007). Both genomic groups co-occur in every state from where isolates have been collected, with the exception of Colorado and Utah, where only a few GGI spirochetes have been isolated to date. At a finer spatial resolution, both genomic groups have been found in Lake Co., MT, Siskiyou Co., CA, Okanogan Co., WA, and the Okanagan Valley in southern British Columbia. The ecological epidemiology of this system remains poorly understood. This research focused on the phylogeographic structure of *B. hermsii* isolates obtained from infections in humans, rodent hosts, and tick vectors across the western United States and southern British Columbia, Canada. MLST analyses of housekeeping genes have shown little sequence divergence among isolates within each genomic group. We compared whole-chromosome sequences of *B. hermsii* using coalescent-based techniques to ask the following questions:

- How genetically different are isolates of *B. hermsii* within each genomic group?
- Are geographically proximate isolates of *B. hermsii* genetically similar to each other?
- Is there evidence of long distance dispersal of *B. hermsii*, and how common are dispersal events?

Identifying the phylogeographic structure of *B. hermsii* will provide important information about dispersal and the occurrence and frequency with which these events may occur. The ability for dispersal has strong implications for the introduction of *B. hermsii* to new geographic areas of suitable habitat, and may impact the future distribution of TBRF in the face of climate change (Chapter 5).

## 4.3 Methods

### 4.3.1 *Borrelia hermsii* Samples

Isolates of *B. hermsii* included specimens in the RML collection obtained from 30 human infections, 1 chipmunk (*Tamias* sp.), 2 ticks (*O. hermsi*), 1 dog (*Canis familiaris*) (Schwan *et al.* 2007, 2009, *unpublished data*), and 15 isolates obtained from pine squirrels (*Tamiasciurus hudsonicus*) and *O. hermsi* collected during field studies described in Chapter 2 (Table 4-1a,b). *B. hermsii* spirochetes in whole blood of infected squirrels were inoculated into laboratory mice (RML Colony Strain, *Mus musculus*) via intraperitoneal injection. Individual *O. hermsi* were allowed to feed on laboratory mice. Mice were monitored daily for the presence of spirochete infection by examining a blood smear (<3 uL) obtained from the tail vein by nicking the tip of the tail. When an adequate level of spirochetemia was reached (10 or more spirochetes per field), we euthanized the mouse, collected blood by intracardiac puncture, and placed 500 uL of infected blood into BSK-H (Sigma-Aldrich<sup>®</sup>) culture medium with 12% rabbit serum. Purified *B. hermsii* genomic DNA was prepared by harvesting spirochetes from the medium, treating with a lysozyme, a detergent (TES, 1% DOC) and Proteinase K, followed by two phenol/chloroform extractions, a single chloroform extraction and lastly precipitation by ethanol.

Purified genomic *B. hermsii* DNA was submitted to the RML Genomics Unit, Research Technologies Branch, Division of Intramural Research, National Institutes of Health, for whole genome sequencing using a SOLiD 3 System (Applied Biosystems) and identification of SNPs. Two reference genomes assembled previously at RML, DAH (GGI) and MTW (GGII), were used for sequence alignment (DAH – GenBank accession number NC\_010673; MTW2 – *unpublished*). Data generated by the SOLiD sequencer were analyzed using Bioscope (Applied Biosystems) and Zoom (Bioinformatics Solutions, Inc.) to identify SNPs in 21 GGI and 28 GGII



*B. hermsii* isolates. SNP number and locations (within open reading frames or intergenic) were identified. SNPs found within open reading frames were identified as being either synonymous or non-synonymous. The number of pair-wise SNP differences among all GGI isolates and among GGII isolates was quantified using Arlequin v 3.5 (Excoffier and Lischer 2010).

We tested for the presence of significant recombination using SplitsTree4 and the Phi test (Bruen *et al.* 2006; Hudson and Bryant 2006). Sites having undergone significant recombination were identified using DNAsp v5 (Librado and Rozas 2009). The coalescent process assumes a neutral model in which no recombination occurs (Kingman 1982). We tested the effect of violating this assumption and observed no differences in the output when including or excluding recombination, therefore, the complete data set was used in the analysis.

#### **4.3.2 Phylogenetic analysis**

Concatenated sequences were created for each genomic group and analyses of GGI and GGII were performed separately. Coalescent-based Bayesian phylogenetic analyses were implemented for both genomic groups in BEAST v1.5.4 (Drummond and Rambaut 2007). We ran models with and without the dates for when the spirochetes were isolated. The Generalized Time Reversible (GTR) model was chosen as the genetic distance model using the web implemented version of j-modeltest, FindModel based on MODELTEST (Posada and Crandall 1998, available at <http://www.hiv.lanl.gov/content/sequence/findmodel/findmodel.html>). Other parameter settings included an estimated base frequency and no site heterogeneity.

A relaxed, uncorrelated, lognormal clock allowing for different lineages to evolve at different rates was chosen (Drummond *et al.* 2006; Lemey *et al.* 2010). Due to the lack of knowledge of demographic history, we chose a coalescent model using the Bayesian Skyline

setting with 5 groups. We ran 200 million iterations in BEAST and used the ESS provided by Tracer v1.5.4 to assess model convergence. Coalescent trees were produced using TreeAnnotator v1.5.4 with 10000 burn-in replicates and a maximum clade credibility tree and viewed with FigTree. The maximum-credibility method evaluates each of the trees created by the Bayesian analysis and each clade within the tree is given a score based on the number of times that it appears in other sampled posterior trees. Scores are added to give a total score for the tree; the tree with the highest score represents the maximum clade credibility tree (Drummond 2010).

#### **4.4 Results**

We identified single nucleotide polymorphisms (SNPs) along the chromosome of 49 isolates of *B. hermsii*; 28 isolates were from endemic TBRF areas including Idaho, Washington, California, Utah, Colorado, and British Columbia and 21 isolates were from Montana. Prior MLST analyses showed high genetic similarity among isolates within each group, yet whole-chromosome sequencing revealed large numbers of SNPs among each group. Geographically proximate isolates tended to be more similar, however there were some isolates in both genomic groups that were quite genetically distinct from other isolates found nearby. In the Flathead Lake area of Montana, both genomic groups were found but only three out of 21 isolates were GGI and all GGI isolates originated from Wild Horse Island. GGII spirochetes were documented at two island study sites and one mainland study site at Flathead Lake, Montana. These data suggest one GGI introduction and at least two separate introductions of GGII *B. hermsii* to Wild Horse Island.

#### **4.4.1 GGI *B. hermsii***

We compared chromosomal sequences of 21 GGI *B. hermsii*. There were 3,425 SNPs located across the 922,307 bp chromosome of these isolates (Figure 4-2); 57% of SNPs were synonymous, 34% were non-synonymous, and 9% were located in intergenic regions. Synonymous and non-synonymous SNPs occurred in 533 different open reading frames and significant recombination was detected among GGI isolates ( $p < 0.001$ ), however the presence of recombination did not affect the results and thus the complete dataset was used.

There was a high degree of heterogeneity among GGI isolates. EST and ALL accounted for > 50% of all GGI SNPs (1,735 and 1,698 SNPs, respectively) when compared with the reference strain (Table 4-2a, Figure 4-2a). Two GGI isolates, LAK-4 and LAK-6, were identical to each other and differed from the only other GGI Montana isolate, WHS90, by just 14 SNPs (Table 4-2a). GGI isolates EST and ALL always grouped separately from the other GGI isolates. These isolates were also geographically the most distant isolates compared to all other spirochetes. Isolates MAN, WAD and ELD-2 from the Sierra Nevada Mountains of eastern California were also geographically and genetically distinct from other GGI isolates including SIS and RAL from northern California (Figure 4-3).

#### **4.4.2 GGII *B. hermsii***

We compared 28 GGII isolates of *B. hermsii*. There were 1,833 SNPs located across the 920,644 bp chromosome of these isolates (Figure 4-2b); 52% of SNPs were synonymous, 40% were non-synonymous, and 8% were located in intergenic regions. Synonymous and non-synonymous SNPs were distributed evenly across the chromosome and were present in 363 open reading frames. No significant recombination was detected among these isolates ( $p = 0.536$ ).

Five GGII isolates, LAK-1, LAK-2, HAN, SIL, and DOG, accounted for > 70% of SNP diversity when compared with the reference strain MTW. Additionally, there were ~750 base pair differences between MTW and the other GGII isolates (Table 4-2b). All other Montana GGII isolates differed from each other by only 1 to 40 SNPs (Table 4-2b).

GGII isolates LAK-1, LAK-2, SIL, HAN, and DOG from western Montana, northern Idaho, and Washington were genetically similar to each other but distinct from all other GGII isolates collected from the same geographic areas (Figure 4-4). The MTW isolate was also the most genetically distinct from and geographically distant from other isolates. Remaining isolates from Washington and British Columbia as well as YOR from northern California were alike and grouped more closely with the remaining Montana isolates. All GGII Montana isolates, with the exception of the aforementioned of LAK-1 and LAK-2, grouped closely together.

#### **4.5 Discussion**

Whole-chromosome analyses of *B. hermsii* isolates provided new insight into genetic differences and similarities among and between the two genomic groups. There was a high amount of genetic differentiation within each of the genomic groups. Overall, GGI isolates had longer coalescent times and longer genetic distances among isolates (Figure 4-3 and 4-4). SNP analysis of GGI and GGII *B. hermsii* revealed differences between genomic groups. *B. hermsii* spirochetes displayed low genetic diversity across the chromosome with at most one SNP per 269 bases in GGI spirochetes and one SNP per 502 bases in GGII spirochetes. GGII spirochetes had almost half as many SNPs, shorter genetic distances and shorter coalescent times between the most genetically divergent isolates. Mutations (SNPs) and recombination events are expected to accumulate over time and therefore the prediction is that individuals with more SNPs

should be older. This analysis corresponds to previous findings in which GGI has been proposed to be ancestral to GGII because of the large number of polymorphisms and high nucleotide diversity of GGI compared to GGII at several loci (Porcella *et al.* 2005)

Isolates were generally geographically clustered; however, there were some exceptions that suggested the possibility of dispersal events. Phylogeographic analysis of *B. hermsii* suggests that dispersal events have occurred in the past and that there have been at least three introductions of *B. hermsii* to Montana; a single introduction of GGI spirochetes and at least two separate introductions of GGII spirochetes (Figures 4-3 and 4-4). Coalescent phylogenies estimated using the date of spirochete collection or those estimated without consideration of collection date showed similar topologies. GGI isolates showed three divergent groups: 1) ALL and EST from Utah and Colorado, respectively, 2) WAD, MAN and ELD-2 from the Sierra Nevada Mountains in eastern California, and 3) all other isolates from northern California, eastern Washington, the Idaho panhandle and the three Wild Horse Island isolates (Figure 4-3). Isolates belonging to GGII also showed three distinct groups; 1) SIL, DOG, HAN, LAK-1 and LAK-2 were closely related and genetically distinct from all other isolates and represented collections from Idaho, Washington, and Montana; 2) the MTW isolate from near Los Angeles, California, was distinct from all other isolates; 3) the remaining isolates from Idaho, Washington, Montana, northern California and British Columbia grouped closely together (Figure 4-4). With the exception of the five genetically divergent isolates from Montana, Idaho, and Washington, the phylogeny showed clear geographic clustering. All Montana isolates (except LAK-1 and LAK-2) were genetically similar and grouped by collection site. Most Yellow Bay isolates from both ticks and squirrels formed a monophyletic group. A single isolate from Yellow Bay (YBS60) grouped most closely with isolates from Wild Horse Island, and the single isolate from

Melita Island was distinct from, but most closely related to the other Montana isolates (Figure 4-4). Results suggest that long distance dispersal events are possible. Some isolates from Idaho, Washington and Montana collected in close proximity to each other were highly genetically distinct. In Montana, all three GGI isolates were genetically similar; however, some GGII isolates from here were very distinct from each other. Two GGII Montana isolates were dissimilar from all other Montana isolates, yet were highly similar to isolates obtained from Idaho and Washington. These results indicate that at least three introductions of *B. hermsii* to the Flathead Lake region of Montana may have occurred in the past.

Until 2009, all *B. hermsii* isolates examined consistently grouped into the two genomic groups described previously (Porcella *et al.* 2005; Schwan *et al.* 2007). In 2009, we trapped an infected pine squirrel (*Tamiasciurus hudsonicus*) at Yellow Bay Biological Station, Lake Co., MT (See Chapter 2; Fischer *et al.* 2009). This squirrel was dually infected with two genetically distinct strains of *B. hermsii*. We isolated one strain (YBS60) and obtained DNA sequence for housekeeping genes from the other strain. YBS60 was identified as GGII, whereas the other spirochete detected grouped more closely to GGI but was clearly genetically distinct from other members of this group. The DNA sequences obtained from the uncultured spirochete were identical to sequences obtained from a spirochete found in a northern spotted owl (*Strix occidentalis*) (Fischer *et al.* 2009).

Identification of infection in an owl and a squirrel located > 200 km apart suggest that birds may be capable of dispersing *B. hermsii* to new geographic areas. Infection of the spotted owl with *B. hermsii* is the first documentation of infection in a wild bird; however, Schwan *et al.* (2007) demonstrated subcutaneous infection with *B. hermsii* in a 14-day-old chicken (*Gallus domesticus*). The tick vector, *O. hermsi* has been found associated with a variety of wild birds

and in the laboratory all stages of *O. hermsi* have successfully fed on chickens and northern bobwhite quail (*Colinus virginianus*) (Schwan *et al.* 2007). *O. hermsi* have been documented in association with blue birds (*Sialia* sp.) (Gregson 1949; Longanecker 1951), house sparrows (*Passer domesticus*), California gulls (*Larus californicus*) (Furman and Loomis 1984), and American robins (*Turdus migratorius*) (Schwan *et al.* 2003). In addition to the rodent hosts and the potential avian hosts described above, bats (*Myotis* sp.) may also be hosts of *O. hermsi*. Longanecker (1951) found several *O. hermsi* occupying dead tree snags and in attics containing bats, and found an *O. hermsi* attached to one bat.

Long-distance dispersal events are possibly occurring via movement of *B. hermsii* infected birds or bats or the dispersal of infected *O. hermsi* via these species; however our data cannot discern the mechanism at work here. The results presented here, together with data from the niche modeling (Chapter 5) suggest that these organisms may be dispersed long geographic distances, which may have important implications in the face of global climate change. In 2050, the predicted distribution of *B. hermsii* and *O. hermsi* indicate a substantial shift in range due to climate change (Chapter 5). If these organisms are able to move or be moved across the landscape, it is probable that new niches can be exploited.

Table 4-1a. GGI *B. hermsii* isolates included in SNP analysis. The name includes the state or province from where the isolate originated, the year of isolation, and the three letter isolate designation. The biological origin of each isolate is listed under source.

<b>Name</b>	<b>Location</b>	<b>Source</b>
BC_2001_GAR	Okanagan Valley, B.C.	Human
CA_1960s_MAN	Sierra Nevada Mtns., CA	Human
CA_1997_RAL	Siskiyou Co., CA	Human
CA_1998_SIS	Siskiyou Co., CA	Tick
CA_1998_WAD	Placer Co., CA	Human
CA_2005_ELD-2	El Dorado Co., CA	Tick
CO_1996_EST	Larimer Co., CO	Human
ID_1996_CAR	Benewah Co., ID	Human
ID_1996_SWA	Kootenai Co., ID	Human
ID_1996_MIL	Kootenai Co., ID	Human
ID_1996_BRO	Kootenai Co., ID	Human
ID_1998_HAL	Kootenai Co., ID	Human
ID_2004_MAT	Clearwater Co., ID	Human
MT_2004_LAK-4	WHI, Lake Co., MT	Human
MT_2009_LAK-6	WHI, Lake Co., MT	Human
MT_2008_WHS90	WHI, Lake Co., MT	Squirrel
UT_1997_ALL	Duchesne Co., UT	Human
WA_1987_FRO	Eastern WA	Human
WA_1991_DAH	Spokane Co., WA	Human
WA_1996_FRE	Pend Oreille Co., WA	Human
WA_1997_BAK	Okanogan Co., WA	Human



Table 4-1b. GGII *B. hermsii* isolates included in SNP analysis. The name includes the state or province from where the isolate originated, the year of isolation, and the three letter isolate designation. The biological origin of each isolate is listed under source.

<b>Name</b>	<b>Location</b>	<b>Source</b>
BC_1995_OKA-1	Okanagan Valley, B.C	Human
BC_1996_OKA-3	Okanagan Valley, B.C	Human
CA_1964_YOR	Siskiyou Co., CA	Human
CA_2008_MTW	Los Angeles Co. CA	Tick
ID_1990_HAN	Boundary Co., ID	Human
ID_2002_SIL	Boundary Co., ID	Human
MT_2002_LAK-1	WHI, Lake Co., MT	Human
MT_2002_LAK-2	WHI, Lake Co., MT	Human
MT_2004_LAK-3	WHI, Lake Co., MT	Human
MT_2004_LAK-5	WHI, Lake Co., MT	Human
MT_2008_WHS40	WHI, Lake Co., MT	Squirrel
MT_2008_WHS81	WHI, Lake Co., MT	Squirrel
MT_2008_WHS88	WHI, Lake Co., MT	Squirrel
MT_2008_YBS60	YB, Lake Co., MT	Squirrel
MT_2008_YBS70	YB, Lake Co., MT	Squirrel
MT_2009_YBS266	YB, Lake Co., MT	Squirrel
MT_2010_YBS479	YB, Lake Co., MT	Squirrel
MT_2010_YBS1143	YB, Lake Co., MT	Squirrel
MT_2010_YBT10	YB, Lake Co., MT	Tick
MT_2010_YBT13	YB, Lake Co., MT	Tick
MT_2010_YBT17	YB, Lake Co., MT	Tick
MT_2010_YBT18	YB, Lake Co., MT	Tick
MT_2010_YBT20	YB, Lake Co., MT	Tick
MT_2010_MIS491	MI, Lake Co., MT	Squirrel
WA_1992_REN	Okanogan Co., WA	Human
WA_1997_GMC	Stevens Co., WA	Human
WA_1997_RUM	Stevens Co., WA	Human
WA_2009_DOG	Chelan Co., WA	Dog

Table 4-2a. Number of SNPs between all GGI *B. hermsii* isolates. LAK-4 and LAK-6 are grouped together because they were identical and thus all pair-wise differences between them and other isolates are also identical.

	DAH	LAK4/6	WHS90	BRO	GAR	MAN	FRE	CAR	BAK	RAL	SIS	WAD	HAL	ELD-2	MAT	SWA	MIL	FRO	ALL	EST
DAH	0																			
LAK4/6	32	0																		
WHS90	44	14	0																	
BRO	383	379	391	0																
GAR	388	384	396	427	0															
MAN	855	847	861	827	875	0														
FRE	425	421	433	62	431	813	0													
CAR	596	590	604	521	588	947	503	0												
BAK	423	419	431	64	431	805	26	503	0											
RAL	208	212	224	429	400	804	455	582	451	0										
SIS	209	213	225	428	401	805	456	584	452	2	0									
WAD	762	752	766	725	754	796	707	868	703	710	711	0								
HAL	22	16	30	379	388	849	421	580	419	204	205	756	0							
ELD-2	602	596	610	635	624	780	623	774	617	546	547	592	600	0						
MAT	339	339	351	430	121	872	436	609	434	373	374	761	339	611	0					
SWA	465	455	469	380	429	821	370	289	368	451	452	708	451	635	470	0				
MIL	58	70	82	371	374	846	399	570	397	226	227	766	60	606	329	445	0			
FRO	177	189	201	418	405	851	448	615	446	197	198	753	181	589	356	492	195	0		
ALL	1698	1690	1702	1709	1700	1665	1677	1796	1673	1650	1651	1617	1692	1623	1719	1647	1696	1691	0	
EST	1734	1726	1740	1745	1732	1705	1715	1834	1711	1688	1689	1649	1728	1659	1751	1685	1732	1729	552	0

Table 4-2b. Number of SNPs between all GGII *B. hermsii* isolates.

	MTW	LAK 1	SIL	YBS 70	YOR	WHS 40	WHS 81	WHS 88	YBS 60	LAK 5	HAN	REN	OKA 1	GMC	LAK 2	LAK 3	YBS 266	YBT 10	YBT 13	YBT 17	YBT 18	YBT 20	DOG	RUM	OKA 3	MIS 491	YBS 479	YBS 1143	
MTW	0																												
LAK1	1313	0																											
SIL	1350	129	0																										
YBS70	756	1104	1127	0																									
YOR	760	1110	1133	44	0																								
WHS40	748	1106	1127	34	54	0																							
WHS81	755	1103	1130	25	41	19	0																						
WHS88	755	1103	1128	23	39	17	2	0																					
YBS60	754	1102	1129	24	40	18	1	1	0																				
LAK5	756	1106	1133	28	44	16	5	5	4	0																			
HAN	1321	30	135	1108	1114	1110	1109	1107	1108	1110	0																		
REN	749	1091	1130	53	63	61	54	52	53	57	1093	0																	
OKA1	827	1175	1214	139	149	147	140	138	139	141	1175	114	0																
GMC	748	1092	1131	58	68	66	59	57	58	62	1094	33	119	0															
LAK2	1315	25	139	1106	1112	1110	1107	1105	1106	1108	24	1089	1171	1088	0														
LAK3	744	1100	1125	24	46	20	11	11	10	12	1102	45	129	52	1100	0													
YBS266	753	1105	1132	7	51	37	28	28	27	29	1111	56	140	61	1109	23	0												
YBT10	755	1107	1134	9	49	39	26	26	25	29	1113	62	148	67	1111	31	14	0											
YBT13	752	1114	1139	14	54	40	29	29	28	26	1116	65	149	70	1116	32	17	11	0										
YBT17	756	1108	1133	8	48	40	23	23	22	24	1112	59	145	64	1108	28	13	5	8	0									
YBT18	753	1111	1136	9	49	41	26	26	25	29	1117	62	148	67	1115	31	14	8	9	7	0								
YBT20	752	1112	1137	14	54	46	29	29	28	30	1116	63	149	68	1112	32	17	11	12	6	9	0							
DOG	1346	95	96	1143	1147	1145	1140	1140	1139	1143	97	1128	1212	1129	97	1137	1146	1142	1145	1141	1142	1141	0						
RUM	762	1099	1140	76	82	86	69	69	68	72	1103	57	137	62	1099	72	79	73	70	70	69	70	1128	0					
OKA3	827	1129	1170	143	149	151	138	138	137	139	1135	126	66	131	1131	139	144	142	139	141	138	145	1162	127	0				
MIS491	752	1110	1135	42	54	54	37	37	36	40	1114	63	149	68	1112	40	45	39	38	36	37	40	1143	72	143	0			
YBS479	755	1111	1136	11	51	39	26	26	25	27	1115	62	148	67	1113	31	16	8	9	5	8	9	1142	71	144	39	0		
YBS1143	753	1109	1134	11	51	39	28	28	27	29	1113	62	146	67	1113	29	12	8	11	7	8	9	1142	73	142	39	6	0	

Figure 4-1. Geographic locations by county of *B. hermsii* isolates included in SNP analysis (in black). Blue circles show locations of *B. hermsii* isolates and yellow triangles correspond to locations where *O. hermsii* and *B. hermsii* were found. Multiple isolates from a single county are denoted by a single symbol (See Table 1).

Figure 4-2. Alignment of concatenated chromosomal SNPs of 49 *B. hermsii*, a) genomic group 1 (GGI), b) genomic group 2 (GGII), created in BEAST. Black bars represent the presence of a SNP and grey areas represent sequence consensus. Isolates grouped by state of origin.

Figure 4-3. Coalescent-based phylogeny of concatenated chromosomal SNPs from 21 GGI *B. hermsii* isolates based on BEAST output created using TreeAnnotator and viewed using FigTree. Scale bar is in years.

Figure 4-4. Coalescent-based phylogeny of concatenated chromosomal SNPs from 28 GGII *B. hermsii* isolates based on BEAST output created using TreeAnnotator and viewed using FigTree. Scale bar is in years.

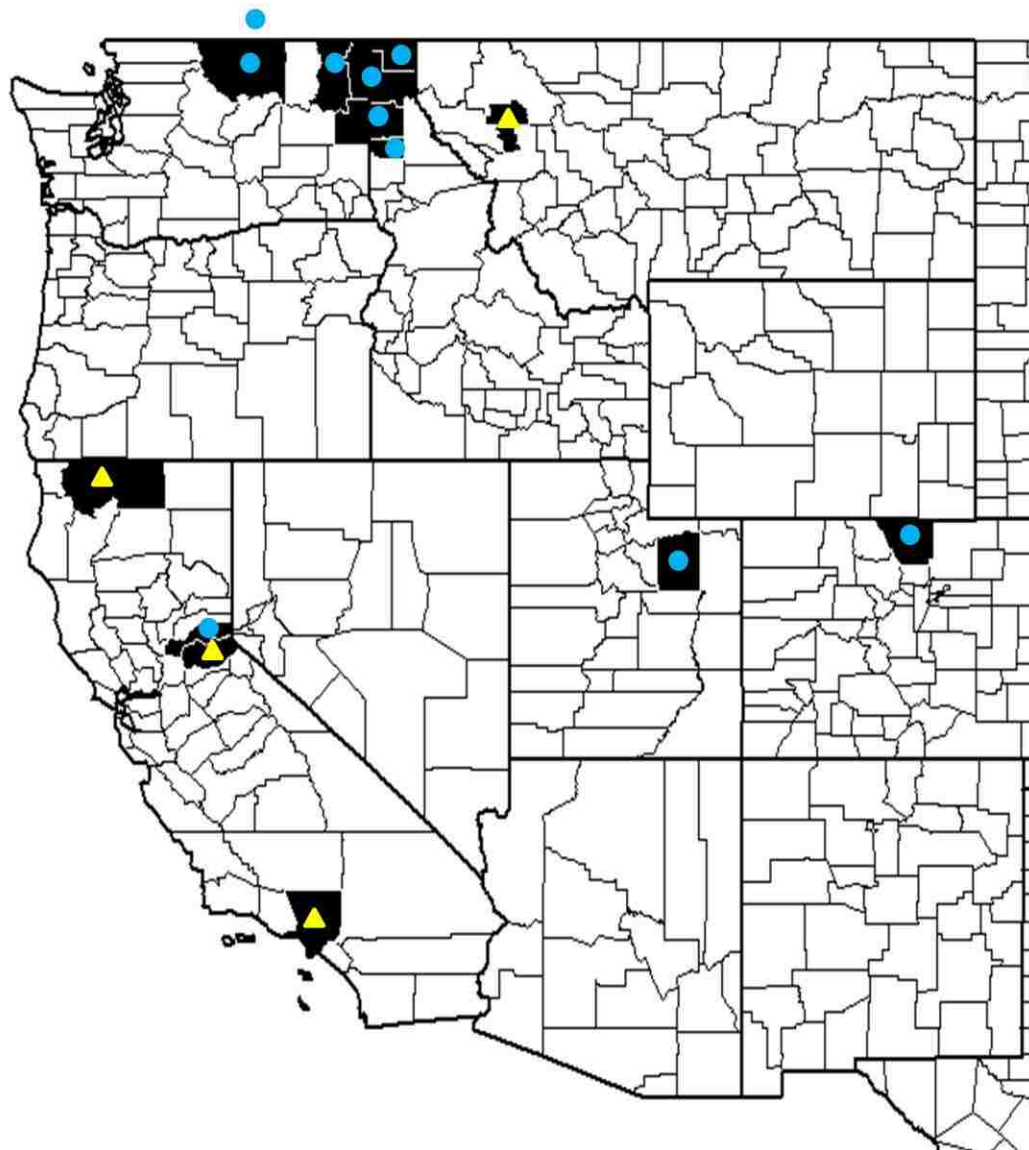


Figure 4-1.

BC\_2001\_GAR  
 CA\_1960S\_MAN  
 CA\_1997\_RAL  
 CA\_1998\_SIS  
 CA\_1998\_WAD  
 CA\_2005\_ELD2  
 CO\_1996\_EST  
 ID\_1996\_BRO  
 ID\_1996\_CAR  
 ID\_1996\_SWA  
 ID\_1996\_MIL  
 ID\_1998\_HAL  
 ID\_2004\_MAT  
 MT\_2004\_LAK-4  
 MT\_2009\_LAK-6  
 MT\_2008\_WHS90  
 UT\_1997\_ALL  
 WA\_1987\_FRO  
 WA\_1991\_DAH  
 WA\_1996\_FRE  
 WA\_1997\_BAK

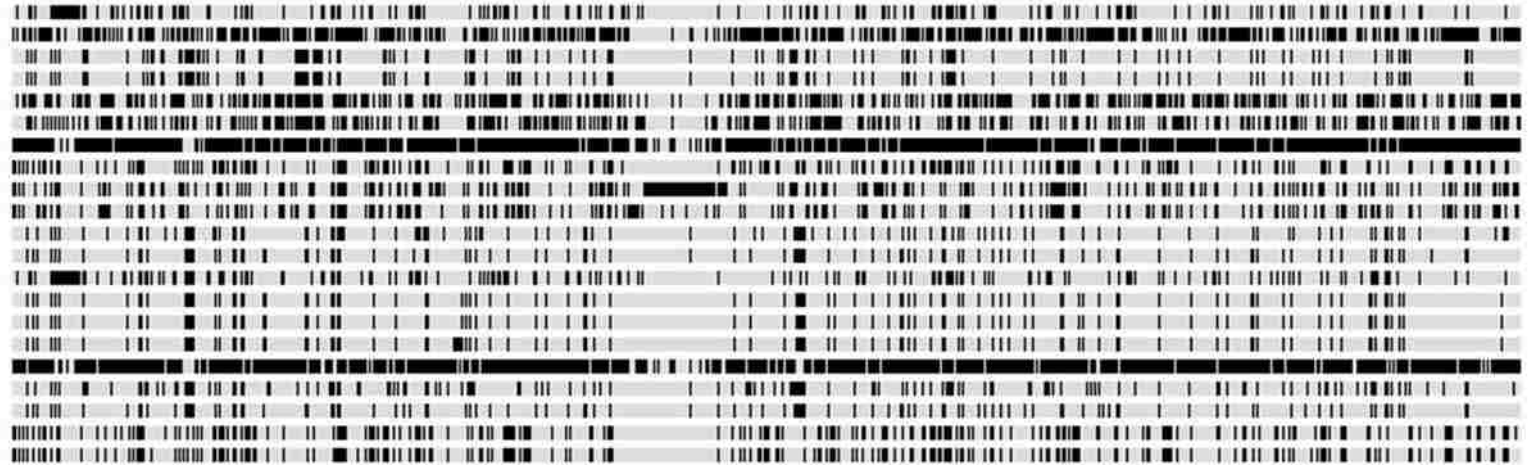


Figure 4-2a.

BC\_1995\_OKA-1  
 BC\_1996\_OKA-3  
 CA\_1964\_YOR  
 CA\_2008\_MTW  
 ID\_1990\_HAN  
 ID\_2002\_SIL  
 MT\_2002\_LAK-1  
 MT\_2002\_LAK-2  
 MT\_2004\_LAK-3  
 MT\_2004\_LAK5  
 MT\_2008\_WHS40  
 MT\_2008\_YBS60  
 MT\_2008\_YBS70  
 MT\_2008\_WHS81  
 MT\_2008\_WHS88  
 MT\_2009\_YBS266  
 MT\_2010\_YBS479  
 MT\_2010\_MIS491  
 MT\_2010\_YBS1143  
 MT\_2010\_YBT10  
 MT\_2010\_YBT13  
 MT\_2010\_YBT17  
 MT\_2010\_YBT18  
 MT\_2010\_YBT20  
 WA\_1992\_REN  
 WA\_1997\_RUM  
 WA\_2009\_DOG

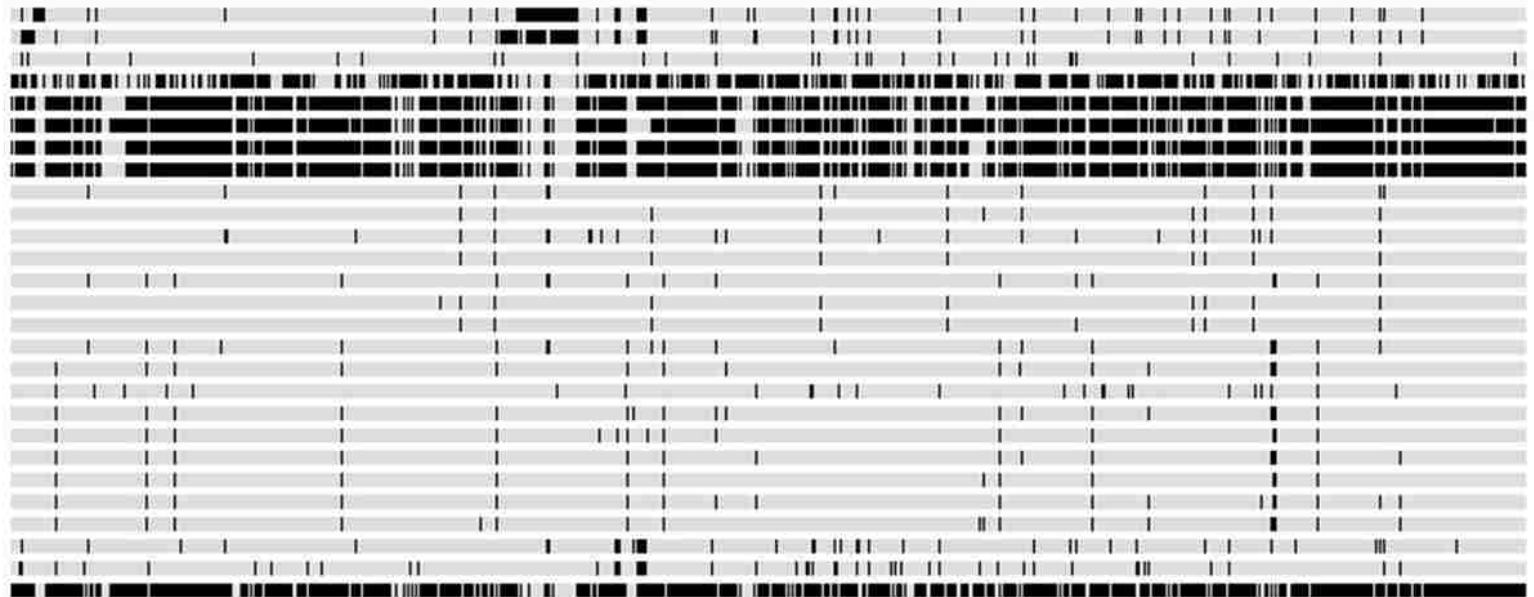


Figure 4-2b.

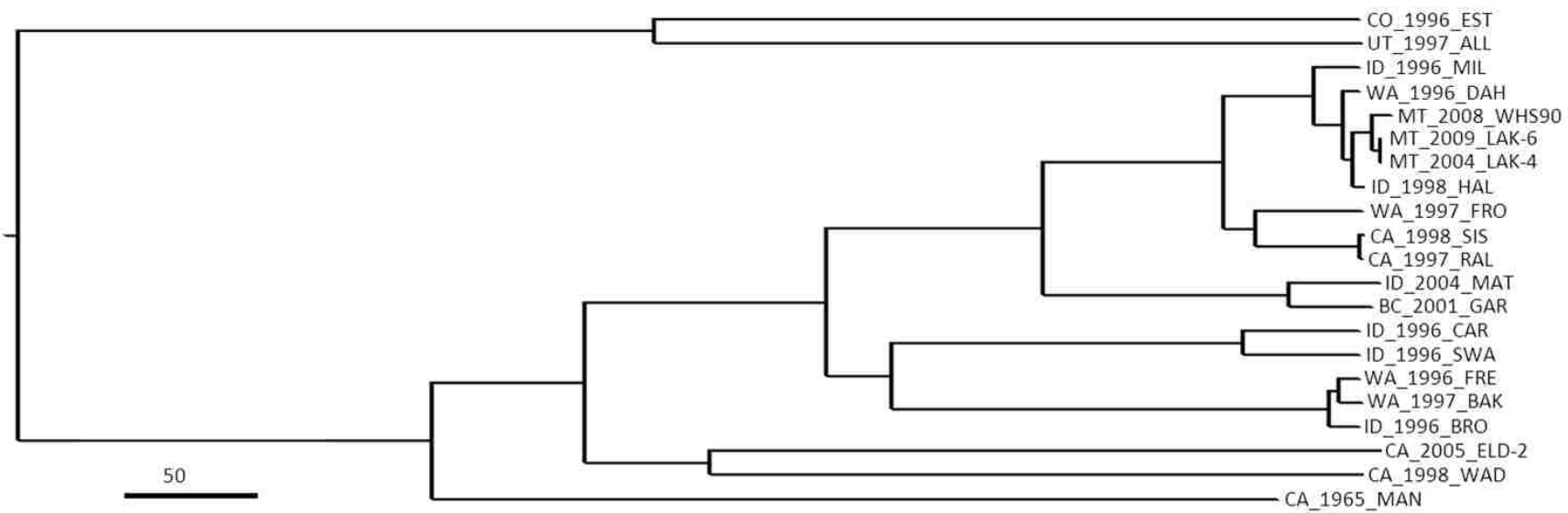


Figure 4.3

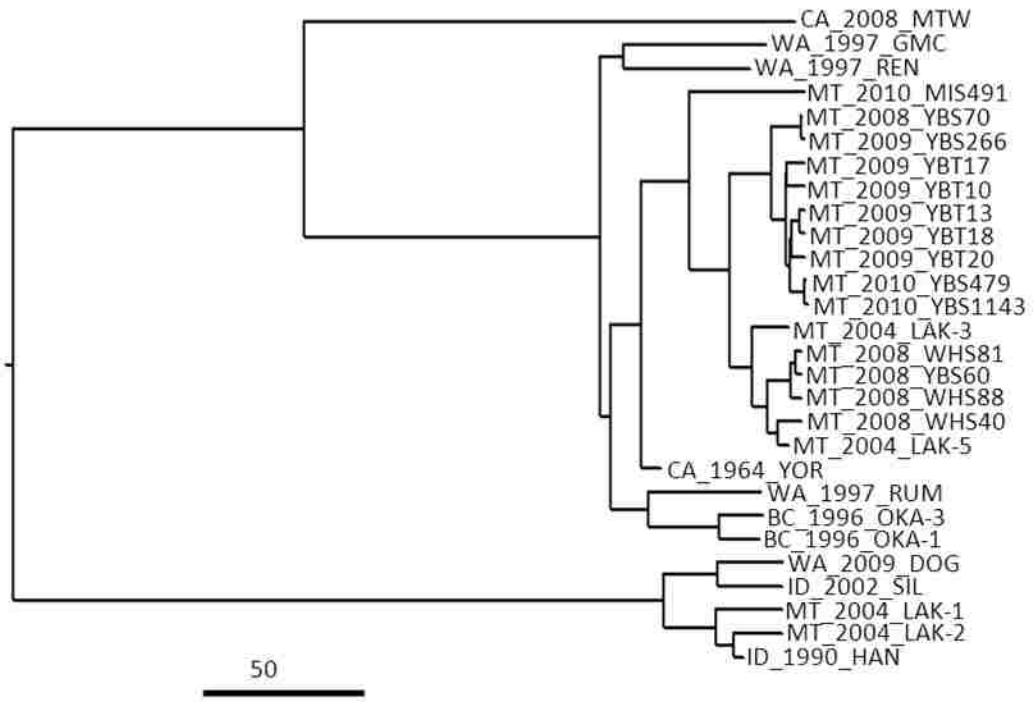


Figure 4.4



## **Chapter 5 – The Potential Distribution of *Ornithodoros hermsi*, a Vector of Tick-borne Relapsing Fever Spirochetes, in Western North America**

### **5.1 Abstract**

An ecological niche model was created using the Maximum Entropy Species Distribution Model (Maxent) to estimate the probability of the predicted distribution of *Ornithodoros hermsi*, the soft tick vector for the relapsing fever spirochete *Borrelia hermsii*. The preference of coniferous forest habitats at a range of higher elevations and the preferred hosts for these ticks has been recognized for many years; however, the climatic factors driving the distribution are not well understood. Here we show that five climate variables combined contributed more than 75% to predicting the distribution of *O. hermsi*. Temperature extremes accounted for four of the five most important variables. Minimum temperature during the coldest month, mean temperature of the wettest month, maximum temperature during the warmest month and annual temperature range all contributed equally to the model. Predicted shifts in distribution of the tick were examined using climate change models for the year 2050. The geographic distributions with the highest probabilities of tick occurrence were predicted to decrease in all models for the year 2050.

## 5.2 Introduction

Tick-borne relapsing fever (TBRF) is a vector-borne zoonotic disease caused by many species of helical, highly motile *Borrelia* bacteria and is endemic to the Americas, Africa, and Asia (Davis 1940). In North America, there are three species of tick-borne relapsing fever spirochetes, each vectored by a different species of *Ornithodoros* tick: *B. hermsii*, *B. turicatae*, and *B. parkeri*, vectored by *O. hermsi*, *O. turicata*, and *O. parkeri*, respectively (Davis 1942). Tick-borne relapsing fever in humans is characterized by recurring episodes of fever with general symptoms including headache, myalgia, nausea, arthralgia, and vomiting, and causes human infections each year (Dworkin *et al.* 1998). The illness was first reported in the western United States in Colorado in 1915 (Meader 1915), and has been considered endemic there since 1935 when *O. hermsi* was documented in Jefferson County (Davis 1939).

The geographic distribution of TBRF in North America has been broadly defined based largely on investigations of reported human cases, elevation, and host distribution (Schwan *et al.* 2007). Human cases of TBRF have been reported throughout the western United States and in southern British Columbia, Canada (Dworkin *et al.* 2002), and presence of the tick vector has been documented at elevations ranging from less than 3,000 feet to over 8,000 feet in areas of Colorado and California (Wheeler *et al.* 1935; Longanecker 1951). Human exposure is often reported to be in rustic settings, such as cabins, at higher elevations of coniferous forests and often in association with rodents such as tree squirrels (*Tamiasciurus* spp.) and chipmunks (*Tamias* spp.) (Porter *et al.* 1932; Beck 1937; Davis 1940; Dworkin *et al.* 1998, 2002).

Infection and exposure to *B. hermsii* in a diverse array of rodent species has been documented. Early investigations of human TBRF cases near Big Bear Lake, Lake Tahoe and Placer Lake, California, noted the presence and abundance of several species of ground squirrels

(*Spermophilus* spp.), chipmunks (*Tamias* spp.), and Douglas squirrels (*Tamiasciurus douglasii*), and documented infections in Douglas squirrels and chipmunks (Beck 1937). Identification of relapsing fever antibodies has been detected in pine squirrels (*T. hudsonicus*), flying squirrels (*Glaucomys sabrinus*), yellow-pine and red-tailed chipmunks (*T. amoenus* and *T. ruficaudus*), deer mice (*Peromyscus maniculatus*), voles (*Microtus* sp.), jumping mice (*Zapus princeps*), Columbian ground squirrels (*Spermophilus columbianus*), as well as two species of shrews (*Sorex* spp.) (Chapter 2). A single wild bird, a northern spotted owl (*Strix occidentalis*) was infected with *B. hermsii* (Thomas *et al.* 2002, Bunikis *et al.* 2004). Current and past exposures to *B. hermsii* suggest interactions of these vertebrate host species with the tick vector *O. hermsi*.

In addition to a known association with rodents, *O. hermsi* has been associated with a variety of wild birds, and in the laboratory all stages of *O. hermsi* have successfully fed on chickens and northern bobwhite quail (*Colinus virginianus*) (Schwan *et al.* 2007). *O. hermsi* have been documented in the nests of wild blue birds (*Sialia* sp.) (Gregson 1949; Longanecker 1951), house sparrows (*Passer domesticus*), California gulls (*Larus californicus*) (Furman and Loomis 1984), and American robins (*Turdus migratorius*) (Schwan *et al.* 2003). Bats (*Myotis* sp.) may also serve as hosts to *O. hermsi* as Longanecker (1951) found several *O. hermsi* occupying dead tree snags and in attics containing bats and a single *O. hermsi* was attached to one bat.

The geographic range of potential hosts associated with the *O. hermsi* system provides a nearly ubiquitous distribution across the entirety of western North America and southern to central British Columbia; however most human cases of relapsing fever have originated in a relatively small number of locations. Human infections in only 13 counties accounts for approximately 50% of all cases (Dworkin *et al.* 2008). Known endemic areas of repeated human

infection are well documented and include many popular tourist destinations including the north rim of the Grand Canyon (AZ), Estes Park (CO), and several mountain lakes including Lake Coeur D'Alene (ID), Lake Tahoe and Big Bear Lake (CA) and Flathead Lake (MT), (Dworkin *et al.* 2008). Reported human cases of TBRF provide a basis for much of what is known about the distribution of TBRF in North America and research on the underlying ecology of the system is lacking. Despite the ubiquity of potential hosts across the landscape, cases of TBRF are clustered in distinct foci suggesting that there may be constraints beyond just the presence of a suitable host for the tick vector. Like other vector-borne diseases, the spatial distribution of TBRF is likely limited by the environmental restrictions of *O. hermsi*.

The spatial distribution of zoonotic diseases, especially vector-borne diseases, depends heavily on environmental features and the presence of both host and vector is often geographically limited by environmental constraints (Kitron 1998). The distribution of tick-borne pathogens and the effect of climate on hard (Ixodid) ticks has been modeled extensively (Randolph 1993, 2004; Rogers and Randolph 1993; Randolph and Rogers 2000; Randolph *et al.* 2000; Estrada-Peña 2001; Cumming 2002; Brownstein *et al.* 2003, 2005; Wimberly *et al.* 2008). However, these studies have been carried out almost exclusively on hard ticks (Acari: Ixodidae), with the exception of Cumming and Van Vuuren (2006) who simultaneously modeled both hard and soft ticks in Africa. Hard and soft ticks have vastly different life histories, and thus are exposed to different environmental pressures. Hard ticks are only associated with a host while feeding, which results in spending greater than 90% of their life off the host (Needham and Teel 1991). Although hard ticks have developed mechanisms to increase the chance of survival upon detachment, when hard ticks drop off their hosts they are exposed to surrounding environmental conditions at least until they can seek shelter to lessen the effects of environmental pressures

(Needham and Teel 1991). Soft ticks (Acari: Argasidae) also spend most of their life off-host, having the unique ability to feed and detach in very short amounts of time to ensure they remain in or very near to the burrow or nest of the host (Sonenshine 1991). Thus when soft ticks drop of their host, they likely remain in the confines of the host's nest or burrow, which maintains a relatively stable microclimate (Davis 1942). Soft ticks may be less affected by rapidly changing environmental conditions as compared to hard ticks, and therefore may be most affected by extremes in environmental conditions over the course of their lifetime.

Ecological niche modeling (ENM) is an important tool for ecologists, conservationists, and more recently disease ecologists. The previously mentioned attempts to model the distribution of hard tick vectors of human disease and the predicted effect of climate change have utilized GIS- and statistically-based methods including logistic regression, autologistic regression, and geographically weighted regression. More recently, several computer-based machine-learning programs including GARP, BIOCLIM, and Maxent have been used to model the distribution of many species, and model performance has been compared thoroughly (Elith *et al.* 2006). The Maximum Entropy Species Distribution Model (Maxent) developed and described by Phillips *et al.* (2004, 2006) routinely outperforms other models and is most appropriate to use when only small numbers of presence-only data points exist (Elith *et al.* 2006).

Maxent has been used extensively to model current and future distributions of a variety of species including invasive species (Ficetola *et al.* 2007; Mukherjee *et al.* 2010), rare or elusive species (Marino *et al.* 2011) and a variety of human diseases and vectors including mosquitoes and malaria (Moffett *et al.* 2007; Foley *et al.* 2010), triatomines and Chagas disease in Texas

(Sarkar *et al.* 2010), plague in California (Holt *et al.* 2009), West Nile virus (Larson *et al.* 2010) and leishmaniasis vectored by sand flies in North America (González *et al.* 2010).

A more thorough understanding of the relationship between *O. hermsi* and environmental conditions is necessary to understand the current distribution of the tick and predict suitable areas yet unknown, thereby better defining areas of potential human risk of infection. Identifying environmental conditions necessary for the persistence of *O. hermsi* allows for the identification of potential areas of disease emergence in the face of climate change by projecting known climate limitations onto future climate surfaces. Vial (2009) suggests that because soft ticks occupy a stable microclimate, the broad-scale analyses applied to hard ticks should not be applicable to them. Because so little is known about the ecology and behavior of soft ticks, macroclimate-scale analyses, as performed here, may be useful to accurately define the distribution of these ticks and other nidicolous (nest-dwelling) species.

This research investigated the current and future potential distribution of *O. hermsi*, the soft-bodied tick vector of *B. hermsii*, in western North America. We used the Maxent model (Phillips *et al.* 2004, 2006) to predict the geographic distribution of *O. hermsi* and thus, indirectly also predict the potential for the presence of *B. hermsii*. Applying this type of model will provide a basis for guiding future research efforts in North America and provide a public health service. Tick-borne relapsing fever is underreported in the United States, due in part to the lack of information on the exact location of endemic foci, the generality of symptoms, and because most physicians have little or no experience with TBRF patients. We used known locations of *O. hermsi* and *B. hermsii* to identify the current potential distribution in western North America and applied these environmental constraints to model the effects of climate change on their distribution in the year 2050. The objectives of this research were to: 1) present

the first detailed distribution map of *O. hermsi*, 2) assess the effect of climate change on this distribution, and 3) evaluate the potential to use the proposed distribution map as a risk assessment tool for medical practitioners.

## 5.3 Methods

### 5.3.1 Presence data

We used 40 georeferenced presence points that included three types of data (Table 5-1): 1) human TBRF cases with known point of exposure, 2) documented presence of *O. hermsi*, and 3) locations of rodents that tested positive for the presence of relapsing fever *Borrelia* antibodies. Most human cases were followed up by a case investigation including complete travel histories to identify the most likely point of exposure. These sites included several popular vacation destination lakes in Washington, Idaho, and California, as well as several other locations along the Cascade, Sierra-Nevada, San Bernardino and Rocky Mountain ranges (Dworkin *et al.* 2002). *O. hermsi* has been documented desperately in many of these areas (Longanecker 1951). Since *B. hermsii* is vector-specific we were confident that confirmed human cases represented areas where *O. hermsi* was present even if no specimens were collected, especially if the point of exposure was consistent with known endemic foci of *B. hermsii*. The resulting model estimated the potential distribution of *O. hermsi* under current climate conditions, which thereby represents the potential human risk of *B. hermsii* infection. *B. hermsii* may not be found everywhere that *O. hermsi* is predicted to occur, but the presence of the vector allows for the potential of disease emergence. To ensure that only a single presence point was located in each pixel, we eliminated points that were < 1km apart, therefore, a single presence point represents each study site around Flathead Lake described in Chapter 2.

### 5.3.2 Current and future climate data

We downloaded 19 bioclimatic data layers from the WorldClim database ([www.worldclim.org](http://www.worldclim.org); last accessed July 2010) (Hijmans *et al.* 2005) and a digital elevation model from GTOPO 30 elevation model developed by the U.S. Geological Survey's Center for Earth Resources Observation and Science (EROS) ([http://eros.usgs.gov/#/Find\\_Data/Products\\_and\\_Data\\_Available/gtopo30](http://eros.usgs.gov/#/Find_Data/Products_and_Data_Available/gtopo30); last accessed July 2010), at a spatial resolution of 30 arc-sec (~1 km). To eliminate redundant information in the model, we identified correlations between the 20 variables by creating a correlation matrix (based on Pearson correlation) using the band correction tool in the spatial analyst toolbox in ArcMap 9.3.1 (ESRI®) (Table 5-2). Variables with a correlation  $\geq 0.75$  were represented by a single variable. Redundant variables were reduced to a single variable that best represented the most extreme environmental pressure of cold and humidity tolerance. For example, minimum or maximum monthly or quarterly variables were chosen over mean or annual variables (Table 5-2). Extremes in environmental conditions were chosen due to the life-history characteristics of *O. hermsi*. This tick spends most of its life unattached to the host and remains sheltered in the relatively stable microclimate of the host's nest or burrow, thus these ticks are most likely to be affected by extreme climate events that may impact the microclimate of the ticks' environment. To avoid extrapolating too far out of the known potential range of *O. hermsi*, the geographic extent of all variables was clipped using the extract by mask feature in ArcMap 9.3.1 to only include the western three tiers of states, portions of southern Canada and Northern Mexico (Figure 5-1).

Climate change models based on the Intergovernmental Panel on Climate Change 3<sup>rd</sup> Assessment (IPCC3) were downloaded at a resolution of 30 arc-sec (~1 km) from the WorldClim



website ([www.worldclim.org](http://www.worldclim.org); last accessed July 2010), from three modeling centers: the Canadian Centre for Climate Modelling and Analysis (CCCMA), the Commonwealth Scientific and Industrial Research Organisation (CSIRO), and the Hadley Centre for Climate Prediction and Research (HADCM). Two emissions scenarios were used. The conservative B2 scenarios as put forth by the IPCC describe a world with intermediate population and economic growth, emphasizing local solutions to economic, social, and environmental sustainability. The more extreme A2 scenarios describe a very heterogeneous world with high population growth, slow economic development and slow technological change (IPCC 2000). Predicted minimum and maximum temperature and precipitation were downloaded for each month for the year 2050. Monthly climate estimates were transformed into the 19 Bioclim variables using the Bioclim feature in the freely available DIVA-GIS program (<http://www.diva-gis.org/>, last accessed June 2011; Ramírez and Bueno-Cabera 2009). The 19 Bioclim variables were clipped to the same extent as the current variables.

### **5.3.3 Maxent modeling**

The predicted distributions of *O. hermsi* and *B. hermsii* were modeled using Maxent v. 3.3, (<http://www.cs.princeton.edu/~schapire/maxent/>; last visited February 2011), a machine-learning program that estimates the probability of presence based on several environmental variables (Phillips *et al.* 2006). The Maxent algorithm is based on the principle of maximum entropy and estimates the probability distribution, subject to the constraint that the distribution follows the observed averages of the presence points. Thus, there is a constraint placed on the model to ensure that the distribution reflects information contained in the presence points and to avoid over fitting of the model (Elith *et al.* 2011). Maxent requires only presence data for input

(Phillips *et al.* 2006) and utilizes background data to inform the model about the entire distribution of each environmental variable (Elith *et al.* 2006; Phillips *et al.* 2006). Some programs like GARP create pseudoabsence points, which may not represent true absence, which potentially confounds model results (Peterson and Cohoon 1999). Other methods such as regression require true absence data, which are rarely absolute in disease systems; it is often difficult to confirm the absolute absence of a disease due to sampling challenges including cryptic species, sampling bias, etc. The model produces an estimate of the suitability of each pixel on the map as a function of the environmental variables contained in that cell and the variable values at presence points (Elith *et al.* 2006).

We ran ten replicate runs for cross-validation. The presence data were randomly split into ten equal-size groups and models were created leaving out each group in turn; all points were randomly chosen using the “random seed” option. This cross-validation technique is useful for small sample sizes, as it ensures that all occurrence data points are used to validate the model. Cross-validated receiver operating characteristic (ROC) curves were created to show the variability between models. Model fit was assessed using the area under the curve (AUC) statistic which represents the probability that a presence point chosen at random will rank higher than an absence (background) point (Hanley and McNeil, 1982). AUC values range from 0-1, with a value of 1 representing a perfect model, while a value of 0.5 indicates the model performs no better than random (Elith *et al.* 2006; Phillips and Dudik 2008). Models with AUC of  $> 0.75$  are considered potentially useful (Elith *et al.* 2006). Default parameters included “Auto features”, regularization parameter = 1, 10,000 random background points, and jackknife to measure variable importance in testing and training datasets and model performance.

## 5.4 Results

The distribution of suitable environmental conditions for the presence of *O. hermsi* and therefore potentially *B. hermsii* as well, was created in Maxent based on 10 variables. The predicted probabilities corresponded well with presence points; more than 90% of presence points (37 out of 40) occurred in areas with greater than 50% predicted probability of occurrence. Suitable areas occurred throughout the known distribution of TBRF and showed additional areas of high predicted suitability (Figure 5-2). High probabilities occurred in known TBRF endemic areas of coniferous forests at a range of elevations in mountainous regions throughout California, Washington, Oregon, the Idaho panhandle, southern British Columbia, the Flathead Valley in western Montana, and the north rim of the Grand Canyon (Figure 5-2). Areas of high suitability were also identified in areas not previously identified as TBRF foci including areas of northern Baja, the southern Big Horn Mountains and Laramie Mountains in Wyoming, and additional smaller foci in southern Nevada and southeastern Utah (Figure 5-2).

Pearson correlation analysis resulted in nine climate variables that were < 75% correlated with other variables used in the model and elevation (Table 5-2; shown in bold). Average training AUC for the 10 replicate runs was 0.982 (SD = 0.003) and average test AUC for replicate runs was 0.957 (SD = 0.029). Four temperature-related climate variables and precipitation during the warmest quarter contributed greater than 75% of model fit (Table 5-3). Temperature extremes contributed relatively equally to the model and included the minimum temperature during the coldest month (BIO6), mean temperature of the wettest month (BIO8), maximum temperature during the warmest month (BIO5) and annual temperature range (BIO7). The highest contributing precipitation variable was precipitation of the warmest quarter (11.3%). All remaining variables contributed 22.9% to the model.

Jackknife estimates assessed the training, testing, and AUC regularization gains for the model (Figure 5-3). These estimates showed how much better or worse the model did with only a single variable as well as without that single variable, for all variables in the model. The environmental variable with highest regularized training gain was the minimum temperature of coldest month (BIO6), which contained more information that was not explained by the other variables (shown by the light blue/aqua colored bar in Figure 5-2). Jackknife results on training, testing, and AUC showed a similar pattern as observed in Table 5-3. The variables with the most information not explained by other variables for the training set included the minimum temperature during the coldest month (BIO6) and precipitation during the wettest month (BIO13). When testing data were concerned, jackknife plots showed that minimum temperature during the coldest month (BIO6) and maximum temperature during the warmest month (BIO5) were the most influential to the model when used alone. Maximum temperature during the warmest month (BIO5) had the most information not explained by other variables, as can be seen by the decrease in test gain when this variable was omitted (Figure 5-3). Values shown are averages for all replicate runs.

Logistic response curves illustrated that the probability of presence of the tick changed as the variable values changed. Each curve showed the effect of an individual variable on the model and showed the dependence of the predicted suitability on each of the variables shown (Figure 5-4). The peak for each curve corresponded to the threshold at which the probability of presence of *O. hermsi* was highest: 1) minimum temperature of the coldest month = 18°F, 2) mean temperature of the wettest quarter = 35°F, 3) maximum temperature of the warmest month = 79°F, 4) temperature annual range (BIO5-BIO6) = 61°F, and 5) precipitation of warmest

quarter = 3.13". The predicted logistic probability distribution of *O. hermsi* and *B. hermsii* is shown in Figure 5-2 and the total area (km<sup>2</sup>) in each probability class is shown in Table 5-4.

Projections of the current model onto 6 future climate models for the year 2050 with two emissions scenarios (A2 and B2) showed an obvious shift in the potential distribution of the tick and a decrease in the proportion of area predicted to have high probabilities of presence of tick-borne relapsing fever (Figure 5-5). The predicted distribution showed an apparent geographic shift to the east and to higher mountain ranges in Wyoming and Colorado. The extreme A2 emissions scenarios for all three models predicted a dramatic decrease in the amount of high probability areas and therefore an increase in the amount of area with low probability. The more conservative emissions scenarios (B2) for the three models showed that similar patterns of predicted suitability and probabilities remained high (> 0.50) in many areas of northwestern Wyoming, north central Colorado and northeastern Utah (Figure 5-5).

## 5.5 Discussion

The model presented here helps to better define the environmental niche for tick-borne relapsing fever caused by *B. hermsii* and vectored by *O. hermsi* in the western United States and for identifying areas of increased risk for human disease. The model supports previously known endemic foci and also provides insight into additional areas suitable for *O. hermsi* and therefore the potential threat for human infections with *B. hermsii*. Areas with high probability of presence include the entire Sierra Nevada range in eastern California, the Cascade Mountains stretching through Washington and Oregon, and finally the northern Bitterroot Mountains in Idaho as well as much of the Idaho panhandle including areas around Coeur d'Alene, Bonners Ferry, Priest Lake, and eastern Washington near Spokane, the Flathead Valley in Montana, and

finally the north rim of the Grand Canyon. The modeled probability distribution also identified areas where the probability of presence is high, but no reports of relapsing fever have been reported (Figure 5-2). These areas include small but highly suitable regions in northern Baja California, Mexico, the southern Big Horn Mountains and Laramie Mountains in Wyoming, and additional smaller foci in southern Nevada and southeastern Utah.

The shape of the response curves (Figure 5-4) demonstrated the narrow environmental suitability range for ticks, with dramatic peaks in the range of conditions most suitable. This is consistent with previous findings that soft ticks show a strict and narrowly defined tolerance to temperature and humidity for development and activity (Vial 2009). Logistic probability distributions indicated that *O. hermsi* are semi-cold tolerant, with an optimum minimum temperature during the coldest month of approximately 18°F and mean temperature of the wettest month of approximately 35°F. Additionally, areas with high probability have mild warm temperature tolerances; maximum temperatures during the warmest month of the year reach the highest probability around 79°F and an annual temperature range of about 61°F. Finally, areas with high predicted probability receive roughly 3” of rain during the warmest quarter.

Climate change models trained on the existing potential distribution showed a decrease in suitable future environments for *O. hermsi* and therefore *B. hermsii* across western North America. There was a predicted shift in the distribution with suitable areas moving from the lower elevation, presumably warmer climates, to climates at higher elevations where conditions may become more suitable. High predicted probability regions in the year 2050 were found in northeastern Wyoming, near Yellowstone National Park, an area encompassed by the Teton and Wind River Mountain ranges, and the western front of the Rocky Mountains in Colorado. Climate change models for the predicted probability distribution in the year 2050 showed an

overall decrease in the highest probability category ( $> 0.75$ ). In fact, all three models run under the extreme emissions scenarios (A2) predicted no areas to have a probability of presence  $> 0.75$ , while the more conservative emissions scenarios (B2) showed a dramatic decrease from 115,205 km<sup>2</sup> for current predictions to 82,231 km<sup>2</sup>, 73,761 km<sup>2</sup>, and 15,508 km<sup>2</sup> for climate change models CCCMA, CSIRO, and HADCM, respectively. Geographic areas predicted in the lowest probability category ( $< 0.05$ ) also decreased across all models except CSIRO-A2, which showed a slight increase in predicted area (Table 5-4).

We did not consider additional ecological factors that may contribute to the distribution of the tick and pathogen. For example, the primary rodent hosts implicated in maintaining *O. hermsi* and *B. hermsii* are tree squirrels (*Tamiasciurus* spp.) and chipmunks (*Tamias* spp.). We did not explicitly map the environmental distribution of these species, but we did overlay distributions of both species complexes (Figure 5-6) (Columbia University 2008). Distributions of these rodent species completely overlap the predicted probability distribution of *B. hermsii* and *O. hermsi* for both current and future predicted distributions. We did not attempt to model future distributions of these rodent species; however, if the ranges do not change substantially, there may be adequate hosts in the future for the predicted shift in the geographic distribution of these ticks and spirochetes based on a warmer climate.

Additionally, we did not consider the dispersal ability of either the tick vector or the spirochete. Dispersal of infected or uninfected *O. hermsi* and the potential for infected hosts to disperse *B. hermsii* across the landscape is not well understood, however the possibility for aerial dispersal exists for both organisms. *O. hermsi* are known to associate with and feed on wild birds and bats (Gregson 1949; Longanecker 1951; Furman and Loomis 1984; Thompson *et al.* 2002; Schwan *et al.* 2003; Bunikis *et al.* 2004; Fischer *et al.* 2009). The role of birds in

dispersing pathogens infectious to humans across the landscape is well documented (see Tsiodras *et al.* 2008). The possibility of the dispersal of *O. hermsi* via aerial vertebrates is uncertain, however birds are well-known dispersers of *Ixodes* ticks that transmit Lyme disease spirochetes and tick-borne encephalitis virus (Anderson *et al.* 1986; Nichols *et al.* 1996; Durdern *et al.* 1997; Rand *et al.* 1998; Scott *et al.* 2001; Waldernstrom *et al.* 2007). Finally, humans should not be ruled out as potential dispersers of *O. hermsi*. Human cases of TBRF are often reported after visiting popular tourist destinations and *O. hermsi* has been found in sleeping bags and bedding from a cabin (Beck 1942; Cooley and Kohls 1944; Schwan and Winkler 1984).

Many environmental niche models of vector-borne diseases projected onto future climates show not only a shift in species distribution, but often an increase in the amount of suitable habitat and thus a greater threat to public health. Studies of *Ixodes*/Lyme disease systems in North America and Europe consistently predict a continued expansion or range to higher latitudes (Randolph 2001; Ogden *et al.* 2006). The range of leishmaniasis and their sand fly vectors are also predicted to expand in the face of climate change in North America and in Portugal (Casimiro *et al.* 2006; González *et al.* 2010). Similar trends have been predicted in the southern hemisphere, where mosquito-borne viruses are expected to expand southward as temperatures rise (Russell 1998). The TBRF system modeled here showed that overall risk may decrease as the amount of suitable geographic area decreases, but the predicted distribution does follow observed trends of moving to higher, presumably cooler, climates. A similar trend was predicted for tick-borne encephalitis (TBE) in Europe, where by 2080 the risk of TBE may have practically disappeared with endemic areas confined to very small geographic islands with suitable climates (Randolph 2001).



Few field studies, other than site investigations associated with human infections, of tick-borne relapsing fever caused by *B. hermsii* and vectored by *O. hermsi* have been done. Our study described in other chapters of this dissertation is the exception along with a single monitoring program in California implemented in cooperation with the California Department of Health, the U.S. Forest Service, and the Rocky Mountain Laboratories, along with records of field investigations that date back to the mid 1930's (Beck 1937). Despite TBRF being a reportable disease in many of the United States where it is endemic, less than 25 infections are reported annually (<http://www.cdc.gov/ncidod/dvbid/relapsingfever/>) probably due, in part, to misdiagnosis. Infection poses little threat of mortality except to the fetus of pregnant women. This research should provide additional information to researchers interested in studying the ecology of relapsing fever and provide health care practitioners with a better understanding of where threatening foci exist. Ultimately, we hope to enhance recognition and increase the likelihood of diagnosis of TBRF. Many of the areas with high probability of presence are recreational sites that experience high numbers of human visitation and use. This research will help managers in those areas to warn visitors of the potential risks of contracting relapsing fever and what the preventative measures are that could be undertaken to lessen the risk of exposure. Visitors to endemic areas should be made aware of potential threats so that if they do contract the disease and return home, they can advise the attending physician that they had visited an endemic area for tick-borne relapsing fever.

Finally, as mentioned previously, two other species of soft ticks in North America are vectors for relapsing fever *Borrelia*, *O. parkeri* and *O. turicata* (Davis 1942). Modeling the potential distribution of these other *Ornithodoros* species to determine if there is any environmental overlap in distributions with *O. hermsi* might offer insights for understanding this

vector-pathogen specificity. Additionally, with future climate changes, vector species may begin to overlap, potentially providing the opportunity for the adaptation of these ticks to transmit additional relapsing fever *Borrelia*. The model presented here only utilized 40 locations where *O. hermsi* is known, and future research should attempt to verify the model for the current distribution of *O. hermsi* and *B. hermsii* and to expand on the known distribution of these species. The distribution map can provide researchers with potential previously unidentified “hot spots” to investigate. The high correlation of known presence points with areas of high predicted suitability suggest the model presented here is a good representation of the risk for human TBRF risk.

Table 5-1. Description of 40 georeferenced presence locations of *O. hermsi*, *B. hermsii* infected hosts, hosts with antibodies specific to relapsing fever spirochetes, and isolates resulting from human cases with known site of exposure.

Location	Location
Browne Mtn., Spokane Co., WA <sup>1*</sup>	East of Yellow Bay, East side Flathead Lake, Lake Co., MT <sup>6*</sup>
West shore of Okanagan Lake, Kelona, B.C. <sup>2*</sup>	Melita Island, Flathead Lake, Lake Co., MT <sup>6*</sup>
Badger Mtn., near Waterville, Douglas Co., WA <sup>3*</sup>	Between Polson and Big Arm, Lake Co., MT <sup>6</sup>
Echo Summit, Eldorado Co., CA <sup>3</sup>	North Rim of Grand Canyon National Park, Coconino Co., AZ <sup>7*</sup>
Bonner's Ferry, Boundary Co., WA <sup>3</sup>	Manzanita Lake Campground, Lassen Volcanic National Park, Shasta Co., CA <sup>8‡</sup>
Winthrop, Okanogan Co., WA <sup>3</sup>	Blue Lake Campground, Modoc National Forest, Modoc Co., CA <sup>8‡</sup>
Newport, Pend Oreille Co., WA <sup>3</sup>	Laguna/El Prado Campground, Cleveland National Forest, San Diego Co., CA <sup>8‡</sup>
West side of Lake Coeur d'Alene, Kootenai Co., ID <sup>3</sup>	Crooked Creek Station, Inyo National Forest, Inyo Co., CA <sup>8‡</sup>
Spirit Lake, Kootenai Co., ID <sup>3</sup>	Lake Sabrina Campground, Inyo National Forest, Inyo Co., CA <sup>8‡</sup>
East side of Lake Coeur d'Alene, Kootenai Co., ID <sup>3</sup>	Swall Meadows, Inyo National Forest, Inyo Co., CA <sup>8‡</sup>
Loon Lake, Stevens Co., WA <sup>3</sup>	Lee Vining Ranger Station, Inyo National Forest, Inyo Co., CA <sup>8‡</sup>
Colville, Stevens Co., WA <sup>3</sup>	Four Jeffery Campground, Inyo National Forest, Inyo Co., CA <sup>8‡</sup>
West of Mt. Hebron, Siskiyou Co., CA <sup>4</sup>	Holocomb Valley Campground, San Bernardino National Forest, San Bernardino Co., CA <sup>8‡</sup>
Alpine Meadows, West Lake Tahoe, Placer Co., CA <sup>4</sup>	Krakatoa Island, Mono Lake, Mono Co., CA <sup>9*</sup>
East side of Okanagan Lake, Kelona, B.C. <sup>2*</sup>	East of Salt Lake City, Duchesne Co., UT <sup>3</sup>
Mt. Wilson Observatory, Los Angeles Co., CA <sup>5*</sup>	Estes Park, Larimer Co., CO <sup>10*</sup>
Meeks Bay, Lake Tahoe, Eldorado Co., CA <sup>3</sup>	Cordova, Rio Arriba Co., NM <sup>11</sup>
Wild Horse Island, Flathead Lake, Lake Co., MT(South side) <sup>3*</sup>	Sheep Springs, San Juan Co., NM <sup>12*</sup>
Wild Horse Island, Flathead Lake, Lake Co., MT(North side) <sup>6</sup>	Estes Park, Larimer Co., CO <sup>11*</sup>
Yellow Bay, East side Flathead Lake, Lake Co., MT <sup>6*</sup>	Huntington Lake, Fresno Co., CA <sup>13</sup>

<sup>1</sup>Thompson *et al.* 1969; <sup>2</sup>Banerjee *et al.* 1998; <sup>3</sup>Schwan *et al.* 2007, <sup>4</sup>Fritz *et al.* 2004; <sup>5</sup>Schwan *et al.* 2009; <sup>6</sup>This research; <sup>7</sup>Boyer *et al.* 1977; <sup>8</sup>California

Department of Health Services 2005; <sup>9</sup>Schwan and Winkler 1984; <sup>10</sup>Trevejo *et al.* 1998; <sup>11</sup>K. Gage, Centers for Disease Control and Prevention, *unpublished*

*data*; <sup>12</sup>Espinoza *et al.* 1977; <sup>13</sup>T. Schwan, unpublished data. \* indicates where *O. hermsi* has also been documented. \*\* Unpublished data. ‡Indicates

presence of seropositive rodents.

Table 5-2. Pearson correlation between 19 Bioclim variables and elevation. The 10 environmental variables included in the Maxent model are shown in bold. Bold numbers within the matrix indicate variables with a Pearson correlation  $\geq 0.75$ . A short description of each variable is given in the footnote of the table.

Layer*:	ELV	BIO9	<b>BIO5</b>	BIO4	<b>BIO8</b>	<b>BIO6</b>	<b>BIO7</b>	BIO3	<b>BIO2</b>	BIO17	BIO16	<b>BIO18</b>	BIO19	<b>BIO15</b>	<b>BIO14</b>	<b>BIO13</b>	BIO12	BIO11	BIO10	BIO1
<b>ELV</b>	1																			
BIO9	-0.172	1																		
<b>BIO5</b>	-0.288	0.527	1																	
BIO4	-0.063	-0.714	-0.138	1																
<b>BIO8</b>	-0.240	0.027	0.613	0.040	1															
<b>BIO6</b>	-0.269	<b>0.843</b>	0.614	<b>-0.827</b>	0.304	1														
<b>BIO7</b>	0.089	-0.605	0.095	<b>0.923</b>	0.150	-0.727	1													
BIO3	0.089	0.687	0.532	<b>-0.818</b>	0.331	<b>0.825</b>	-0.578	1												
<b>BIO2</b>	0.291	0.257	0.708	-0.079	0.449	0.254	0.295	0.580	1											
BIO17	0.196	-0.186	<b>-0.766</b>	-0.070	-0.602	-0.298	-0.290	-0.406	-0.673	1										
BIO16	-0.163	0.142	-0.357	-0.454	-0.177	0.240	-0.614	0.131	-0.477	0.520	1									
<b>BIO18</b>	0.074	-0.251	-0.301	-0.085	0.230	-0.080	-0.161	0.022	-0.206	0.297	0.469	1								
BIO19	-0.156	0.233	-0.413	-0.427	-0.451	0.199	-0.610	0.011	-0.552	0.634	<b>0.872</b>	0.058	1							
<b>BIO15</b>	-0.382	0.240	0.416	-0.337	0.594	0.513	-0.285	0.529	0.218	-0.497	0.309	0.344	-0.016	1						
<b>BIO14</b>	0.220	-0.233	<b>-0.770</b>	-0.022	-0.591	-0.343	-0.237	-0.443	-0.660	<b>0.984</b>	0.434	0.289	0.546	-0.524	1					
<b>BIO13</b>	-0.162	0.146	-0.324	-0.461	-0.128	0.259	-0.608	0.161	-0.442	0.484	<b>0.995</b>	0.513	<b>0.838</b>	0.356	0.399	1				
BIO12	-0.086	0.080	-0.514	-0.387	-0.362	0.109	-0.585	-0.031	-0.595	0.731	<b>0.953</b>	0.379	<b>0.936</b>	0.045	0.652	<b>0.932</b>	1			
BIO11	-0.229	<b>0.809</b>	0.702	<b>-0.779</b>	0.423	<b>0.982</b>	-0.629	<b>0.873</b>	0.399	-0.410	0.148	-0.052	0.065	0.568	-0.447	0.175	-0.007	1		
BIO10	-0.420	0.531	<b>0.960</b>	-0.195	0.703	0.689	-0.034	0.530	0.551	-0.717	-0.239	-0.173	-0.342	0.538	-0.724	-0.204	-0.413	<b>0.766</b>	1	
BIO1	-0.349	0.721	<b>0.856</b>	-0.556	0.596	<b>0.905</b>	-0.396	<b>0.769</b>	0.484	-0.579	-0.008	-0.078	-0.123	0.615	-0.605	0.026	-0.189	<b>0.953</b>	<b>0.922</b>	1

\* ELV Elevation above sea level, BIO1 = Annual Mean Temperature, BIO2 = Mean Diurnal Range (Mean of monthly (max temp - min temp)), BIO3 = Isothermality (BIO2/BIO7) (\* 100), BIO4 = Temperature Seasonality (standard deviation \*100), BIO5 = Max Temperature of Warmest Month, BIO6 = Min Temperature of Coldest Month, BIO7 = Temperature Annual Range (BIO5-BIO6), BIO8 = Mean Temperature of Wettest Quarter, BIO9 = Mean Temperature of Driest Quarter, BIO10 = Mean Temperature of Warmest Quarter, BIO11 = Mean Temperature of Coldest Quarter, BIO12 = Annual Precipitation, BIO13 = Precipitation of Wettest Month, BIO14 = Precipitation of Driest Month, BIO15 = Precipitation Seasonality (Coefficient of Variation), BIO16 = Precipitation of Wettest Quarter, BIO17 = Precipitation of Driest Quarter, BIO18 = Precipitation of Warmest Quarter, BIO19 = Precipitation of Coldest Quarter

Table 5-3. Contribution of selected variables to the Maxent model. The five most influential variables contributed > 75% to explain the distribution of *O. hermsi* and *B. hermsii*.

Temperature-related variables contributed the most to explain the observed distribution produced by the model.

<b>Variable</b>	<b>BIOCLIM Variable</b>	<b>Percent Contribution</b>
Min Temperature of Coldest Month	BIO6	17.7
Mean Temperature of Wettest Quarter	BIO8	17.1
Max Temperature of Warmest Month	BIO5	15.7
Temperature Annual Range	BIO7	15.2
Precipitation of Warmest Quarter	BIO18	11.3
Precipitation of Wettest Month	BIO13	8
Elevation	ELV	6.3
Mean Diurnal Range	BIO2	5.9
Precipitation of Driest Month	BIO14	2
Precipitation Seasonality	BIO15	0.7

Table 5-4. Area (km<sup>2</sup>) of each probability class (< 0.05, 0.05-0.25, 0.25-0.50, 0.50-0.75, and > 0.75) for the predicted distribution of *O. hermsi* by Maxent. Estimates are based on the current distribution of 9 climate layers and elevation. Climatic requirements identified for current environmental conditions were projected onto future climate change models to predict the probability distribution of the tick in the year 2050. Three climate change models under two emissions scenarios were used; conservative (B2) and extreme (A2) emissions, created by the Canadian Centre for Climate Modelling and Analysis (CCCMA), the Commonwealth Scientific and Industrial Research Organisation (CSIRO), and the Hadley Centre for Climate Prediction and Research (HADCM), based on the Intergovernmental Panel on Climate Change 3<sup>rd</sup> Assessment (IPCC3).

Probability of Predicted Distribution	Current	CCCMA		CSIRO		HADCM	
		<u>A2</u>	<u>B2</u>	<u>A2</u>	<u>B2</u>	<u>A2</u>	<u>B2</u>
< 0.05	5,148,611	4,710,764	1,952,027	5,719,990	1,834,023	3,346,980	2,947,951
0.05-0.25	1,695,386	2,944,254	3,367,906	2,127,868	4,858,090	4,127,027	4,126,808
0.25-0.50	594,298	229,414	1,889,005	37,172	873,315	407,172	618,408
0.50-0.75	331,531	599	593,862	0	245,842	3,851	176,356
> 0.75	115,205	0	82,231	0	73,761	0	15,508

Figure 5-1. Map of 40 presence locations for infected hosts, hosts with *Borrelia* antibodies, *O. hermsi* collections and georeferenced points of bacterial isolates obtained from the blood of infected human patients.

Figure 5-2. Logistic predicted probability of occurrence/ecological suitability of *B. hermsi* and *O. hermsi*. Presence points (as defined in Figure 5-1) are shown in red, and probability of occurrence increases as the shading becomes darker.

Figure 5-3. Jackknife plots for: a) regularized training gain, b) regularized test gain, and c) AUC gain. Gain is how much better or worse the model performs based on the inclusion or exclusion of variables and is measured in three ways: the omission of a single variable, the inclusion of only a single variable, and the inclusion of all variables. The red bar shows model performance with all variables included. Dark blue bars show model performance with only a single variable included, while the light blue bars display model performance when a single variable is omitted. Variables with the longest blue bars have the most individual influence on the model, while light blue bars that are the shortest contain the most information that is not present in other variables in the model. Training gain (a) shows variation in model performance of presence points included in the training dataset, test gain (b) is based on model performance based on 25% of presence points withheld to test model performance, and AUC gain (c) assesses model fit as a whole.

Figure 5-4. Variable response curves produced by Maxent for the 5 most influential variables contributing to the model. Each curve shows the effect of an individual variable on the model and the dependence of the predicted suitability on each of the variables shown. Peaks for each curve correspond to the threshold at which the probability of presence is highest: 1) Min Temperature of Coldest Month = 18°F, 2) Mean Temperature of Wettest

Quarter = 35°F, 3) Max Temperature of Warmest Month = 79°F, 4) Temperature Annual Range (BIO5-BIO6) = 61°F, and 5) Precipitation of Warmest Quarter = 3.13".

Figure 5-5. Predicted changes in distribution of *O. hermsi* and *B. hermsii* in western North America based on three climate change models under extreme emissions scenarios (A2) and more conservative emissions scenarios (B2) for the year 2050. Models were created by the Canadian Centre for Climate Modelling and Analysis (CCCMA), the Commonwealth Scientific and Industrial Research Organisation (CSIRO), and the Hadley Centre for Climate Prediction and Research (HADCM), based on the Intergovernmental Panel on Climate Change 3<sup>rd</sup> Assessment (IPCC3).

Figure 5-6. Overlay of Douglas squirrel (*Tamiasciurus douglasii*) and pine squirrel (*T. hudsonicus*) distributions (hatched overlay with dark outline) and all chipmunks (*Tamias* spp.) (stippled overlay) in western North America on the: a) current and b) the year 2050 predicted distribution of *O. hermsi* and *B. hermsii* with a probability of presence > 0.50 (dark gray underlay), Center for International Earth Science Information Network (CIESIN), Columbia University. 2008. Species Distribution Grids [online data]. Palisades, NY: Socioeconomic Data and Applications Center (SEDAC), Columbia University. Available at <http://sedac.ciesin.columbia.edu/species> , retrieved [7/30/2011].



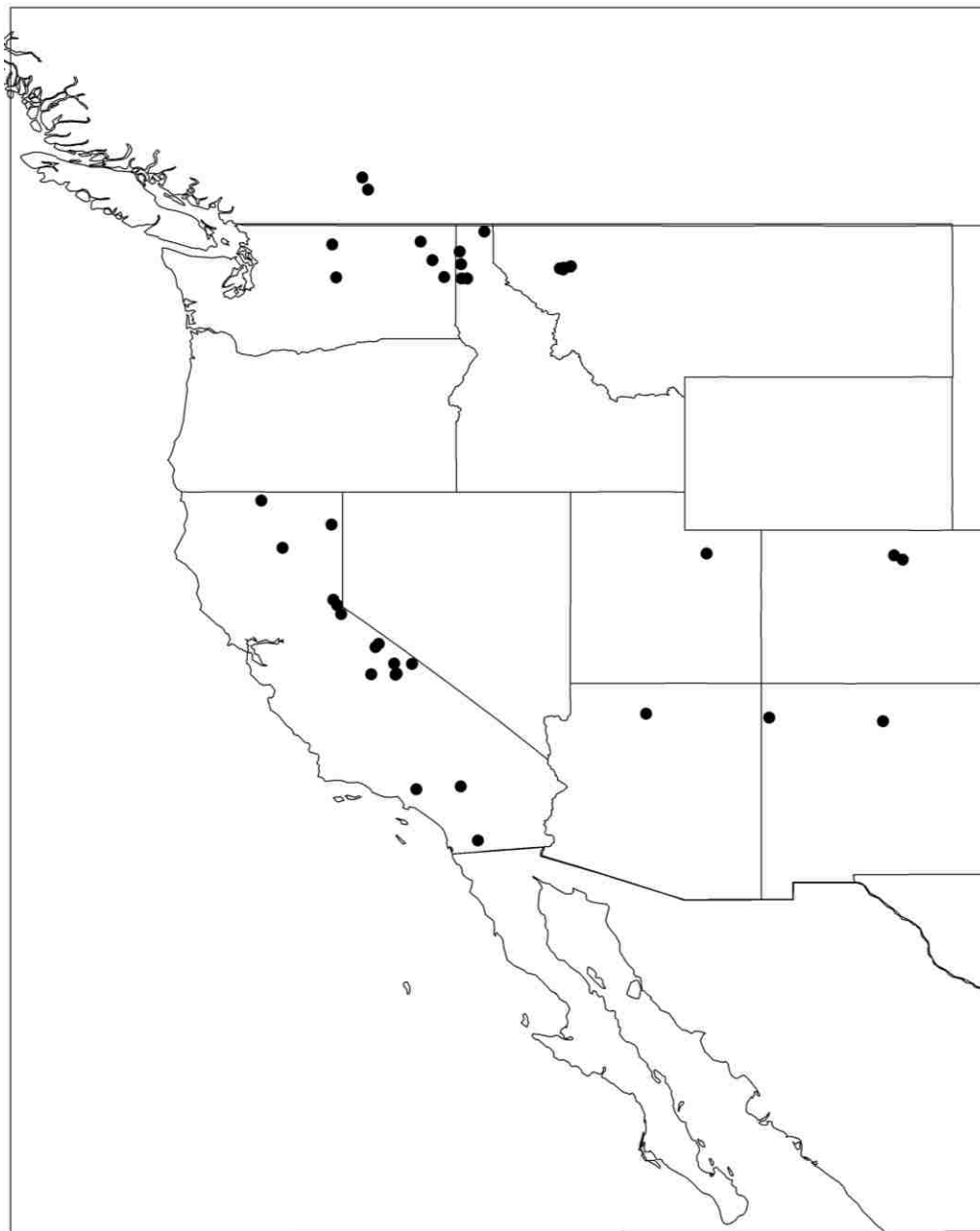


Figure 5-1.

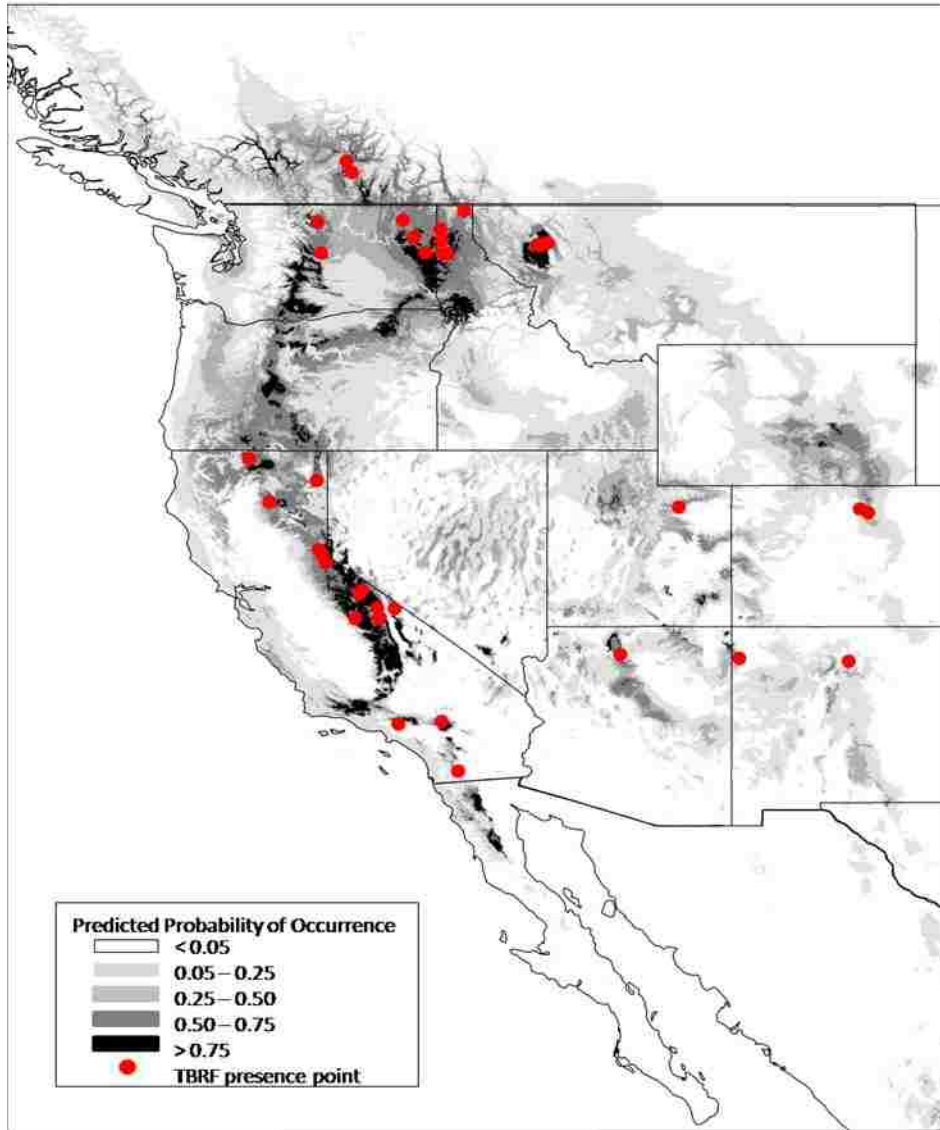


Figure 5-2.

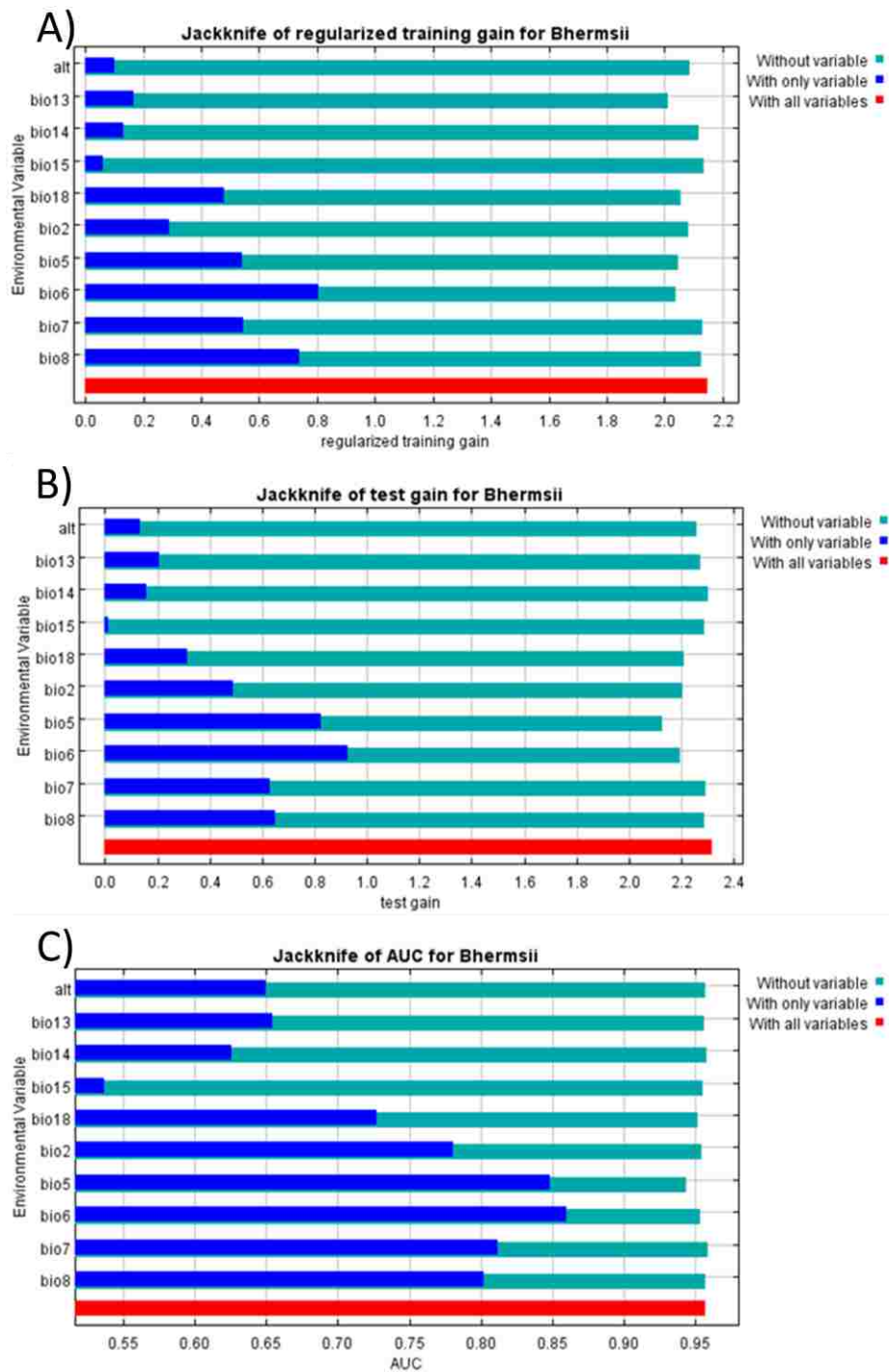


Figure 5-3.

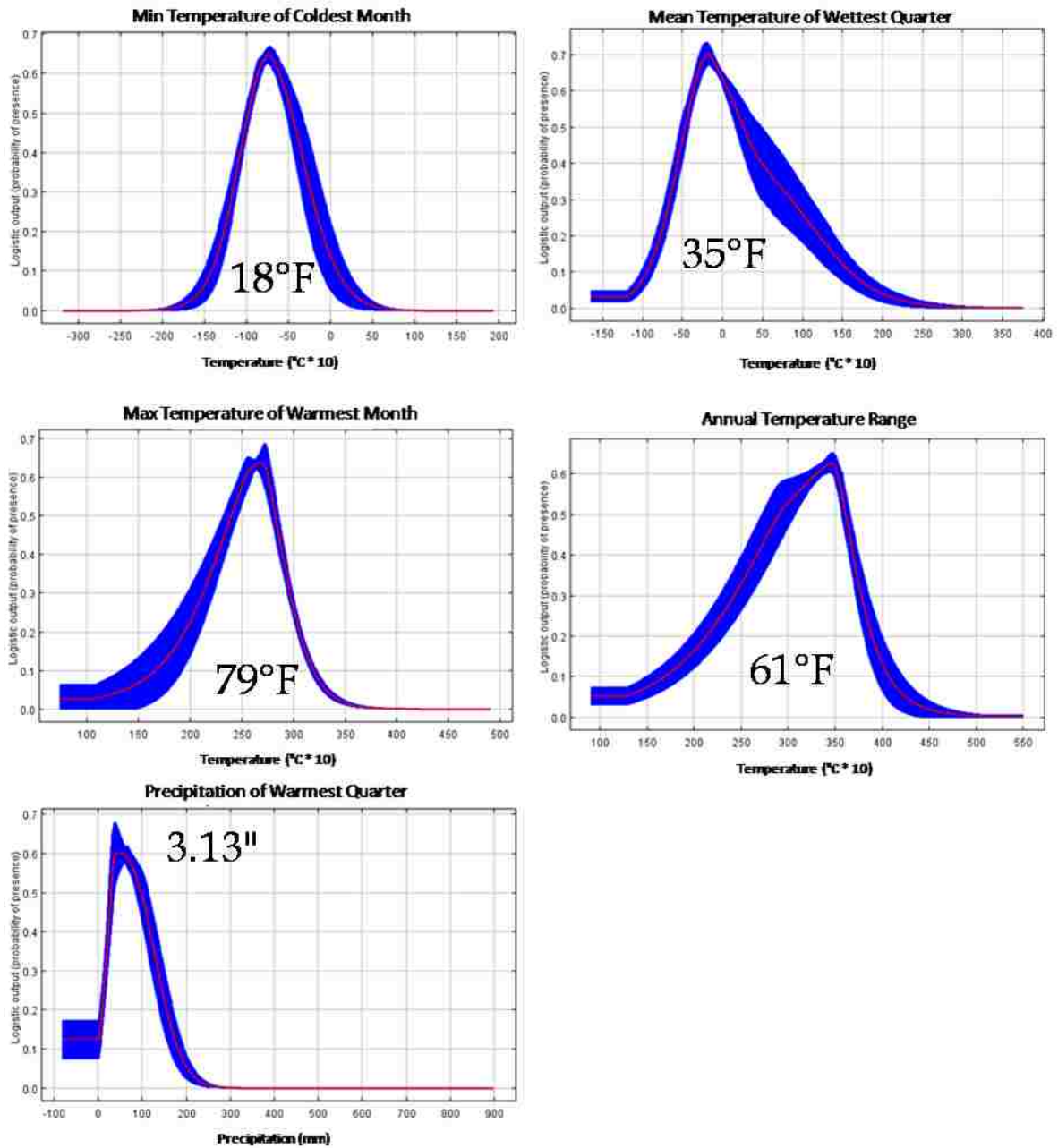


Figure 5-4.

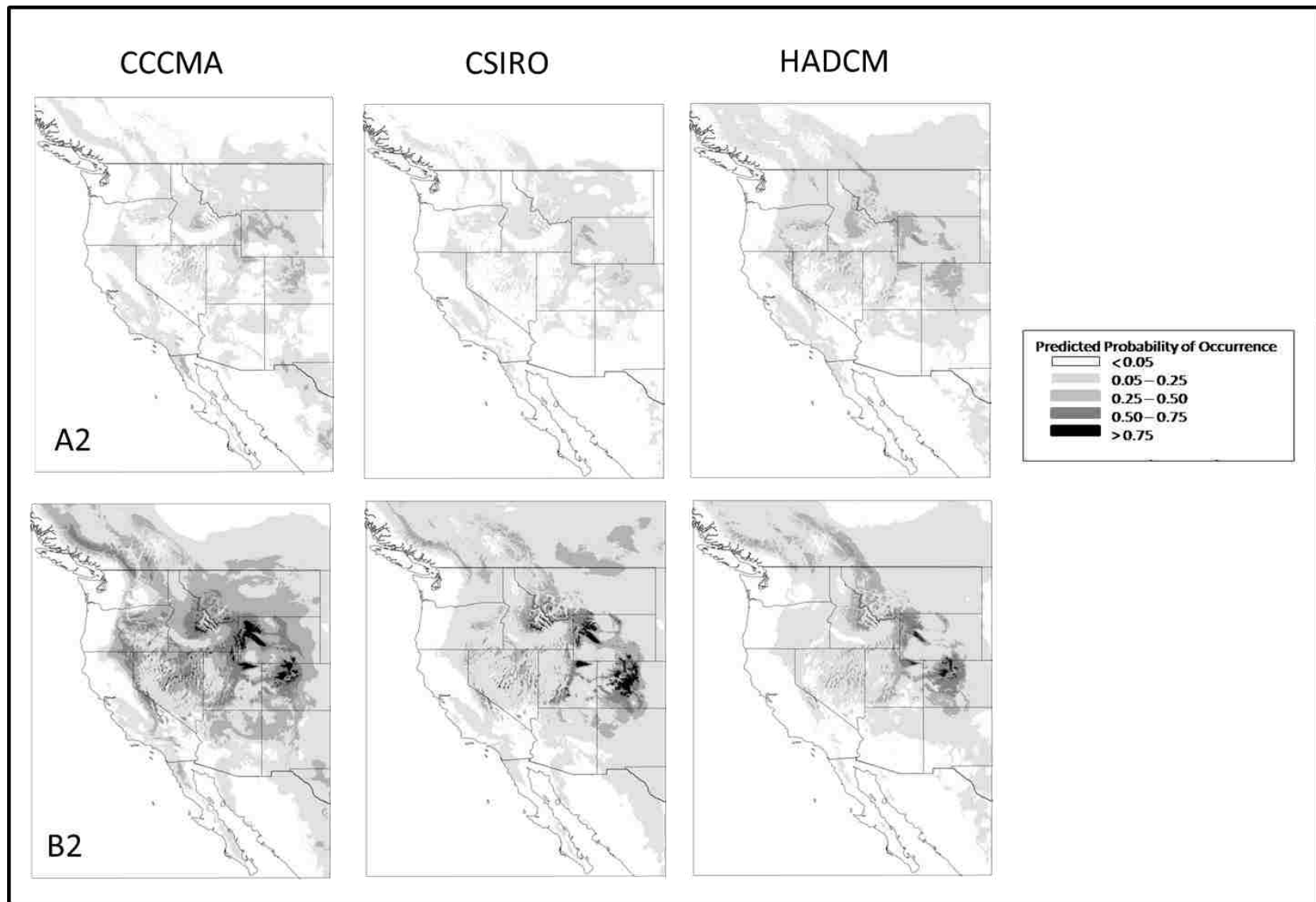


Figure 5-5.

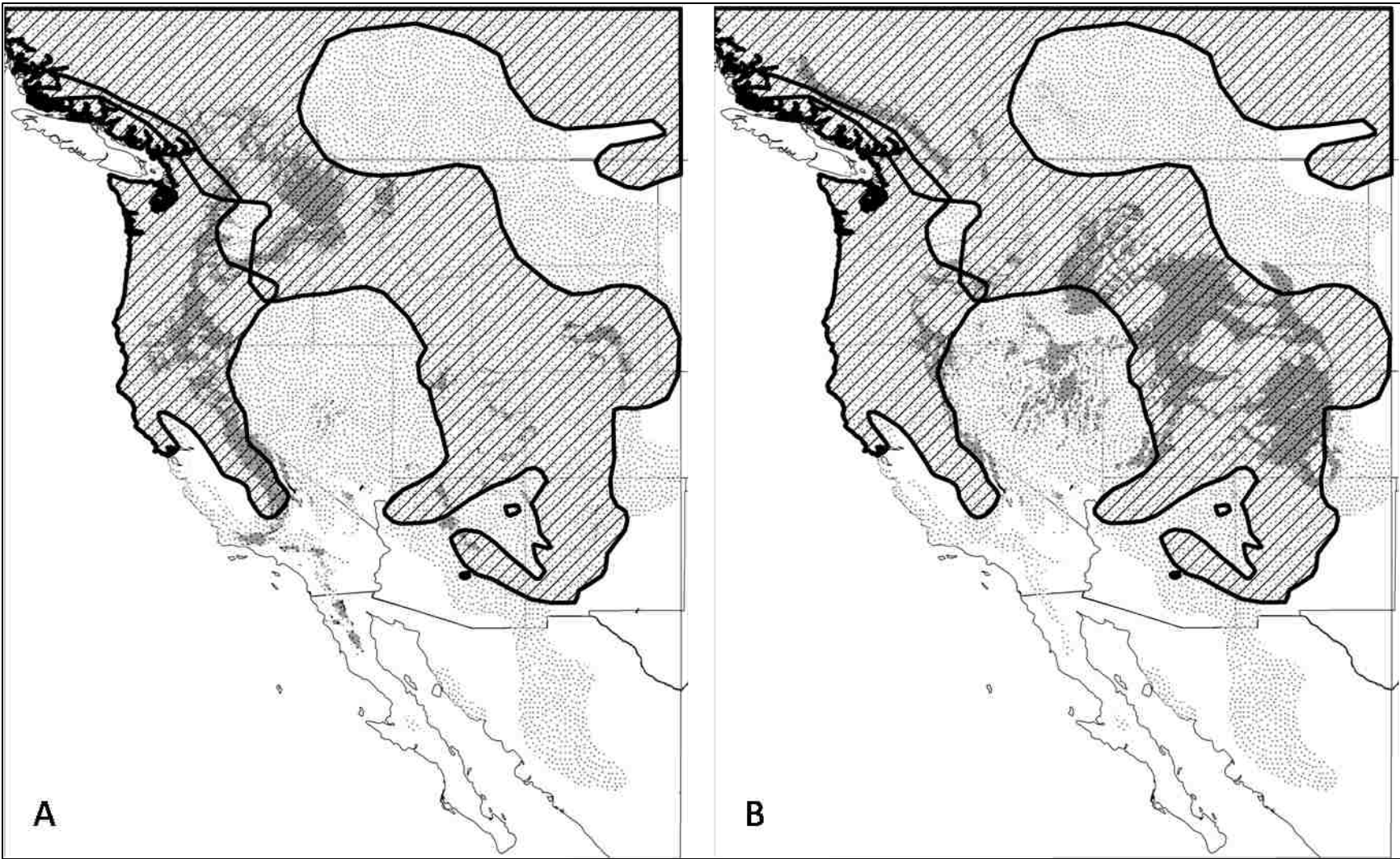


Figure 5-6.

# Appendix A – Virulence of Two Genomic Groups of *Borrelia hermsii* in deer mice (*Peromyscus maniculatus*)

## A.1 Introduction

Differences may exist in the competency among rodent species to become infected with *Borrelia hermsii* and subsequently transmit the infection to uninfected *Ornithodoros hermsi* ticks. Burgdorfer and Mavros (1970) examined several species of wild rodents including pine squirrels (*Tamiasciurus hudsonicus*), yellow pine chipmunks (*Tamias amoenus*), meadow voles (*Microtus pennsylvanicus*), northern flying squirrels (*Glaucomys sabrinus*), bushy tailed wood rats (*Neotoma cinerea*), golden-mantled ground squirrels (*Spermophilus lateralis*), Columbian ground squirrels (*S. columbianus*), and deer mice (*Peromyscus maniculatus*) for their susceptibility to infection with *B. hermsii*. Individuals were either inoculated with infected *O. hermsi* tick material or fed on by infected *O. hermsi*. All individuals were monitored daily for the presence of spirochetes in the blood. Pine squirrels, chipmunks, and voles became spirochetemic and varied in their duration and intensity of spirochetes in the blood, suggesting different potentials for transmitting spirochetes to naive ticks. Spirochetes were not detected in the blood of the other four species, including deer mice, which suggested that the other species were incompetent hosts for *B. hermsii*.

In 2008 we trapped a deer mouse infected with *B. hermsii* on Wild Horse Island, Flathead Lake, Lake Co., Montana. Infection was determined by visualizing the spirochetes in a thin blood smear with a microscope and confirmed using PCR. We performed multi-locus sequencing of *B. hermsii* genes and identified the spirochete as belonging to genomic group (GG) II. The discovery of a deer mouse infected with *B. hermsii* prompted us to repeat the

experiment performed by Burgdorfer and Mavros (1970). In the original experiment, potential hosts were either inoculated with crushed suspensions of infected *O. hermsi* or by allowing two to five experimentally infected ticks to feed on them (Burgdorfer and Mavros 1970). The infected ticks were collected during an outbreak of human tick-borne relapsing fever on Browne Mountain near Spokane, WA (Thompson *et al.* 1969). This *B. hermsii* (HS1) is a GGI spirochete (Porcella *et al.* 2005). Therefore, Burgdorfer and Mavros (1970) probably infected individuals with GGI spirochetes. We wanted to determine if GGI and GGII spirochetes showed differences in infectivity and used DAH, a GGI isolate of *B. hermsii* and MTW, a GGII isolate of *B. hermsii* to infect deer mice by intraperitoneal needle inoculation and infected tick bite.

## A.2 Methods

First, we inoculated two deer mice (RML colony New Mexico strain) with 200  $\mu$ L of PBS containing  $1 \times 10^6$  spirochetes per mL of either DAH (GGI) or MTW (GGII) *B. hermsii*. We also challenged deer mice with infection via tick bite. Five deer mice were fed upon by ticks infected with DAH (GGI) and five deer mice were fed upon by ticks infected with MTW (GGII) *B. hermsii* (Table A-1). Mice were monitored daily for spirochetemia by clipping the end of the tail. A thick-drop blood mount was prepared and 50 fields were counted using a dark-field microscope (Nikon Eclipse E600) at  $\times 400$  magnification. We quantified the density of spirochetes in the blood of deer mice infected by tick bite. A 3/8" diameter circle was etched onto a microscope slide and 2.5  $\mu$ L of blood was spread evenly within the circle (area of circle =  $71.22 \text{ mm}^2$ ). Slides were air-dried at room temperature, stained with Giemsa for 30 minutes, rinsed in de-ionized water, and air-dried at room temperature. Slides were examined under a bright-field microscope (Nikon Eclipse E800) at  $\times 600$  magnification with a 60 $\times$  oil immersion



objective (area per field = 0.126 mm<sup>2</sup>). Fifty fields were examined on each slide for the presence of spirochetes and the total number of spirochetes per milliliter of blood was determined. Mice were followed for 21 days. Two white mice (RML Laboratory Strain) were also fed on by infected ticks from both genomic groups and served as a control to ensure tick infection, as white mice are highly susceptible to both genomic groups of *B. hermsii*. Laboratory procedures were approved by Rocky Mountain Laboratories Animal Care and Use Committee (2007-39; 2010-53).

### **A.3 Results/Discussion**

The deer mouse inoculated with DAH (GGI) had a single spirochete on day one post-inoculation; however, no spirochetes were observed beyond day one in this mouse. The mouse infected with MTW (GGII) became spirochetemic on day one and spirochetes persisted in the blood continuously until day 11. Following the initial peak in spirochetemia on day four, two relapses were observed. Peak spirochetemia for each relapse was observed on days 10 and 15 (Figure A-1). No spirochetes were observed in the blood smear between days 11 to 13 and 16 to 21.

The tick-challenge experiment yielded similar results to those observed during the needle inoculation experiment. Both control white mice became spirochetemic after being fed on by infected ticks. Five deer mice were fed upon by infected nymphal ticks that transmitted MTW (GGII) spirochetes. One deer mouse expired on day one post-infection and was excluded from the analysis; three more mice expired on day 10. All four mice reached peak spirochetemia between days four and five post infection. Spirochete levels in these mice were extremely high,

reaching  $> 10^8$  spirochetes/mL. The mouse that survived until day 21 underwent two complete relapses and spirochete levels were again increasing on the final day of the experiment. There were only four days (day 6, 12, 13, and 20) when no spirochetes were observed (Figure A-2). Peaks in spirochete levels persisted for three to five days and the initial peak in spirochetemia showed the highest level of infection compared with subsequent relapses.

In sharp contrast, none of the five deer mice fed upon by *B. hermsii* DAH (GGI) infected ticks became spirochetemic, despite having been fed upon by many more infected ticks (Table A-1). Therefore, we observed striking differences in the infectivity of *B. hermsii* in deer mice depending on which genomic group the spirochete belonged.

Differences in virulence among genomic groups of *B. hermsii* and the effects on various rodent hosts have strong implications for the persistence of *B. hermsii*. Dynamical systems (susceptible, infected, recovered – SIR) models show an overall decrease in disease persistence with the addition of incompetent hosts (Chapter 3). If GGI spirochetes are unable to establish a high spirochetemia in deer mice and other hosts, such as northern flying squirrels and ground squirrels, there should be an overall decrease of prevalence of spirochete infection. However, if both genomic groups are present in an area, spirochetes may be more likely to persist if multiple rodents act as competent hosts for spirochete infection and are capable of passing the infection back to an uninfected tick. The GGII spirochete MTW used here is extremely virulent and causes high spirochetemias in laboratory mice. We aim to repeat the infection via tick bite experiments using two isolates of *B. hermsii* obtained from the Flathead Lake area in Montana to determine if other GGII *B. hermsii* are equally virulent to deer mice.

Table A-1. Number and stage of *B. hermsii*-infected *O. hermsi* fed on each deer mouse (*P. maniculatus*). N = nymphal tick stage.

<i>Borrelia hermsii</i> Strain	Mouse #	Number & Stage of Ticks
DAH(GGI)	1	51/2 <sup>nd</sup> N
	2	87/2 <sup>nd</sup> N
	3	79/2 <sup>nd</sup> N
	4	48/2 <sup>nd</sup> N
	5	88/2 <sup>nd</sup> N
MTW(GGII)	1	4/1 <sup>st</sup> N
	2	7/1 <sup>st</sup> N
	3*	16/1 <sup>st</sup> N
	4	12/2 <sup>nd</sup> N
	5	14/2 <sup>nd</sup> N

\* Died on day one post-infection, removed from further analysis.

Figure A-1. Differences in susceptibility of deer mice to infection with GGI and GGII *B.*

*hermsii*. The number of spirochetes observed in 50 microscopic fields for 21 days after intraperitoneal needle inoculation of two deer mice (*P. maniculatus*). One mouse was inoculated with *B. hermsii* DAH (GGI) spirochetes (black box) and the other mouse was inoculated with *B. hermsii* MTW (GGII) spirochetes (red circle). P.I. = post-inoculation.

Figure A-2. Spirochete densities in the blood of four deer mice (*P. maniculatus*) infected with *B.*

*hermsii* MTW (GGII) via nymphal *O. hermsi* tick bite. Data for the fifth deer mouse are not shown because it died on day one post-exposure. Three out of four mice died on day 11 and therefore data are only presented for the first 11 days. P.I. = post-inoculation. No spirochetes were observed in the five mice fed upon by ticks infected with *B. hermsii* DAH (GGI) during the 21 days following exposure to infected ticks (*data not shown*).

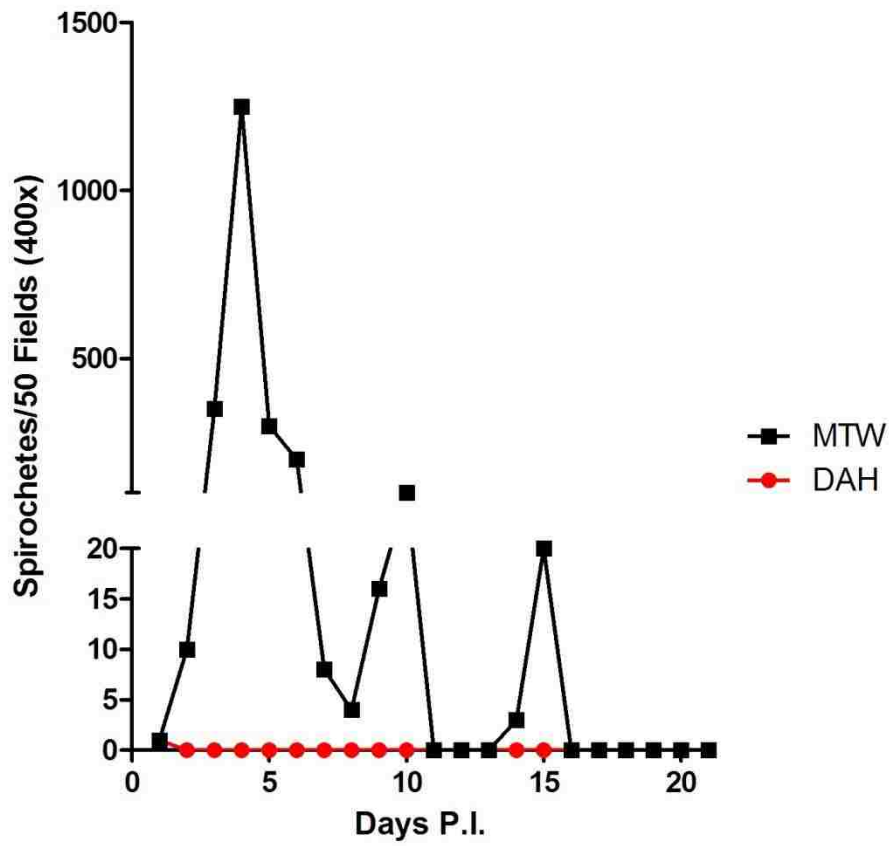


Figure A-1.

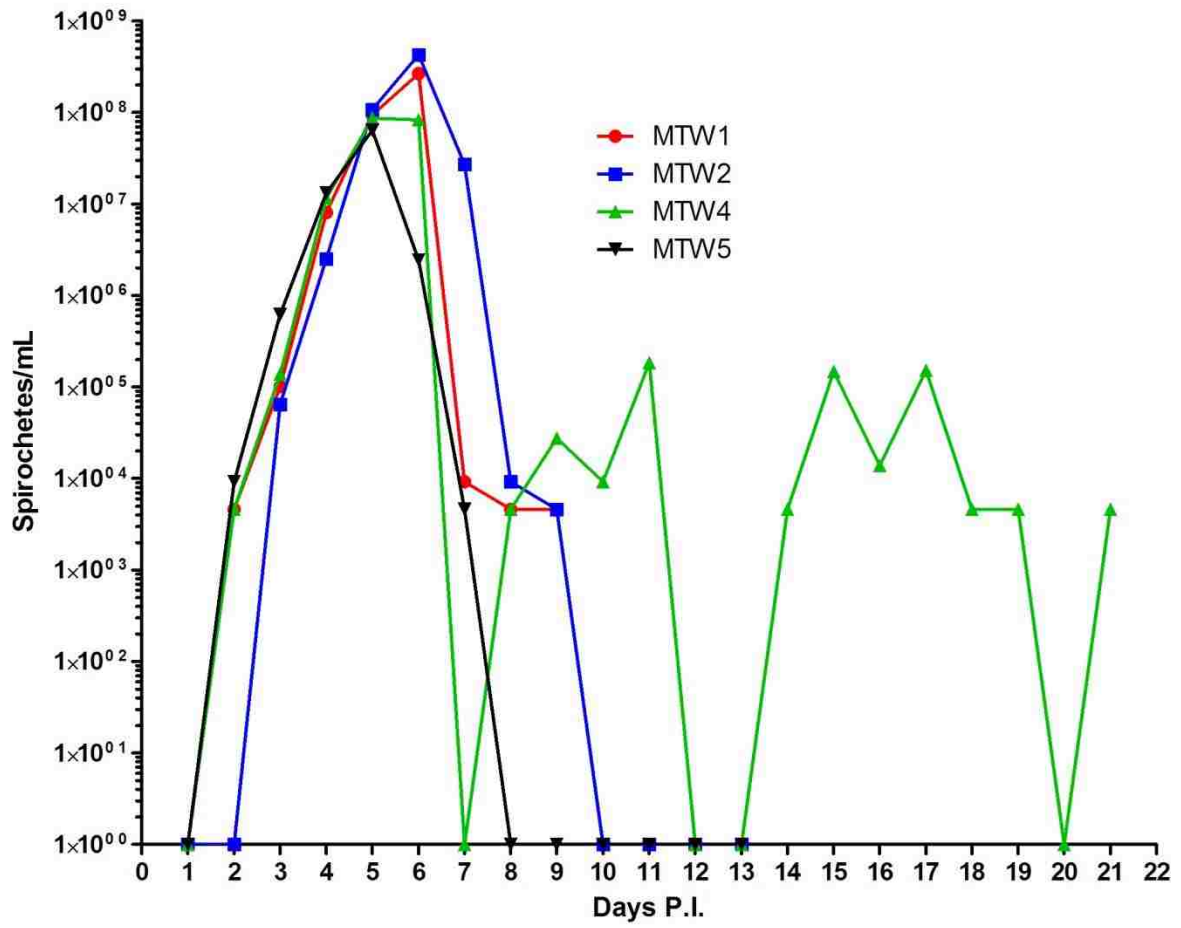


Figure A-2.

## **Appendix B – Population Genetics of *Ornithodoros hermsi*, a Vector of Tick-borne Relapsing Fever in Western North America**

### **B.1 Introduction**

Infected *Ornithodoros hermsi* transmit *Borrelia hermsii* to uninfected vertebrate hosts and infected vertebrate hosts are probably the main source of infection to uninfected *O. hermsi*; however, the mechanisms responsible for widespread dissemination of *B. hermsii* across the landscape remain unknown. The life history characteristics of *O. hermsi* make it less likely that they are dispersed long distances by hosts, however these ticks will feed on birds (Schwan *et al.* 2007). Wild birds have been shown to be infected with *B. hermsii* and found in association with *O. hermsi* (Gregson 1949, Thomas *et al.* 2002, Fischer *et al.* 2009), and bats (*Myotis* sp.) have been found in association with *O. hermsi* (Longanecker *et al.* 1951). *Ornithodoros* ticks may live > 10 years, and can survive for several (>3) years without feeding (Francis 1938). *O. hermsi* obtains a blood meal from the host in < 90 min. Additionally, these ticks are nest dwelling ticks that rarely leave the confines of the host nest or burrow. Finally, soft ticks only require a blood meal about once every three months. Associations between ticks and aerial vertebrates present the potential opportunity for dispersal of *O. hermsi* and/or *B. hermsii*. Here we determined the population genetic structure of *O. hermsi* to identify possible past dispersal events.

### **B.2 Methods**

Individual ticks were obtained from colonies of *O. hermsi* maintained at Rocky Mountain Laboratories (RML), Hamilton, MT. Colonies included the Rocky Mountain Laboratory colony (RML), the Siskiyou colony (SIS), the Wild Horse Island colony (WHI), and the Mount Wilson

colony (MTW). Little information exists regarding the history of the RML colony, but it was likely started sometime in the late 1960s from ticks collected during a human TBRF outbreak near Browne Mountain, Spokane Co., WA. The exact origin and number of founders is unknown. The SIS colony was started in 1998 following the collection of a single uninfected (with *B. hermsii*) pregnant female tick (T. Schwan *personal communication*). The Wild Horse Island colony was established with 12 *O. hermsi* collected from nest material removed from a cabin on Wild Horse Island, Lake County, MT, in which 5 human TBRF cases had been confirmed. Nine nymphs, two males and a single female were the founders of this colony (Schwan *et al.* 2003). The Mount Wilson colony was established in 2007-2008 with 3 nymphs collected in 2007 and 2008. One molted into an adult female and the others molted into males (Schwan *et al.* 2009). Ten ticks (12 from the SIS) were used from each colony for sequencing (Table B-1).

Between 2008 and 2010 we collected nest material from cavity nests in trees and snags, and material from pine squirrel (*Tamiasciurus hudsonicus*) middens to look for *O. hermsi*. Material from nests was collected into Ziploc bags and brought back to Rocky Mountain Laboratories for processing in Berlese extraction funnels. Individual ticks collected from nest material were allowed to feed on laboratory mice to determine if they were infected with *B. hermsii*. A total of 49 “field-caught” and colony ticks were included (Table B-1).

Ticks were frozen with liquid nitrogen and triturated with a mortar and pestle. DNA was extracted using the QIAGEN DNeasy Blood and Tissue Kit according to the manufacturer’s instructions. PCR was performed using the Promega GoTaq Flexi DNA polymerase (Promega Corp, USA) and 6 primers for mt16S rDNA. Primers included 16S+1 (CTGCTCAATGATTTTTTAAATTGCTGTGG), 16S+2 (TTGGGCAAGAAGACCCTATGAA),



16S+3 (ATACTCTAGGGATAACAGCGT), 16S-1 (CCGGTCTGAACTCAGATCAAGT), 16S-2 (TTACGCTGTTATCCCTAGAG), 16S-3 (AAATTCATAGGGTCTTCTTGTC) (Black and Peisman 1994), to ensure complete coverage of the locus. The PCR conditions were as follows: initial denaturation, 96°C for 3 min, followed by 35 cycles of 94°C, 30 s, 55°C, 30 s and 72°C, 2 min 30 s followed by a final extension of 7 min at 72°C. Samples were analyzed by agarose (2%) gel electrophoresis and positive samples were submitted for Sanger sequencing. Sequences were visually inspected and manually corrected using Sequencher 4.7 (Gene Codes Corporation). We obtained good sequence data for 49 ticks (Table B-1). The partial 421 bp sequence of mt16S rDNA was aligned using Geneious Pro 5.3.4 (Drummond *et al.* 2011, available at <http://www.geneious.com/>) (Figure B-1).

Ticks were assigned population groupings based on colony or collection site. Six populations were defined: 1) MTW, 2) RML, 3) SIS, 4) WHI and WHT9, 5) Melita Island ticks (MIT) and 6) Yellow Bay ticks (YBT). We used DnaSP 5.10 (Librado and Rozas 2009) to verify neutral mutations using Tajima's (1989) *D*-statistic and to check for recombination using the four gamete test developed by Hudson and Kaplan (1985). Recombination was not expected to occur between colony populations, therefore we tested each colony separately for recombination. However, we tested all Montana ticks for recombination because we have no knowledge of how often gene flow may have occurred between the islands and the mainland.

An analysis of molecular variance (AMOVA) was used to examine genetic differences within and among tick populations using the software package Arlequin 3.5 (Excoffier and Lischer 2010, available at <http://cmpg.unibe.ch/software/arlequin35>). For AMOVA analyses, ticks were separated into populations based on collection site or colony identity, Montana ticks were further separated into three groups based on collection site, i.e. Melita Island, Wild Horse

Island, and Yellow Bay.  $F_{ST}$  values were obtained to estimate genetic distances between populations.

Phylogenetic trees were generated using Geneious 5.3.4 Neighbor Joining tree building option and the HKY genetic distance model. The closely related species *O. coriaceus* was included as an outgroup and 1000 bootstrap replicates were performed. The genetic distance model was chosen using the web implemented version of j-modeltest, FindModel based on MODELTEST (Posada and Crandall 1998, available at <http://www.hiv.lanl.gov/content/sequence/findmodel/findmodel.html>).

### **B.3 Results**

A partial 421 bp sequence of the mt16S rDNA region of *O. hermsi* was obtained from 49 ticks. This region was extremely AT rich, with an AT content = 0.752. The region showed surprisingly low diversity, with only seven variable bases (Table B-1, Figure B-2). No recombination was detected within any population of ticks. Multiple ticks from individual colonies were included to ensure colonies were genetically pure, as would be the prediction, since colonies are housed and maintained individually at RML.

Seven haplotypes were identified in the mitochondrial 16S rDNA sequences of the 49 *O. hermsi* examined. Most haplotypes differed from its nearest neighbor by only a single base (Table B-1). All WHI colony ticks and field-collected ticks from Melita Island were the same haplotype (Haplotype 1). All MTW colony ticks were the same haplotype (Haplotype 2), as were all RML colony ticks (Haplotype 3). Ticks from the SIS colony represented two distinct haplotypes (Haplotype 4 and Haplotype 5). A single field-caught tick from Wild Horse Island (WHT9) and a single field-caught tick from Yellow Bay were the same haplotype (Haplotype 6).

Finally, all other field-caught Yellow Bay ticks had identical haplotypes (Haplotype 7), despite these ticks having been collected from 3 different nests.

AMOVA analysis of populations revealed that most genetic variation occurred between populations ( $F_{ST} = 0.752$ ,  $p < 0.05$ ) and when all pair-wise population comparisons of  $F_{ST}$  were considered, only Melita Island ticks and Wild Horse Island ticks had a non-significant  $F_{ST}$ , suggesting a lack of genetic variation among the ticks on these two islands (Table B-1). Pair wise  $F_{ST}$  values supported population differentiation (Table B-4). A neighbor-joining tree rooted with *O. coriaceus*, supported the topology depicted in the haplotype analysis (Figure B-3).

## **B.4 Discussion**

Although sample size was relatively small and genetic variation very low in the *O. hermsi* ticks sampled, there is evidence of dispersal among Melita Island, Wild Horse Island and Yellow Bay, on the mainland of Flathead Lake, Lake Co., MT. Ticks collected from these areas between 2008 and 2009 and ticks collected from a cabin on Wild Horse Island during a human outbreak investigation were represented by three haplotypes. Ticks from WHI and MEL had the same haplotype while ticks collected at YB had a different haplotype. Further, one tick from WHI and one tick from YB had the same haplotype that was different from all of the aforementioned haplotypes. If each location was only represented by a single haplotype and each location had a unique haplotype, we would infer that there is no mixing of these populations. On the other hand, the same haplotype at multiple locations suggests that dispersal events between islands and mainland may have occurred in Montana.

It is inconceivable that these ticks have dispersed any distance without the facilitation of a host; however, it is also unlikely that *O. hermsi* are transported long distances by rodents.

Primary hosts of *O. hermsi* that occur on both the islands and the mainland in this area are pine squirrels and deer mice (*Peromyscus maniculatus*). More probable is the dispersal of *O. hermsi* via an aerial vertebrate. *Ornithodoros hermsi* and *B. hermsii* have both been found in association with both birds and bats (Gregson 1949, Longanecker *et al.* 1951, Thomas *et al.* 2002, Schwan *et al.* 2007, Fischer *et al.* 2009). The feeding behavior of *O. hermsi* makes it more plausible that these ticks may be more likely to be transported long distances by birds or bats rather than terrestrial vertebrates. *Ornithodoros hermsi* is able to obtain a blood meal in as little as 15 minutes but will often remain attached feeding for an hour or more and feed primarily at night when diurnal rodent hosts return to the nest/burrow. Results from Chapter 2 show, however, that nocturnal rodents are also regularly exposed to infection with *B. hermsii*. Further investigation into the potential role played by aerial vertebrates in the long distance dispersal of *B. hermsii* and/or *O. hermsi* should be explored.

Table B-1. Location, origin, date of collection, and haplotype of 49 *O. hermsi* ticks from which mitochondrial 16S rDNA sequence was obtained. Tick samples consisted of *O. hermsi* maintained in laboratory colonies at Rocky Mountain Laboratories, Hamilton, MT and *O. hermsi* collected during field studies described in Chapter 2 (MIT, WHT, and YBT). MTW = Mount Wilson colony, RML = Rocky Mountain Laboratory colony, SIS = Siskiyou County colony, WHI = Wild Horse Island colony, MIT = Melita Island ticks, WHT = Wild Horse Island tick, YBT = Yellow Bay tick.

Name	Location	Date of Collection	Haplotype #	Haplotype Seq.	Name	Location	Date of Collection	Haplotype #	Haplotype Seq.
MIT26	Field/log	2009	1	CATTGTA	SIS1	Colony	1998	4	CTTAATG
MIT27	Field/log	2009	1		SIS11	Colony	1998	4	
MIT30	Field/log	2009	1		SIS13	Colony	1998	4	
WHI1	Colony	2002	1		SIS14	Colony	1998	4	
WHI2	Colony	2002	1		SIS15	Colony	1998	4	
WHI3	Colony	2002	1		SIS17	Colony	1998	4	
WHI11	Colony	2002	1		SIS18	Colony	1998	4	
WHI12	Colony	2002	1		SIS19	Colony	1998	4	
WHI13	Colony	2002	1		SIS2	Colony	1998	5	CATTGCG
WHI14	Colony	2002	1		SIS12	Colony	1998	5	
WHI15	Colony	2002	1		SIS16	Colony	1998	5	
WHI16	Colony	2002	1		SIS20	Colony	1998	5	
MTW1	Colony	2007-08	2	TACTATG	YBT14	Field/nest	2009	6	CTTTGTA
MTW11	Colony	2007-08	2		WHT9	Field/nest	2009	6	
MTW12	Colony	2007-08	2		YBT1	Field/nest	2009	7	CATAATG
MTW13	Colony	2007-08	2		YBT2	Field/nest	2009	7	
MTW14	Colony	2007-08	2		YBT4	Field/nest	2009	7	
MTW15	Colony	2007-08	2		YBT10	Field/nest	2009	7	
RML1	Colony	?	3	CTTAGTG	YBT11	Field/nest	2009	7	
RML11	Colony	?	3		YBT12	Field/nest	2009	7	
RML12	Colony	?	3		YBT13	Field/nest	2009	7	
RML13	Colony	?	3		YBT16	Field/nest	2009	7	
RML14	Colony	?	3		YBT18	Field/nest	2009	7	
RML16	Colony	?	3		YBT20	Field/nest	2009	7	
					YBT22	Field/nest	2009	7	

Table B-2. Genetic characteristics of the seven haplotypes represented by the mt16S rDNA of 49 *Ornithodoros hermsi*.

# Sequences	49
# Sites	421
# Polymorphic Sites	7
# Haplotypes	7
Haplotype Diversity	0.842
Nucleotide div. ( $\pi$ )	0.006
Tajima's D (p-value)	1.536 (p > 0.10)
AMOVA (% var. among populations)	75.250 (p < 0.001)
AMOVA (% var. within populations)	24.750 (p < 0.001)
F <sub>ST</sub>	0.752 (p < 0.05)

Table B-3. Pair-wise  $F_{ST}$  values between collection sites (lower diagonal), and the  $p$ -values for pair wise  $F_{ST}$  comparisons (upper diagonal), (+) denotes a significant  $p$ -value ( $p < 0.05$ ), (-) denotes a non-significant  $p$ -value ( $p > 0.05$ ). MTW = Mount Wilson colony, RML = Rocky Mountain Laboratory colony, SIS = Siskiyou County colony, WHI = Wild Horse Island, MIT = Melita Island ticks, YBT = Yellow Bay tick.

	MIT	MTW	RML	SIS	WHI	YBT
MIT		+	+	+	-	+
MTW	1.000		+	+	+	+
RML	1.000	1.000		+	+	+
SIS	0.562	0.688	0.314		+	+
WHI	-0.184	0.968	0.956	0.657		+
YBT	0.810	0.860	0.781	0.267	0.844	

Figure B-1. Geneious maximum likelihood alignment of the 421 bp sequences of the mitochondrial 16S rDNA of 49 *O. hermsi* and *O. coriaceus*. The green bar on top shows the base position and the consensus among ticks. Each row represents a different haplotype. Black bars show areas of disagreement among bases and gray regions depict identical bases.

Figure B-2. Alignment of seven haplotypes (shown in parentheses) identified for *O. hermsi* mitochondrial 16S rDNA sequences. The (•) represents agreement with the base call in Haplotype 1.

Figure B-3. A) Neighbor joining tree of *O. hermsi* (haplotypes shown in parentheses) and *O. coriaceus* as the outgroup. The evolutionary history was inferred using the Neighbor-Joining method. The bootstrap consensus tree inferred from 1000 replicates is shown. The tree is drawn to scale based on the number of base substitutions per site. All positions containing gaps and missing data were eliminated. Due to two deletions in *O. coriaceus*, there were 421 positions in the final dataset. Evolutionary analyses were conducted using MEGA5. B) Neighbor joining tree showing inset of *O. hermsi* and genetic relationships among seven haplotypes (shown in parentheses).



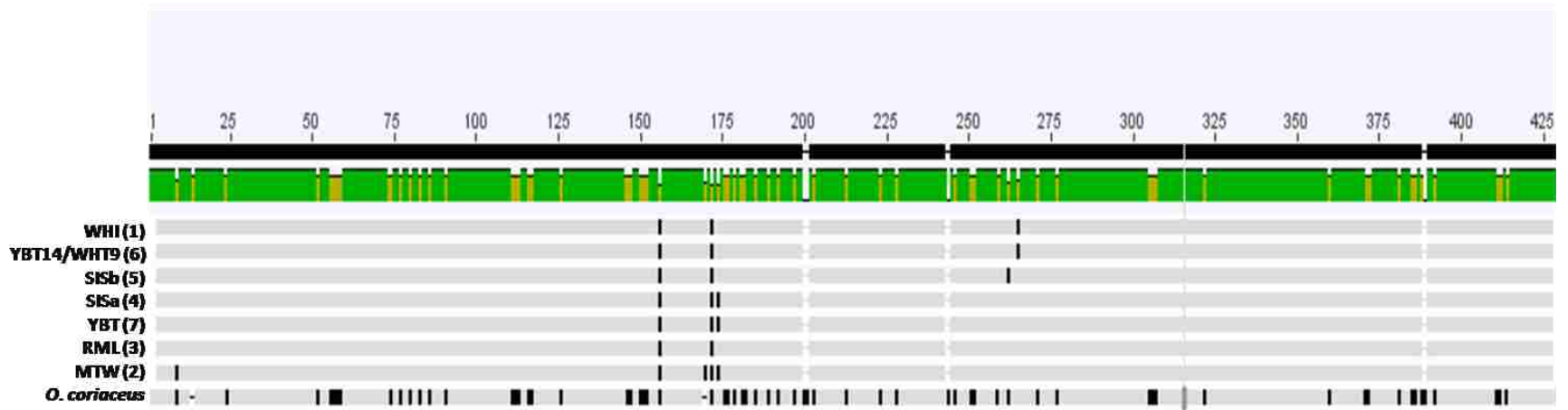


Figure B-1.

<b>WHI (1)</b>	<b>C</b>	<b>A</b>	<b>T</b>	<b>T</b>	<b>G</b>	<b>T</b>	<b>A</b>
<b>MTW (2)</b>	<b>T</b>	<b>:</b>	<b>C</b>	<b>:</b>	<b>A</b>	<b>:</b>	<b>G</b>
<b>RML (3)</b>	<b>:</b>	<b>T</b>	<b>:</b>	<b>A</b>	<b>:</b>	<b>:</b>	<b>G</b>
<b>SISa (4)</b>	<b>:</b>	<b>T</b>	<b>:</b>	<b>A</b>	<b>A</b>	<b>:</b>	<b>G</b>
<b>SISb (5)</b>	<b>:</b>	<b>:</b>	<b>:</b>	<b>:</b>	<b>:</b>	<b>C</b>	<b>G</b>
<b>YBT14/WHT9 (6)</b>	<b>:</b>	<b>T</b>	<b>:</b>	<b>:</b>	<b>:</b>	<b>:</b>	<b>:</b>
<b>YBT(7)</b>	<b>:</b>	<b>:</b>	<b>:</b>	<b>A</b>	<b>A</b>	<b>:</b>	<b>G</b>

Figure B-2.

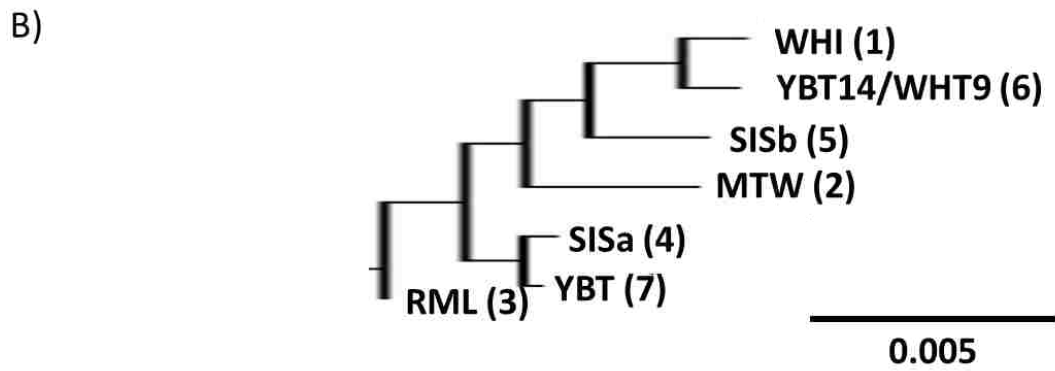
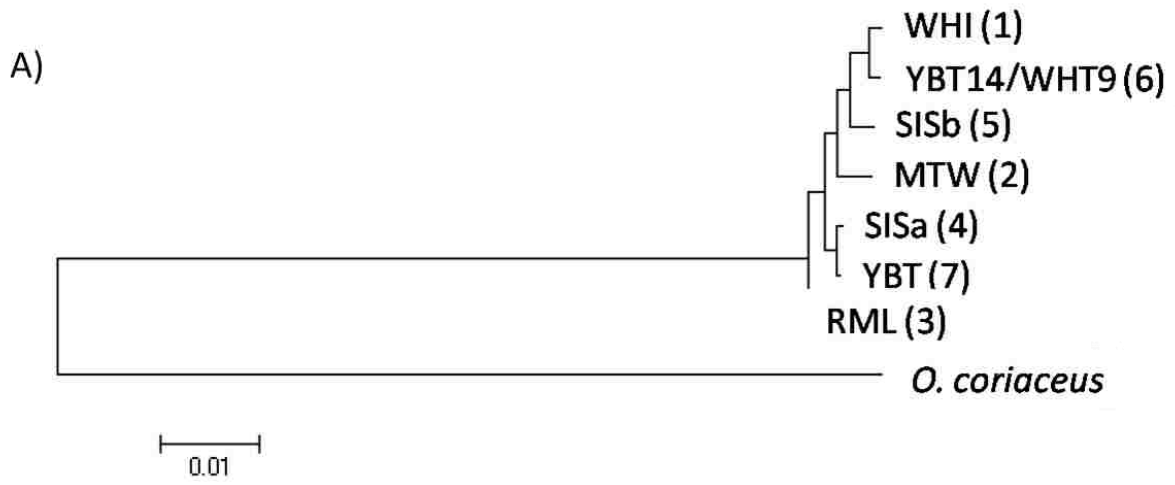


Figure B-3.

## References

- Allen, B.F., R.B. Langerhans, W.A. Ryberg, W.J. Landesman, N.W. Griffin, R.S. Katz, B.J. Oberle, M.R. Schutzenhofer, K.N. Smyth, A. de St. Maurice, L. Cark, K.R. Crooks, D.E. Hernandez, R.G. McLean, R.S. Ostfeld, and J.M. Chase. 2009. Ecological correlates of risk and incidence of West Nile virus in the United States. *Oecologia* 158:699–708.
- Anderson, J.F., R.C. Johnson, L.A. Magnarelli, and F.W. Hyde. 1986. Involvement of birds in the epidemiology of the Lyme disease agent *Borrelia burgdorferi*. *Infection and Immunity* 51:394–396.
- Anderson, M.A. and R.A. May. 1991. *Infectious diseases of humans: dynamics and control*. Oxford University Press, Oxford, UK.
- Archie, E.A., G. Luikart, and V.O. Ezenwa. 2009. Infecting epidemiology with genetics: a new frontier in disease ecology. *TRENDS in Ecology and Evolution* 24:21–30.
- Banerjee, S.N., M. Banerjee, K. Fernando, W. Burgdorfer, and T.G. Schwan. 1998. Tick-borne relapsing fever in British Columbia, Canada: First isolation of *Borrelia hermsii*. *Journal of Clinical Microbiology* 36:3505–3508.
- Barbour, A.G. 1990. Antigenic variation of a relapsing fever *Borrelia* species. *Annual Review of Microbiology* 44:155–171.
- Barbour, A.G. 2005. Relapsing fever. In: *Tick-borne diseases of humans* (Eds. J.L. Goodman, D.T. Dennis, and D.E. Sonenshine). ASM Press, Washington, D.C., U.S.A.
- Barbour, A.G. and B.I. Restrepo. 2000. Antigenic variation in vector-borne pathogens. *Emerging Infectious Diseases* 6:449–457.

- Barbour, A.G., N. Burman, C.J. Carter, T. Kitten, and S. Bergstrom. 1991. Variable antigen genes of the relapsing fever agent *Borrelia hermsii* are activated by promoter addition. *Molecular Microbiology* 5:489–493.
- Barbour, A.G., C.J. Carter, and C.D. Sohaskey. 2000. Surface protein variation by expression site switching in the relapsing fever agent *Borrelia hermsii*. *Infection and Immunity* 68:7114–7121.
- Beck, M.D. 1937. California field and laboratory studies on relapsing fever. *Journal of Infectious Diseases* 60:64–80.
- Beck, M.D. 1942. Present distribution of relapsing fever in California. In: *A symposium on relapsing fever in the Americas* (Ed. F.R. Moulton). Washington: American Association for the Advancement of Science pp. 20–25.
- Begon, M. 2008. Effects of host diversity on disease dynamics. In: *Infectious Disease Ecology: Effects of ecosystems on disease and disease on ecosystems* (Eds. R.S. Ostfeld, F. Keesing, and V.T. Eviner). Princeton University Press, Princeton, NJ, USA.
- Black, W.C. and J. Piesman. 1994. Phylogeny of hard- and soft-tick taxa (Acari: Ixodida) based on mitochondrial 16S rDNA sequences. *Proceedings of the National Academy of Sciences* 91:10034–10038.
- Boyer, K.M., R.S. Munford, G.O. Maupin C.P. Pattison, M.D. Fox, A.M. Barnes, W.L. Jones, and J.E. Maynard. 1977. Tick-borne relapsing fever: an interstate outbreak originating at Grand Canyon National Park. *American Journal of Epidemiology* 105:469–479.
- Brownstein, J.S., T.R. Holford, and D. Fish. 2003. A climate-based model predicts the spatial distribution of the Lyme disease vector *Ixodes scapularis* in the United States. *Environmental Health Perspectives* 111: 1152–1157.

- Brownstein, J.S., T.R. Holford, and D. Fish. 2005. Effect of climate change on Lyme disease risk in North America. *EcoHealth* 2:38–46.
- Bruen, T., H. Phillipe, and D. Bryant. 2006. A quick and robust statistical test to detect the presence of recombination. *Genetics* 172:2665–2681.
- Bunikis, J., J. Tsao, U. Garpmo, J. Berglund, D. Fish, and A.G. Barbour. 2004. Typing of *Borrelia relapsing fever* group strains. *Emerging Infectious Diseases* 10:1661–1664.
- Burgdorfer, W.A. and G.R. Varma. 1967. Trans-stadial and transovarial development of disease agents in arthropods. *Annual Review of Entomology* 12:347–376.
- Burgdorfer, W.A. and A.J. Mavros. 1970. Susceptibility of various species of rodents to the relapsing fever spirochete, *Borrelia hermsii*. *Infection and Immunity* 2:256–259.
- California Department of Public Health Services, Vector-borne Disease Section. 2005. Annual Report. <http://www.cdph.ca.gov/programs/vbds/Documents/VBDSAnnualReport05.pdf>.
- California Department of Public Health Services, Vector-borne Disease Section. 2008. Annual Report. <http://www.cdph.ca.gov/programs/vbds/Documents/VBDSAnnualReport08.pdf>
- Carson, S. 2008. Evaluation of habitat models for small mammals in Montana at multiple scales. MS Thesis, University of Montana, Missoula, MT.
- Casimiro, E., J. Calheiros, F.D. Santos, and S. Kovats. 2006. National assessment of human health effects of climate change in Portugal: approach and key findings. *Environmental Health Perspectives* 114:1950–1956.
- Centers for Disease Control and Prevention. 2003. Tickborne relapsing fever outbreak after a family gathering---New Mexico, August 2002. *Morbidity and Mortality Weekly Report* 52:809–812.

Columbia University, Center for International Earth Science Information Network (CIESIN).

2008. Species distribution grids [online data]. Palisades, NY: Socioeconomic Data and Applications Center (SEDAC), Columbia University (Available at <http://sedac.ciesin.columbia.edu/species>, retrieved [7/30/2011]).

Cooley, R.A. and G.M. Kohls. 1944. The Argasidae of North America, Central America, and Cuba. American Midland Naturalist Monograph No. 1.

Cumming, G.S. 2002. Comparing climate and vegetation as limiting factors for species ranges of African ticks. *Ecology* 83:255–268.

Cumming, G.S. and D.P. Van Vuuren. 2006. Will climate change affect ectoparasites species ranges? *Global Ecology and Biogeography* 15:486–497.

Cummings, C.A., C.A. Bormann Chung, R. Fang, M. Barker, P. Brzoska, P.C. Williamson, J. Beaudry, M. Matthews, J. Schupp, D.M. Wagner, D. Birdsell, A.J. Vogler, M.R. Furtado, P. Keim, and B. Budowle. 2010. Accurate, rapid and high-throughput detection of strain-specific polymorphisms in *Bacillus anthracis* and *Yersinia pestis* by next-generation sequencing. *Investigative Genetics* 1:5.

Cutler, S.J. 2006. Possibilities of relapsing fever reemergence. *Emerging Infectious Diseases* 12(3):369–374.

Cutler, S.J. 2010. Relapsing fever – a forgotten disease revealed. *Journal of Applied Microbiology* 108:1115–1122.

Dai, Q., B.I. Restrepo, S.F. Porcella, S.J. Raffel, T.G. Schwan, and A.G. Barbour. 2006. Antigenic variation by *Borrelia hermsii* occurs through recombination between extragenic repetitive elements on linear plasmids. *Molecular Microbiology* 6: 1329–1343.

- Daszak, P., A.A. Cunningham, and A.D. Hyatt. 2000. Emerging infectious diseases of wildlife—Threats to biodiversity and human health. *Science* 287:443–449.
- Davis, G. E. 1939. Relapsing fever: *Ornithodoros hermsi* a vector in Colorado. *Public Health Reports* 54:2178–2180.
- Davis, G. E. 1940. Ticks and relapsing fever in the United States. *Public Health Reports* 55: 2347–2351.
- Davis, G.E. 1941. *Ornithodoros hermsi* and relapsing fever in Oregon. *Public Health Reports* 56:2010–2012.
- Davis, G. E. 1942. Species unity or plurality of the relapsing fever spirochetes. In: A symposium on relapsing fever in the Americas (Ed. F.R. Moulton). Washington: American Association for the Advancement of Science pp. 41–47.
- Diekmann, O., J.A.P. Heesterbeek, and J.A.J. Metz. 1990. On the definition and the computation of the basic reproduction ratio  $R_0$  in models for infectious disease in heterogeneous populations. *Journal of Mathematical Biology* 28:365–382.
- Dietz, K. 1975. Transmission and control of arbovirus disease. In: *Epidemiology* (Ed. K.L. Cooke). Philadelphia: SIAM pp. 104–121.
- Dobson, A., I. Cattadori, R.D. Holt, R.S. Ostfeld, F. Keesing, K. Krichbaum, J.R. Tohr, S.E. Perkins, and P.J. Hudson. 2006. Sacred cows and sympathetic squirrels: The importance of biological diversity to human health. *PLoS Medicine* 3:0714–0718.
- Drummond, A.J. and A. Rambaut. 2007. BEAST: Bayesian evolutionary analysis by sampling trees. *BMC Evolutionary Biology* 7:214.
- Drummond, A.J. 2010. Summarizing posterior trees.  
[http://beast.bio.ed.ac.uk/Summarizing\\_posterior\\_trees](http://beast.bio.ed.ac.uk/Summarizing_posterior_trees)



- Durden, L.A., R.G. McLean, J.H. Oliver, S.R. Ubico, and A.M. James. 1997. Ticks, Lyme disease spirochetes, trypanosomes, and antibody to encephalitis viruses in wild birds from coastal Georgia and South Carolina. *Journal of Parasitology* 83:1178–1182.
- Dworkin, M.S., D.E. Anderson Jr., T.G. Schwan, P.C. Shoemaker, S.N. Banerjee, B.O. Kassen, and W. Burgdorfer. 1998. Tick-borne relapsing fever in the northwestern United States and southwestern Canada. *Clinical Infectious Diseases* 26:122–131.
- Dworkin, M., T.G. Schwan, and D. Anderson, Jr. 2002. Tick-borne relapsing in North America. *Medical Clinics of North America* 86:417–433.
- Dworkin, M., T.G. Schwan, D. Anderson, Jr., and S.M. Borchardt. 2008. Tick-borne relapsing fever. *Infectious Disease Clinics of North America* 22:449–468.
- Elith, J., C.H. Graham, R.P. Anderson, M. Dudík, S. Ferrier, A. Guisan, R.J. Hijmans, F. Huettmann, J.R. Leathwick, A. Lehmann, J. Li, L.G. Lohmann, B.A. Loiselle, G. Manion, C. Moritz, M. Nakamura, Y. Nakazawa, J.C. McOverton, A.T. Peterson, S.J. Phillips, K.S. Richardson, R. Scachetti-Pereira, R.E. Schapire, J. Sobern, S. Williams, M.S. Wisz, and N.E. Zimmermann. 2006. Novel methods improve prediction of species' distributions from occurrence data. *Ecography* 29:129–151.
- Elith, J., S.J. Phillips, T. Hastie, M. Dudik, Y.E. Chee, and C.J. Yates. 2011. A statistical explanation of MaxEnt for ecologists. *Diversity and Distributions* 17:43–57.
- Espinoza, H., N. McCaig, R.E. Cutler, and W.P. Reed. 1977. Relapsing fever in New Mexico. *Rocky Mountain Medical Journal* 74:321–323.
- Estrada-Peña, A. 2001. Forecasting habitat suitability for ticks and prevention of tick-borne diseases. *Veterinary Parasitology* 98:111–132.

- Excoffier, L. and H.E. Lischer. 2010. Arlequin suite ver. 3.5: A new series of programs to perform population genetics analyses under Linux and Windows. *Molecular Ecology Resources*. 10: 564–567.
- Felsenfeld, O. 1971. *Borrelia*. Strains, vectors, human and animal Borreliosis, Warren H. Green, Inc., St Louis, MO, U.S.A.
- Ficetola, G.F., W. Thuiller, and C. Miaud. 2007. Prediction and validation of the potential global distribution of a problematic alien invasive species – the American bullfrog. *Diversity and Distributions* 13:476–485.
- Fischer, R.J., T.L. Johnson, S.J. Raffel, and T.G. Schwan. 2009. Identical strains of *Borrelia hermsii* in mammal and bird. *Emerging Infectious Diseases* 15:2064–2066.
- Foley, D.H., T.A. Klein, H.C. Kim, T. Brown, R.C. Wilkerson, and L.M. Reuda. 2010. Validation of ecological niche models for potential malaria vectors in the Republic of Korea. *Journal of the American Mosquito Control Association* 26:210–213.
- Francis, E. 1938. Longevity of the tick *Ornithodoros turicata* and of *Spirochaeta recurrentis* with this tick. *Public Health Reports* 53:2220–2241.
- Frank, S.A., and A.G. Barbour. 2006. Within-host dynamics of antigenic variation. *Infection, Genetics, and Evolution* 6:141–146.
- Fritz, C.L., L.R. Bronson, C.R. Smith, M.E. Schriefer, J.R. Tucker, and T.G. Schwan. 2004. Isolation and characterization of *Borrelia hermsii* associated with two foci of tick-borne relapsing fever in California. *Journal of Clinical Microbiology* 42:1123–1128.
- Furman D.P. and E.C. Loomis. 1984. Ticks of California (Acari: Ixodida). *Bulletin of the California Insect Survey* vol. 25. University of California Publications, University of California Press, Berkeley, CA, U.S.A.

- Goldberg, T.L., T.R. Gillespie, I.B. Rwego, E. Wheeler, E.L. Estoff, and C.A. Chapman. 2007. Patterns of gastrointestinal bacterial exchange between chimpanzees and humans involved in research and tourism in western Uganda. *Biological Conservation* 135:511–517.
- González, C., O. Wang, S.E. Strutz, C. González-Salazar, V. Sánchez-Cordero, and S. Sarkar. 2010. Climate change and risk of Leishmaniasis in North America: predictions from ecological niche models of vector and reservoir species. *PLoS Neglected Tropical Diseases* 4:e585.
- Gregson J.D. 1949. Notes on the occurrence of *Ornithodoros hermsi* in British Columbia, and its probable relation to relapsing fever: Argasidae, Ixodoidea. *Proceedings of the Entomological Society of British Columbia* 45:15–16.
- Gubler, D.J. 1998. Resurgent vector-borne diseases as a global health problem. *Emerging Infectious Diseases* 4:442–450.
- Gubler, D.J., P. Reiter, K.L. Ebi, W. Yap, R. Nasci, and J.A. Patz. 2000. Climate variability and change in the United States: potential impacts on vector- and rodent-borne diseases. *Environmental Health Perspectives* 109(S2):223–233.
- Gutacker, M.M, J.C. Smoot, C.A. Lux Migliaccio, S.M. Ricklefs, S. Hua, D.V. Cousins, E.A. Graviss, E. Shashkina, B.N. Kreiswirth, and J.M. Musser. 2002. Genome-wide analysis of synonymous single nucleotide polymorphisms in *Mycobacterium tuberculosis* complex organisms: resolution of genetic relationships among closely related microbial strains. *Genetics* 162: 1533–1543.
- Gutacker, M.M., B. Mathema, H. Soini, E. Shashkina, B.N. Kreiswirth, E.A. Graviss, and J.M. Musser. 2006. Single-nucleotide polymorphism–based population genetic analysis of

- Mycobacterium tuberculosis* strains from 4 geographic sites. *Journal of Infectious Diseases* 193: 121–128.
- Hanley, J.A. and B.J. McNeil. 1982. The meaning and use of the area under a receiver operating characteristic (ROC) curve. *Radiology* 143:26–36.
- Harris, S.R., E.J. Feil, M.T.G. Holden, M.A. Quail, E.K. Nickerson, N. Chantratita, S. Gardete, A. Tavares, N. Day, J.A. Lindsay, J.D. Edgeworth, H. de Lencastre, J. Parkhill, S.J. Peacock, and S.D. Bentley. 2010. Evolution of MRSA during hospital transmission and intercontinental spread. *Science* January 22, 327:469.
- Hermes, W. B. 1956. *Medical entomology; with special reference to the health and well-being of man and animals*. The MacMillan Company, New York, NY, U.S.A. pp. 506–513.
- Hethcote, H. W. 2000. The mathematics of infectious diseases. *SIAM Review* 42:599–653.
- Hijmans, R.J., S.E. Cameron, J. L. Parra, P.G. Jones, and A. Jarvis. 2005. Very high resolution interpolated climate surfaces for global land areas. *International Journal of Climatology*. 25:1965–1978.
- Hinnenbusch, J.B, A.G. Barbour, B.I. Restrepo, and T.G. Schwan. 1998. Population structure of the relapsing fever spirochete *Borrelia hermsii* as indicated by the polymorphism of two multigene families that encode immunogenic outer surface lipoproteins. *Infection and Immunity* 66:432–440.
- Holt, A.C., D.J. Salkeld, C.L. Fritz, J.R. Tucker, and P. Gong. 2009. Spatial analysis of plague in California: niche modeling predictions of the current distribution and potential response to climate change. *International Journal of Health Geographics* 8:38–51.
- Hudson, R.R. and N.L. Kaplan. 1985. Statistical properties of the number of recombination events in the history of a sample of DNA sequences. *Genetics* 111:147–164.

- Hudson, D. H. and D. Bryant. 2006. Application of phylogenetic networks in evolutionary studies. *Molecular Biology and Evolution* 23: 254–267.
- Intergovernmental Panel on Climate Change 3rd Assessment. 2000. IPCC Special report: emissions scenarios. <http://www.ipcc.ch/pdf/special-reports/spm/sres-en.pdf>.
- Jones, K.E., N.G. Patel, M.A. Levy, A. Storeygard, D. Balk, J.L. Gittleman and P. Daszak. 2008. Global trends in emerging infectious diseases. *Nature* 451:990–994.
- Keeling, M.J., P. Rohani, and B.T. Grenfell. 2001. Seasonally forced disease dynamics explored as switching between attractors. *Physica D* 148:317–335.
- Keesing, F., R.D. Holt, and R.S. Ostfeld. Effects of species diversity on disease risk. *Ecology Letters* 9:485–498.
- Kermack, W.O. and A.G. McKendrick. 1927. A contribution to the mathematical theory of epidemics. *Proceedings of the Royal Society of London Series A* 115:700–721.
- Kingman, J.F.C. 1982. The coalescent. *Stochastic Processes and their Applications* 13:235–238.
- Kitron, U. 1998. Landscape ecology and epidemiology of vector-borne diseases: Tools for spatial analysis. *Journal of Medical Entomology* 35:435–445.
- Larson, S.R., J.P. DeGroot, L.C. Bartholomay, and R. Sugumaran. 2010. Ecological niche modeling of potential West Nile virus vector mosquito species in Iowa. *Journal of Insect Science* 10:1–17.
- Lemey P., A. Rambaut, J.J. Welch, and M.A. Suchard. 2010. Phylogeography takes a relaxed random walk in continuous space and time. *Molecular Biology and Evolution* 27:1877–1885.

- Lewis, M.A., J. Renclawowicz, P. van den Driessche, and M. Wonham. 2006. A comparison of continuous and discrete-time West Nile virus models. *Bulletin of Mathematical Biology* 68:491–509.
- Librado, P. and J. Rozas. 2009. DnaSP v5: a software for comprehensive analysis of DNA polymorphism data. *Bioinformatics* 25:1451–1452.
- Longanecker, D.S. 1951. Laboratory and field studies on the biology of the relapsing fever tick vector (*Ornithodoros hermsi* Wheeler) in the high mountains of California. *American Journal of Tropical Medicine and Hygiene* 1-31(3):373–380.
- Lopez, J.E., M.E. Schrupf, S.J. Raffel, P.F. Policastro, S.F. Porcella, and T.G. Schwan. 2008. Relapsing fever spirochetes retain infectivity after prolonged *in vitro* cultivation. *Vector-borne and Zoonotic Diseases* 8:813–820.
- Mackie F.P. 1907. The part played by *Pediculus corporis* in the transmission of relapsing fever. *British Medical Journal* 2:1706–1709.
- Marino, J., M. Bennett, D. Crossios, A. Iriarte, M. Lucherini, P. Pilscoff, C. Sillero-Zubiri, L. Villalba, and S. Walker. 2011. Bioclimatic constraints to Andean cat distributions: a modeling application for rare species. *Diversity and Distributions* 17:311–322.
- McCallum, H., N. Barlow, and J. Hone. 2001. How should pathogen transmission be modeled? *TRENDS in Ecology & Evolution* 16:295–300.
- Meader C.N. 1915. Five cases of relapsing fever originating in Colorado, with positive blood findings in two. *Colorado Medicine* 12:365–368.
- Moffett A, N. Shackelford, and S. Sarkar. 2007. Malaria in Africa: vector species' niche models and relative risk maps. *PLoS ONE* 2: e824.

- Morelli, G., Y. Song, C.J. Mazzoni, M. Eoinger, P. Roumagnac, D.M. Wagner, M. Feldkamp, B. Kusecek, A.J. Vogler, Y. Li, Y. Cui, N.R. Thomson, T. Jombart, R. Leblois, P. Lichtner, L. Rahalison, J.M. Peterson, F. Balloux, P. Keim, T. Wirth, J. Ravel, R. Yang, E. Carniel, and M. Achtman. 2010. *Yersinia pestis* genome sequencing identifies patterns of global phylogenetic diversity. *Nature Genetics* 42:1140–1143.
- Morse, S.S. 1995. Factors in the emergence of infectious diseases. *Emerging Infectious Diseases* 1:7–15.
- Moursund, W.H. 1942. Historical introduction to the symposium on relapsing fever. In: *Relapsing fever in the Americas* (Ed. F.R. Moulton). Washington: American Association for the Advancement of Science.
- Mukherjee, S. A. Krishnan, K. Tamma, C. Home, Navya R, S. Joseph, A. Das, and U. Ramakrishnan. 2010. Ecology driving genetic variation: A comparative phylogeography of jungle cat (*Felis chaus*) and leopard cat (*Prionailurus bengalensis*) in India. *PLoS ONE* 5: e13724.
- Murray, C.J.L. and A.D. Lopez. 1996. *The global burden of disease: a comprehensive assessment of mortality and disability from diseases*. Geneva, Switzerland: World Health Organization.
- Needham, G.R. and P.D. Teel. 1991. Off-host physiological ecology of Ixodid ticks. *Annual Review of Entomology* 36:659–681.
- Nicholls, T.H. and S.M. Callister. 1996. Lyme disease spirochetes in ticks collected from birds in midwestern United States. *Journal of Medical Entomology* 33:379–384.
- Nübel, U., P. Roumagnac, M. Feldkamp, J. Song, K. Soo Ko, Y. Huang, G. Coombs, M. Ip, H. Westh, R. Skov, M.J. Struelens, R.V. Goering, B. Strommenger, A. Weller, W. Witte,

- and M. Achtman. 2008. Frequent emergence and limited geographic dispersal of methicillin-resistant *Staphylococcus aureus*. *Proceedings of the National Academy of Sciences* 105:14130–14135.
- Ogden, N.H., A. Maarouf, I.K. Barker, M. Bigras-Poulin, L.R. Lindsay, M.G. Morshed, C.J. O’Callaghan, F. Ramay, D. Waltner-Toews, and D.F. Charron. 2006. Climate change and the potential for range expansion of the Lyme disease vector *Ixodes scapularis* in Canada. *International Journal For Parasitology* 36:63–70.
- Ostfeld, R.S and F. Keesing. 2000a. Biodiversity and disease risk: The case of Lyme disease. *Conservation Biology* 14:722–728.
- Ostfeld, R.S and F. Keesing. 2000b. The function of biodiversity in the ecology of vector-borne zoonotic diseases. *Canadian Journal of Zoology* 78:2061–2078.
- Parola, P. and D. Raoult. 2001. Ticks and tick-borne bacterial diseases in humans: an emerging infectious threat. *Clinical Infectious Diseases* 32:897–928.
- Paterson, S. and M.E. Viney. 2000. The interface between epidemiology and population genetics. *Parasitology Today* 16:528–532.
- Patz, J.A., T.K. Garczyk, N. Geller, and A.Y. Vittor. 2000. Effects of environmental change on emerging parasitic diseases. *International Journal of Parasitology* 30:1395–1405.
- Peterson A.T., and K.C. Cohoon. 1999. Sensitivity of distributional prediction algorithms to geographic data completeness. *Ecological Modelling* 117:159–164.
- Phillips S.J., M. Dudík, and R.E. Schapire. 2004. A maximum entropy approach to species distribution modeling. In: *Proceedings of the Twenty-First International Conference on Machine Learning* pp. 655–662.



- Phillips, S.J., R.P. Anderson, and R.E. Schapire. 2006. Maximum entropy modeling of species geographic distributions. *Ecological Modelling* 190:231–259.
- Phillips S.J. and M. Dudík. 2008. Modeling of species distributions with Maxent: new extensions and a comprehensive evaluation. *Ecography* 31:161–175.
- Porcella, S.F., S.J. Raffel, D.E. Anderson, S.D. Gilk, J.L. Bono. M.E. Schrupf, and T.G. Schwan. 2005. Variable tick protein in two genomic groups of the relapsing fever spirochete *Borrelia hermsii* in western North America. *Infection and Immunity* 73:6647–6658.
- Porter, G.S., M.D. Beck, and I.M. Stevens. 1932. Relapsing fever in California. *American Journal of Public Health* 22:1136–1140.
- Posada, D. and K.A. Crandall. 1998. MODELTEST: testing the model of DNA substitution. *Bioinformatics* 14:817–818.
- Power, A.G. and C.E. Mitchell. 2004. Pathogen spillover in disease epidemics. *The American Naturalist* 164(S5): S79–S89.
- Ramirez J. and A. Bueno-Cabrera. 2009. Working with climate data and niche modeling. I. Creation of bioclimatic variables.  
[http://gisweb.ciat.cgiar.org/GCMPPage/docs/tutorial\\_bcvars\\_creation.pdf](http://gisweb.ciat.cgiar.org/GCMPPage/docs/tutorial_bcvars_creation.pdf)
- Rand P.W., E.H. Lacombe, R.P. Smith, Jr., and J. Ficker. 1998. Participation of birds (Aves) in the emergence of Lyme disease in southern Maine. *Journal of Medical Entomology* 35:270–276.
- Randolph, S.E. 1993. Climate, satellite imagery and the seasonal abundance of the tick *Rhipicephalus appendiculatus* in southern Africa: a new perspective. *Medical and Veterinary Entomology* 7:243–258.

- Randolph, S.E. and D.J. Rogers. 2000. Fragile transmission cycles of tick-borne encephalitis virus may be disrupted by predicted climate change. *Proceedings of the Royal Society B: Biological Sciences* 267:1741–1744.
- Randolph, S.E., R.M. Green, M.F. Peacey, and D.J. Rogers. 2000. Seasonal synchrony: the key to tick-borne encephalitis foci identified by satellite data. *Parasitology* 121:15–23.
- Randolph S.E. 2001. The shifting landscape of tick-borne zoonoses: tick-borne encephalitis and Lyme borreliosis in Europe. *Philosophical Transactions of the Royal Society of London Series B* 356: 1045–1056.
- Randolph, S.E. 2004. Evidence that climate change has caused ‘emergence’ of tick-borne diseases in Europe? *International Journal of Medical Microbiology* 293:5–15.
- Roberts, M.G. and J.A.P. Heesterbeek. 2003. A new method for estimating the effort required to control an infectious disease. *Proceedings of the Royal Society of London B* 270:1359–1364.
- Rogers, D.J. and S.E. Randolph. 1993. Distribution of tsetse and ticks in Africa: past, present and future. *Parasitology Today* 9:266–271.
- Russell, R.C. 1998. Mosquito-borne arboviruses in Australia: the current scene and implications of climate change for human health. *International Journal of Parasitology* 28:955–969.
- Saitou, N. and M. Nei. 1987. The neighbor-joining method: a new method for reconstructing phylogenetic trees. *Molecular Biology and Evolution* 4:406–425.
- Sarkar S, S.E. Strutz, D.M. Frank, C. Rivaldi, B. Sissel, and V. Sánchez-Cordero. 2010. Chagas disease risk in Texas. *PLoS Neglected Tropical Diseases* 4: e836.
- Schrag, S.J. and P. Wiener. 1995. Emerging infectious disease: what are the relative roles of ecology and evolution? *Trends in Ecology and Evolution* 10:319–324.

- Schmidt, K.A. and R.S. Ostfeld. 2001. Biodiversity and the dilution effect in disease ecology. *Ecology* 82:609–619.
- Schwan T.G. and D.W. Winkler. 1984. Ticks parasitizing humans and California gulls at Mono Lake, California. In: *Acarology VI*, Griffiths, D.A., Bowman C.E., (Eds.) Chichester (UK): Ellis Horwood Ltd. pp. 1193–1199.
- Schwan T.G., M.E. Schrupf, B.J. Hinnenbusch, D.E. Anderson, Jr., and M.E. Konkel. 1996. GlpQ: an antigen for serological discrimination between relapsing fever and Lyme borreliosis. *Journal of Clinical Microbiology* 34:2483–2492.
- Schwan, T.G., P.F. Policastro, Z. Miller, R.L. Thompson, T. Damrow, and J.E. Keirans. 2003. Tick-borne relapsing fever caused by *Borrelia hermsii*, Montana. *Emerging Infectious Diseases* 9:1151–1154.
- Schwan, T.G., S.J. Raffel, M.E. Schrupf, and S.F. Porcella. 2007. Diversity and distribution of *Borrelia hermsii*. *Emerging Infectious Diseases* 13:436–442.
- Schwan, T.G., S.J. Raffel, M.E. Schrupf, L.S. Webster, A.R. Marques, R. Spano, M. Rood, J. Burns, and R. Hu. 2009. Tick-borne relapsing fever and *Borrelia hermsii*, Los Angeles County, California, USA. *Emerging Infectious Diseases* 15:1026–1031.
- Scott, J.D., K. Fernando, S.N. Banerjee, L.A. Durden, S.K. Byrne, M. Banerjee, R.B. Mann, and M.G. Morshed. 2001. Birds disperse ixodid (Acari: Ixodidae) and *Borrelia burgdorferi*-infected ticks in Canada. *Journal Medical Entomology* 38:493–500.
- Sonenshine, D.E. 1991. *Biology of Ticks: Volume 1*. Oxford University Press, USA.
- Sonenshine, D.E. 2005. The biology of tick vectors of human disease. In: *Tick-borne diseases of humans* (Eds. J.L. Goodman, D.T. Dennis, and D.E. Sonenshine). ASM Press, Washington, D.C., U.S.A.

- Southern, P.M. and J.P. Sanford. 1969. Relapsing fever: a clinical and microbiological review. *Medicine* 48:129–149.
- Steel, M.A. 1998. Mammalian species - *Tamiasciurus hudsonicus*. *American Society of Mammalogy* 586:1–9.
- Stevenson, B., S.F. Porcella, K.L. Oie, C.A. Fitzpatrick, S.J. Raffel, L. Lubke, M.E. Schrupf, and T.G. Schwan. 2000. The relapsing fever spirochete *Borrelia hermsii* contains multiple, antigen-encoding circular plasmids that are homologous to the cp32 plasmids of Lyme disease spirochetes. *Infection and Immunity* 68:3900–3908.
- Sullivan, J. 1995. *Peromyscus maniculatus*. In: Fire effects information system, [Online]. U.S. Department of Agriculture, Forest Service, Rocky Mountain Research Station, Fire Sciences Laboratory. Available: <http://www.fs.fed.us/database/feis/> [2011, July 22].
- Suzán G., E. Marcé, J.T. Giermakowski, J.N. Mills, G. Ceballos, R.S. Ostfeld, B. Armién, J.M. Pascale, T.L. Yates. 2009. Experimental evidence for reduced rodent diversity causing increased hantavirus prevalence. *PLoS ONE* 4:e5461.
- Swaddle J.P. and S.E. Calos. 2008. Increased avian diversity is associated with lower incidence of human West Nile infection: observation of the dilution effect. *PLoS ONE* 3:e2488.
- Tajima, F. 1989. Statistical method for testing the neutral mutation hypothesis by DNA polymorphism. *Genetics* 123:585–595.
- Tamura, K., D. Peterson, N. Peterson, G. Stecher, M. Nei, and S. Kumar. 2011. MEGA5: molecular evolutionary genetics analysis using likelihood, distance, and parsimony methods. *Molecular Biology and Evolution* 28:2731–2739.

- Thomas, N.J., J. Bunikis, A.G. Barbour, and M.J. Wolcott. 2002. Fatal spirochetosis due to a relapsing fever-like *Borrelia* sp. in a northern spotted owl. *Journal of Wildlife Diseases* 38:187–193.
- Thompson, R.S, W. Burgdorfer, R. Russel, and B.J. Francis. 1969. Outbreak of tick-borne relapsing fever in Spokane County, Washington. *The Journal of the American Medical Association* 210:1045–1050.
- Trevejo R.T., M.E. Schriefer, K.L. Gage, T.J. Safranek, K.A. Orloski, W.J. Pape, J.A. Monteneri, and G.L. Campbell. 1998. An interstate outbreak of tick-borne relapsing fever among vacationers at a Rocky Mountain cabin. *American Journal of Tropical Medicine and Hygiene* 58:743–747.
- Tsiodras, S., T. Kelesidis, I. Kelesidis, U. Bauchinger, M.E. Falagas. 2008. Human infections associated with wild birds. *Journal of Infection* 56:83–98.
- van den Driessche, P. and J. Watmough. 2002. Reproduction numbers and sub-threshold endemic equilibria for compartmental models of disease transmission. *Mathematical Biosciences* 180:29–48.
- van den Driessche, P., L. Wang., and X. Zou. 2007. Modeling disease with latency and relapse. *Mathematical Biosciences and Engineering* 4:205–219.
- Van Ert, M.N., W.R. Easterday, L.Y. Huynh, R.T. Okinaka, M.E. Hugh-Jones, J. Ravel, S.R. Zanecki, T. Pearson, T.S. Simonson, J.M. U'Ren, S.M. Kachur, R.R. Leadem-Dougherty, S.D. Rhoton, G. Zinser, J. Farlow, P.R. Coker, K.L. Smith, B. Wang, L.J. Kenefic, C.M. Fraser-Liggett, D.M. Wagner, and P. Keim. 2007. Global genetic population structure of *Bacillus anthracis*. *PLoS ONE* 2:e461.

- Vial, L. 2009. Biological and ecological characteristics of soft ticks (Ixodida: Argasidae) and their impact for predicting tick and associated disease distribution. *Parasite* 16:191–202.
- Waldenström, J., Å. Lundkvist, K.I. Falk, U. Garpmo, S. Bergström, G. Lindegren, A. Sjöstedt, H. Mejlön, T. Fransson, P.D. Haemig, and B. Olsen. 2007. Migrating birds and tick-borne encephalitis virus. *Emerging Infectious Diseases* 13:1215–1218.
- Wheeler, C.M. 1935. A new species of tick which is a vector of relapsing fever in California. *American Journal of Tropical Medicine and Hygiene* 15:435–438.
- WHO. 2000. World health report – 2000. Geneva, Switzerland: World Health Organization.
- Wilcox, B.A. and D.J. Gubler. 2005. Disease ecology and the global emergence of zoonotic pathogens. *Environmental Health and Preventive Medicine* 10:263–272.
- Wimberly, M.C., M.J. Yabsley, A.D. Baer, V.G. Dugan, and W.R. Davidson. 2008. Spatial heterogeneity of climate and land-cover constraints on distributions of tick-borne pathogens. *Global Ecology and Biogeography* 17:189–202.
- Wonham, M., T. de Camino-Beck, and M.A. Lewis. 2004. An epidemiological model for West Nile virus: invasion analysis and control applications. *Proceedings of the Royal Society of London B* 271:501–507.
- Wonham, M., M.A. Lewis, J. Renclawowicz, and P. van den Driessche. 2006. Transmission assumptions generate conflicting predictions in host-vector disease models: a case study in West Nile virus. *Ecology Letters* 9:706–725.
- Wynns, H.L. and M.D. Beck. 1935. Epidemiological studies on relapsing fever in California. *American Journal of Public Health* 7:270–276.